1994

Whole-cell Voltage Clamp Of Junctional Conductances In Insect Cell Pairs

J Dennis Churchill

WHOLE-CELL VOLTAGE CLAMP OF JUNCTIONAL CONDUCTANCES IN INSECT CELL PAIRS

by

Dennis Churchill

Department of Zoology

Submitted in partial fulfilment
of the requirements for the degree of
Doctor of Philosophy

Faculty of Graduate Studies
The University of Western Ontario
London, Ontario
November, 1993

ISBN 0-315-90525-5

Canada

ABSTRACT

Gap junction (GJ) channels are dynamic intercellular structures that open and close (gate) in response to cellular signals (*e.g.* voltage), and may be important in regulating cell-to-cell communication in insect development. This thesis presents one of the first biophysical characterizations of GJ channels in insect cell pairs. Double whole-cell voltage-clamp techniques were employed on epidermal cells from the larval flour beetle, *Tenebrio molitor*, to measure the conductances and substate gating properties of individual GJ channels and the effects of voltage and ATP on gating. In addition, these techniques were used to examine the early events of rapid GJ formation between hemocyte couplets from the cockroach, *Periplaneta americana*. For this, methods were developed for isolating epidermal cells and for preventing rapid flattening of hemocytes by using lipophorin-coated coverlips.

GJ formation between hemocyte couplets occurred within one second after contact and junctional conductance (G_j) increased in steps of ~345 pS. Each step corresponds to a new channel added to the growing gap junction.

Pharate pupal epidermal (PPE) and newly-moulted epidermal (NME) cells suitable for whole-cell recording were isolated. Single cells from both stages had large nonjunctional resistances (>5 GΩ). NME but not PPE cells expressed a hyperpolarization-activated inward current.

Isolated PPE and NME cell pairs had functional gap junctions. G_j dropped during whole-cell recording, however, adding 5 mM ATP but not nonhydrolysable ATP analogues to the pipette solution slowed uncoupling suggesting that ATP probably acts through an ATP-utilizing enzymatic process.

G_j in epidermal cells is mostly membrane-potential (V_M) dependent, although transjunctional-voltage dependence is also present.

Conductances of individual GJ channels in poorly-coupled PPE cell pairs were large (197 to 403 pS). This GJ channel is one of the first described capable of existing in a range of partially-closed substates.

GJ-channel gating mechanisms presented herein may be important in regulating cell-to-cell communication in insects. For instance, V_M-dependence may provide a mechanism for controlling the overall level of coupling. Moreover, GJ-channel substates may account for selective regulation of junctional permeability in developing tissues.

ACKNOWLEDGEMENTS

So that I don't forget anyone I like to send out a general thanks to all the professors, staff and graduate students who have been in the Department of Zoology during the past 5 years. I have valued the friendly learning environment provided by everyone.

I would especially like to thank Dr. Stanley Caveney for the opportunity to work in his lab. I can only hope that some of his unlimited enthusiasm for science has rubbed off.

I must acknowledge the helpful advice of Dr. Stephen Sims for the many selfless hours of advice on my research.

For the many hours of 'discussing science', and playing hockey and various other goofy activities in addition to their friendship I thank fellow graduate students Sheppy Coodin and my wife Caren Helbing.

I must also acknowledge the support and friendship of everyone who spent time in the lab during my tenure including, Heather (Hez) and the other Heather, Jenny, Jennifer, Erika, Elizabeth, Ian, Matt, Steve, Chris, Randy, Miyo and Gerard.

All those around the department who have helped directly or indirectly with my work I thank as well: Ian Craig, Rick Harris, the secretaries (Mary, Callie, Jane, Marge, Sherry and Melina), the janitorial staff (especially Joe, John, Ron and Rudy) and also Ron Podesta and Michael Locke for sitting on my advisory and examining committees.

TABLE OF CONTENTS

LIST OF FIGURES

LIST OF TABLES

LIST OF APPENDICES

LIST OF ABBREVIATIONS

20HE	20-hydroxyecdysone
A	constant in Boltzmann equation describing the steepness of the relationship
AMP	adenosine 5'-monophosphate
AMP-PNP	5'-adenylylimidodiphosphate
ATP	adenosine 5'-triphosphate
ATPase	adenosine 5'-triphosphatase
ATPγS	adenosine 5'-O-(3-thiotriphosphate)
cAMP	adenosine 2'(3')-monophosphate
CF	5(6)-carboxyfluorescein
cGMP	guanosine 2'(3')-monophosphate
Cx	connexin
Da	Daltons
DMSO	dimethyl sulfoxide
EDTA	ethylene diamine tetraacetic acid
EGTA	ethylene glycol-bis(β-aminoethyl ether) N,N,N',N'-tetraacetic acid
F	Faraday's constant
f_s	sample frequency (units: hertz)
γ_j	single-channel conductance (units: pS)
GΩ	gigaohm
G_j	junctional conductance (units: nS)
GJ	gap junction
G_{j50}	time after break-in to a 50% drop in junctional conductance
G_{jmax}	maximal junctional conductance

GTP	guanosine 5'-triphosphate
h	hours
Hepes	N-2-hydroxyethylpiperazine-N'-2-ethanesulfonic acid
I	total current
I_1	current of cell 1
I_2	current of cell 2
I_J	junctional current ($I_1 - I_2$)
I_L	leak current
I_{NJ}	nonjunctional current
I_P	peak capacitive current
ΔI_1	change in current of cell 1
ΔI_2	change in current of cell 2
Δi_j	change in microscopic junctional current
L	length of channel bore
MΩ	megaohm
min	minutes
msec	milliseconds
mV	millivolts
n	sample size
N	number of active channels
NA	numerical aperture
NME	newly-moulted epidermis
nS	nanoSiemens
pA	picoamperes
PCM	pulse code modulator

pF	picoFarads
Pipes	piperazine-N,N'-bis-2-ethanesulfonic acid
P_o	probability of channel opening
PPE	pharate pupal epidermal
PPS	*Periplaneta* pipette solution
ρ	resistivity of a fluid (units: Ωcm)
R	ideal gas constant
r^2	radius squared
r^2	correlation coefficient
R_M	nonjunctional membrane resistance
RNA	ribonucleic acid
R_S	series resistance
SD	standard deviation
sec	seconds
SEM	standard error of the mean
T	absolute temperature (degrees Kelvin)
TBS	*Tenebrio* bath solution
TPS	*Tenebrio* pipette solution
U	units as in units/ml of an enzyme
V^*	voltage of most hyperpolarized cell of a cell pair
V_1	clamped voltage of cell 1
V_2	clamped voltage of cell 2
V_H	holding or command voltage
V_{I-O}	inside-outside voltage
V_J	transjunctional voltage

V_M	nonjunctional-membrane potential
V_o	constant in Boltzmann equation describing V_M at which half the gates are open
ΔV_P	change in pipette voltage
z	gating charge

I GENERAL INTRODUCTION

I.1 Gap Junctions

The cells of most tissues communicate directly via specialized regions of plasma membrane called gap junctions. Such communication is important in direct cell-to-cell signal transmission, in mediating hormonal responses, in tissue homeostasis, and in coordinating cell growth, patterning and development. Gap junctions consist of a lattice of transmembrane integral-membrane protein channels. The component channels, called gap-junction channels (GJ channels), are made of two hemichannels or connexons, one provided by each of a pair of neighbouring cells. Connexons link up in mirror symmetry across the narrow gap between abutting cell membranes and directly join the cell interiors by a chiefly nonselective pathway that is permeable to inorganic ions and small organic molecules (gap junction structure, molecular biology, function and physiology has been extensively reviewed: Bennett *et al.* 1981; Loewenstein 1981; Spray *et al.* 1984; Caveney 1985b; Sheridan & Atkinson 1985; Spray & Bennett 1985; Spray *et al.* 1985; Neyton & Trautmann 1986b; Ramón & Rivera 1986; Bruzzone & Meda 1988; Guthrie & Gilula 1989; Beyer *et al.* 1990; Dermietzel *et al.* 1990; Bennett *et al.* 1991; Willecke *et al.* 1991).

The connexons of vertebrates are constructed of six protein subunits (connexins) surrounding an aqueous pore. Vertebrate connexins make up a diverse family of more than 20

different proteins that have been isolated and sequenced. They have been named according to their predicted molecular weights, for example, the 43000 Da and 32000 Da gap junction proteins first isolated from mammalian heart and liver (respectively) are called connexin43 (Cx43) and connexin32 (Cx32) (Beyer *et al.* 1990; Willecke *et al.* 1991). Nucleic acid hybridization and anti-vertebrate connexin immunoanalyses have not identified homologous arthropod connexins. This suggests that arthropod gap junctions are probably composed of a different family of proteins.

Ultrastructurally, gap junctions in all tissues appear in thin-section electron micrographs as regions of closely-apposed membranes separated by a 1 to 4 nm gap. In freeze-fractured plasma membranes gap junctions are recognized as tightly-packed arrays of membrane particles (gap junctional plaques) with each particle probably representing an individual GJ channel. When arthropod gap junctions are freeze-fractured the particles stick in the E-face of the membrane instead of the P-face as in vertebrate junctions. In addition to this distinction, the particle size in freeze-fractured arthropod junctions are larger than in vertebrates and the upper cut-off limit for the passage of molecules is 2 to 3 nm *vs* 1 to 2 nm in vertebrates (reviews; arthropod gap junction structure: Caveney & Berdan 1982; Lane 1982).

GJ channels are not just static structures. They are capable of opening and closing, a process called gating, in

response to a variety of signals. Generally factors that gate gap junctions include: intracellular pH (pH_i), intracellular Ca^{++} concentration ($[Ca^{++}]_i$), membrane potential (V_M), transjunctional voltage (V_j), certain volatile anaesthetics, fatty acids and phosphorylation. Details on these mechanisms in insects is sparse (review: Caveney 1985a). Most work in insects (mostly on *Chironomus* salivary gland cells) has focused on the effects of intracellular Ca^{++} (Loewenstein 1966; Loewenstein *et al.* 1967; Politoff *et al.* 1969; Rose & Loewenstein 1976; Lees-Miller & Caveney 1982).

Since dual voltage-clamp techniques were first applied to examine the voltage dependence of gap junctions (Spray *et al.* 1981), only three studies on insect cell pairs from *Chironomus* salivary gland (Obaid *et al.* 1983), *Drosophila* salivary gland (Verselis *et al.* 1991), and a mosquito cell line (Bukauskas *et al.* 1991) have been reported. In each study, junctional conductance was found to be strongly dependent on the nonjunctional-membrane potential. Membrane-potential-dependent gating is rarely observed in vertebrate cell types in which gating depends strictly on transjunctional voltage (reviews: Spray & Bennett 1985; Spray *et al.* 1991a). Transjunctional-voltage dependence is usually symmetric about a transjunctional voltage of 0 mV but may be asymmetric as in the rectifying electrical synapses of some invertebrate giant axons.

Whether gating plays an important physiological role is

uncertain. Given the range of mechanisms that gate GJ channels, however, a sensible proposal is that cellular mechanisms that control the degree of cell-to-cell coupling may control chemical communication within a tissue. The clearest role for gap junctions is in excitable tissues such as muscle and nerve where gap junctions conduct electrical signals (see reviews above). Channel gating performs a physiological role in the rectifying synapses of invertebrates where asymmetric transjunctional-voltage dependence of the gap junctions is responsible for directional electrical transmission (Furshpan & Potter 1959; Giaume *et al.* 1987).

Certainly among the strongest evidence for a physiological role of GJ-channel gating in nonexcitable cells is the broad diversity of vertebrate connexins that are being discovered. Each connexin makes up gap junctions having different physiological, pharmacological and biophysical properties. Specific connexins may be expressed in more than one tissue; one cell can express more than one connexin; the same connexin expressed in different cell types can exhibit distinct properties; cells expressing different connexins can form heterotypic gap junctions having intermediate properties; and connexin expression and permeability can change temporally during development and carcinogenesis (reviews: Beyer *et al.* 1990; Dermietzel *et al.* 1990; Bennett *et al.* 1991; Willecke *et al.* 1991).

I.2 Gap Junctions in Development

One proposed role for gap junctions in nonexcitable tissues is as a direct cell-to-cell route for the transfer of chemical signals that are capable of coordinating cells during growth and development. Recent evidence supports the notion that such direct intercellular signalling can occur. The second messenger molecules, Ca^{++} and inositoltrisphosphate, probably pass through gap junctions in a variety of tissues (Saez *et al.* 1989; Cornell-Bell *et al.* 1990; Sandberg *et al.* 1990; Cornell-Bell & Finkbeiner 1991; Sherman & Rinzel 1991; Boitano *et al.* 1992). Although putative developmental signals that are gap junction permeant have not been discovered, three lines of indirect evidence support a role for gap junctions in development (reviews: Wolpert 1978; Bennett *et al.* 1981; Caveney 1985b; Revel 1986; Guthrie & Gilula 1989; DeHaan & Chen 1990).

First, junctional permeability can change in phase with developmental events. Examples of this include the larval insect epidermis of *Tenebrio* where junctional conductance rises and falls in phase with the moult cycle (see section I.3 below), and also in the developing vertebrate heart where action potential propagation increases with developmental stage (DeHaan & Chen 1990).

Second, changes in the pattern of gap junction permeability throughout embryos often corresponds to regions of developmental fate, creating communication compartments.

This has been demonstrated in a variety of early embryos and later developing tissues including, the larval epidermis in the insect *Calliphora*, *Oncopeltus* and *Drosophila* (Warner & Lawrence 1982; Blennerhassett & Caveney 1984; Ruangvoravat & Lo 1992), *Drosophila* imaginal disk (Weir & Lo 1984; Fraser & Bryant 1985; Weir & Lo 1985), and in several vertebrate and invertebrate embryos (in *Xenopus*, Nagajski *et al.* 1989; mouse, Lo & Gilula 1979; *Lymnaea*, Serras & van den Biggelaar 1987; zebrafish, Kimmel & Law 1985; tunicates, Serras & van den Biggelaar 1988; molluscs, Dorresteijn *et al.* 1983; and teleosts, Gevers & Timmermans 1991).

Lastly, experimental blockage of gap junctions can interfere with normal development. Injecting monoclonal antibodies against gap junctions into single cells of early *Xenopus* embryos (Warner *et al.* 1984), *Hydra* (Fraser *et al.* 1987) and preimplantation mouse embryos (Lee *et al.* 1987) alters junctional communication and subsequent development. Also, injecting antisense RNA to gap junction proteins into preimplantation mouse embryos blocks specific connexin expression and certain developmental events (Bevilacqua *et al.* 1989).

I.3 Gap Junctions in the Insect Epidermis

The outer covering of an insect, the integument, is composed of a monolayer of epidermal cells underlying the hard cuticular exoskeleton they produce (reviews: Hepburn 1976; King & Akai, 1982; Wigglesworth 1984; Binnington & Retnakaran,

1991). The epidermis forms the simple two dimensional pattern of bristles, sensory structures, cuticle types and pigmentation found on insects. In addition to a spatial pattern there is a temporal component embodied in the insect moult cycle, growth and metamorphosis. Thus, the segmented insect epidermis has become a convenient model for studying patterning in development. Moreover, it has been possible to study changes in gap junctions with developmental events in the epidermis of the larval flour beetle, *Tenebrio molitor*. Using conventional microelectrode techniques junctional conductance (*i.e.* permeability to inorganic ions) can be measured. Also, the permeability to small organic molecules can be determined by microinjecting small fluorescent molecules (*e.g.* lucifer yellow & carboxyfluorescein) and quantifying the spread of fluorescence through the tissue (technical reviews: Caveney 1985a; Caveney *et al.* 1986).

In *Tenebrio*, junctional conductance within an epidermal segment changes predictably in phase with each moult cycle, increasing early in the cycle and decreasing as the moult approaches (Caveney 1978). Furthermore, the developmental hormone 20-hydroxyecdysone (20HE), increases junctional conductance when epidermal segments are incubated with it *in vitro* (Caveney & Blennerhassett 1980). This elevation in junctional conductance does not involve an increase in the number of GJ channels deployed at the cell junctions. The number of particles in gap junctional plagues does not

increase and the response to 20HE is unaffected by protein synthesis inhibitors (Caveney *et al*. 1980; Berdan & Caveney 1985). Thus, the elevation in junctional conductance must be due to changes in existing GJ channels. It has been proposed that the proportion of open GJ channels might increase or alternatively, already-opened channels may open to a greater extent.

Unlike junctional conductance, the permeability to fluorescent molecules in *Tenebrio*, does not vary within the moult cycle although it does increase as the insect grows in size (Safranyos & Caveney 1984; Safranyos 1985; Caveney & Safranyos 1989). By an unknown mechanism epidermal GJ channels selectively increase conductance to inorganic ions while still restricting passage to larger molecules. A similar response is exhibited *in vitro* by incubating the epidermal cells in L-glutamate which increases junctional conductance 50% without changing permeability to fluorescent molecules (Caveney 1988).

Discoordinate regulation of inorganic ion and small organic molecule permeability also occurs at the border between adjacent segments of epidermis. Passage of fluorescent molecules is restricted by a strip of border cells at the segment borders in *Calliphora*, *Oncopeltus* and *Drosophila* epidermis while ionic coupling is maintained (Warner & Lawrence 1982; Blennerhassett & Caveney 1984; Ruangvoravat & Lo 1992). This occurs without a reduction in the number of gap junctions at the border in *Oncopeltus* (Lawrence & Green 1975).

The observation is significant because each segment, in addition to forming a communication compartment, is also a lineage compartment arising from one embryonic cell (Lawrence 1973) with the segment borders lining up with developmental boundaries (Locke 1959). It is possible that border cells could be sites where the passage of a putative developmental signal molecule is restricted.

In summary, gap junctions in the insect epidermis appear to have the ability to selectively increase or decrease the rate of cell-to-cell passage of different kinds or sizes of molecules. Thus, discoordinate control of permeability is clearly developmentally significant in the epidermis as it occurs at compartment borders, and changes within epidermal segments in phase with the moult cycle and in response to developmental hormones.

I.4 Double Whole-Cell Recording

The development of patch-clamp techniques have provided the first insights into the gating of nonjunctional-ion channels (Hamill *et al.* 1981). With this technique blunt microelectrodes with tip diameters of 1 μm or more (patch-pipettes) are applied directly to biological membranes containing ion channels. Patches of membrane within the pipette tip become electrically isolated when high resistance seals (gigaohm-seals) form between the pipette glass and membrane. Low background noise created by the seal allows the tiny currents passing through ion channels as they open and

close to be detected.

In one of several variants of the patch-clamp technique the membrane patch within the pipette is ruptured with suction. The gigaohm-seal remains intact providing direct electrical access to the whole cell. Thus the entire plasma membrane of small cells can be voltage clamped and the average properties of all the cell's ion channels examined. Furthermore, the concentrations of exogenous and endogenous substances in the cytoplasm can be controlled since the solution in the pipette diffuses into the cell (Marty & Neher 1983).

The whole-cell recording technique can be applied to cell pairs. A patch-pipette is applied to each cell so that the average properties of populations of GJ channels between the two cells can be examined. If the background noise from nonjunctional channels is low enough, then tiny currents passing through single GJ channels can be recorded when there are only a few GJ channels active. Double whole-cell voltage clamp was used to make the first direct measurements of the conductance of individual channels (*i.e.* single-channel conductance, γ_j). GJ channels behave very much like nonjunctional-ion channels in that they open and close randomly to discrete levels (Neyton & Trautmann 1985; Veenstra & DeHaan 1986). Recently, evidence suggests that some GJ channels open to partially-closed states (*i.e.* subconductance states) in addition to the fully-open state (Neyton &

Trautmann 1985; Chen & DeHaan 1992) similar to that found in some nonjunctional-ion channels (Fox 1987).

In summary, double whole-cell voltage-clamp techniques allow the gating properties of larger populations of GJ channels between well-coupled cell pairs to be characterized. As we shall see this includes voltage dependence and gating by intracellularly applied agents. Furthermore, in poorly-coupled cell pairs, with only a few active channels, single GJ-channel properties including single-channel conductances of main and subconductance states (if they exist), can be measured.

I.5 Forming Gap Junctions in Cockroach Hemocytes

Insect hemocytes have been shown to form gap junctions during a cellular immune response. Hemocytes encapsulate parasitic eggs and other foreign invaders of the hemocoel by encasing them in layers of cells (reviews: Grimstone *et al.* 1967; Götz 1986). During encapsulation gap junctions form between the hemocytes (Baerwald 1975; Norton & Vinson 1977; Han & Gupta 1989). In freeze-fracture and dye transfer studies by fellow graduate student, Sheppy Coodin, hemocyte gap junctions were shown to form within minutes of being bled from a cockroach. Precisely how fast gap junction formation (GJ formation) occurred was unknown. A way to address this question is to use the double whole-cell patch-clamp technique. Individual hemocytes may be patch clamped and manipulated into contact and the development of electrical coupling monitored. Indeed, if the background noise is low

enough then the precise moment that the first GJ channel is formed and opens may be determined.

In addition to providing precise determination of the time to onset of coupling, whole-cell recording of GJ formation provides a unique opportunity to measure GJ-channel conductance in a 'natural' condition. In this thesis GJ-channel conductances are measured in epidermal cell pairs that are artificially-uncoupled. In contrast, during the initial stages of GJ formation one or only a few gap junctions are present naturally. Until recently, whole-cell recordings of this type have only been accomplished in vertebrate muscle (Chow & Young 1987; Rook *et al.* 1988) but now are available from an insect cell line (Bukauskas & Weingart, 1993) and in insect hemocytes (Churchill *et al.* 1993).

I.6 Thesis Rationale and Summary of Objectives

All previous studies of epidermal gap junctions in insects have been done on intact segments of tissue consisting of thousands of well-coupled cells. The techniques used on intact tissue have demonstrated that epidermal gap junctions are gated during development and that inorganic ion and small organic molecule permeabilities are regulated discoordinately. The mechanisms accounting for these observations are unknown. Insight into these may be gained by examining the properties of the individual GJ channels using double whole-cell recording. There may be multiple channel types detectable as distinct channels with different fully-open conductances, or,

there could be one population of channels with subconductance states. Different main or subconductance states could have different permeabilities and undergo differential regulation.

On working with isolated cells, other biophysical aspects of epidermal GJ channels that could not be addressed using intact tissue may also be investigated. For example, any detailed biophysical characterization of biological channels must include a description of their voltage dependence. As discussed, the few insect cell junctions studied exhibit primarily membrane-potential dependence whereas most vertebrate gap junctions either exhibit transjunctional-voltage dependence or no voltage dependence at all. Insect gap junctions also differ from those in vertebrates in several of other ways. Thus, a detailed biophysical analysis of the single-channel properties and voltage dependence of insect epidermal GJ channels would allow them to be compared to gap junctions from other organisms, other insect tissues and especially to those insect gap junctions for which the protein sequences will soon be available (probably in a fly such as *Drosophila*). Evolutionary relationships may then be defined and other properties or functions of the gap junction of interest may then, by analogy, be proposed. Moreover, detailed comparisons may help clarify mechanisms for voltage-dependent or substate gating in gap junctions.

Another aspect of epidermal GJ-channel gating may also be investigated. Many vertebrate cell pairs spontaneously

uncouple as an artifact of recording and this is inhibited by including ATP in the pipette. Is this a property of insect gap junctions as well? Can it be used to examine single GJ-channel properties in epidermal cells? What is the general mechanism whereby ATP stabilizes junctional conductance? Does this general mechanism reflect a physiological process involved in stabilizing gap junctions?

In order to complete each of these studies techniques for isolating insect epidermal cell pairs had first to be developed, their suitability for double whole-cell recording determined including a preliminary characterization of their nonjunctional currents.

I.6.1 Summary of Thesis Objectives

The general objectives of this thesis are:

1. To characterize the biophysical properties of cell-to-cell communication in isolated pairs of insect epidermal cells. This work may provide new information that further elucidates the role of gap junctions in insect development and indeed may expand our knowledge of the function of gap junctions in organisms generally.
2. To examine with high temporal resolution the early events of gap junction formation in insect hemocyte couplets.

The specific questions addressed by this thesis are:

1. Can cells be isolated from the insect epidermis? An isolated epidermal cell preparation has yet to be developed.

2. If cells can be isolated are they suitable for double whole-cell recording? What are their nonjunctional electrical properties?
3. Do isolated cells maintain functional gap junctions?
4. Do insect epidermal cells spontaneously uncouple during whole-cell recording as do some vertebrate cell pairs?
5. Does ATP stabilize insect gap junctions and by what general mechanism does it prevent spontaneous uncoupling?
6. What is/are the single-channel conductance(s) of epidermal GJ channels? Do epidermal gap-junction channels have subconductance states?
7. Does information about the single gap-junction channel properties give insight into the selective permeability properties of epidermal gap junctions?
8. What kind of voltage dependence is expressed by epidermal gap junctions? Could voltage dependence play a physiological role?
9. How fast do cockroach hemocytes form gap junctions? What is the single-channel conductance of the first forming gap junctions? Is it similar to that found for epidermal gap junctions?

II WHOLE-CELL VOLTAGE-CLAMP RECORDING TECHNIQUES

This chapter describes in detail the whole-cell voltage-clamp techniques used in these studies. Short methods sections are included in later chapters to detail any additional materials or methods specific to those chapters (Chapters III, IV, VII).

II.1 Chemicals

Piperazine-N,N'-bis-2-ethanesulfonic acid (Pipes), N-[2-hydroxyethyl]piperazine-N'-[2-ethanesulfonic acid] (Hepes), ethylene diamine tetraacetic acid (EDTA), ethylene glycol-bis(β-aminoethyl ether) N,N,N',N'-tetraacetic acid (EGTA) and adenosine 5'-triphosphate (Na_2ATP) were all from Sigma (St. Louis, Missouri).

All basic salts were analytical grade from BDH (Toronto, Ontario).

5(6)-carboxyfluorescein (376 Da) was obtained from Eastman Kodak (Rochester, NY).

II.2 *Tenebrio* Solutions

Pipette solution

TPS in mM: 100 KCl, 10 NaCl, 1 $CaCl_2$, 2 $MgCl_2$, 10 EGTA/45 KOH (added from a 50 mM EGTA/225 mM KOH stock solution), 20 Pipes, 80 sucrose; pH 6.7 with 1 M KOH. For pipette solutions containing any added components such as ATP the component was added before the pH was adjusted and the saline brought up to final volume with double distilled H_2O.

Bath solutions:

TBS in mM: 80 NaCl, 43 KCl, 3 $CaCl_2$, 10 $MgCl_2$, 90 sucrose, 10 glucose, 20 Pipes; pH 6.7 with 1 M NaOH.

II.3 Statistical Analysis

All averaged data are expressed as mean ± SEM unless stated otherwise. The Student's t-test was used to test the difference between two sample means ($p < 0.05$).

II.4 Recording Chamber and Superfusion

Following isolation cells were placed in a Plexiglas recording chamber (Appendix 2) with a volume of approximately 0.5 to 1.0 ml and a glass coverslip fixed to the bottom with white bees wax (Fisher Scientific, Toronto). For whole-cell recording from cuticle-attached epidermal cells the chamber was outfitted with a stainless steel spring-clamp which pressed the cuticle against the coverslip with the cuticle-attached cells on the upper surface. The cells were superfused with 5 to 10 ml of saline once placed in the recording chamber and were frequently superfused with bath saline throughout the experiment (4 to 10 ml/min). Superfusion was achieved by gravity feed using a 60 ml syringe body as a reservoir with a teflon needle-valve, three-way stopcock and drip (to break electrical continuity of the solution), all inserted between the reservoir and recording chamber. Bath saline was aspirated from the recording chamber by vacuum. A three-way stopcock was inserted in the vacuum line so that vacuum could be turned off to prevent drying out of the recording chamber when gravity

feed was turned off. Tygon tubing (Canlab, Toronto) was attached to the components of the perfusion system (through luer lock fittings) by slipping the tubing over stainless steel hypodermic needles. Disposable components of the perfusion system were replaced every few months and were rinsed with 70% ethanol and distilled water after each use.

II.5 Whole-Cell Recording

All experiments were performed on single cells, cell pairs or cell groups at a room temperature of 24 to 29°C (heater controlled) within 8 to 10 h of cell preparation using whole-cell voltage-clamp techniques (Hamill *et al.* 1981). Descriptions of some of these specific methods have appeared elsewhere (Churchill & Caveney 1993a; Churchill *et al.* 1993).

Patch-pipettes with a 1 to 2 μm tip diameter were pulled on the day of use on a two stage vertical pipette puller (model 750; Kopf, Tujunga, California) from 1.5/1.12 mm OD/ID thin-walled borosilicate glass capillary tubing without filament (TW150-4; World Precision Instruments, Sarasota, Florida). Just before use the pipettes were first tip-filled with pipette solution using suction and then backfilled (through a 0.2 μm low protein-binding syringe filter) using a home made teflon needle or a fine quartz metal-free pipette-filling needle (MF28G-5, WPI). Stray capacitance across the pipette wall was reduced by coating to within several hundred μm of the pipette tip (under a dissecting microscope) with pure white beeswax (Fisher Scientific, Toronto). These

pipettes, which had series resistances of 1 to 10 MΩ, were attached to the hydraulic micromanipulator-mounted (model MO-202; each attached to a MN-2/3 3-D micromanipulator, Narishige, Japan) head stages of two independent List L/M EPC-7 patch-clamp type voltage-clamp amplifiers (Medical Systems, New York). Electrical contact to the pipette and bath solutions was made with silver-silver chloride pellets attached to teflon-coated silver wires (HLA-003; Axon Instruments, Foster City, California) or on occasion teflon coated silver wire (AGT1010, 0.25 mm dia.; WPI) with the exposed tip chlorided by submerging in bleach (5% Javex) for 20 to 60 min (just until black).

Current signals were monitored using a 2 channel digital storage oscilloscope (model 2220, Tektronix, Washington) and permanent analogue records of the current and voltage signals were made using a 4 channel ink type chart recorder (model RS 3400, Gould, Cleveland, Ohio). Digital records of the signals were stored to a betamax home video cassette recorder (VCR) (SL-330, Sony) using a 4 channel A/D VCR recorder adaptor (*i.e.* pulse code modulator; PCM) with a maximum sampling frequency (f_s) of 22 kHz (PCM-4; Medical Systems, New York); and to the hard disk of an IBM compatible 386 computer (an upgraded Premium286; AST, Irvine, California) using a 125 kHz TL-1 DMA AD/DA interface (Axon Instruments).

Voltage commands and acquisition to disk for double whole-cell experiments was controlled by in-house software

(TWOCELL) designed specifically for double whole-cell recording (written in Axobasic; Axon Instruments and Quickbasic; Microsoft, Bellevue, Washington; see Appendix 3 for part of program). For single cell studies the commercially available Pclamp stimulation, acquisition and analysis suite of programs was used (Axon Instruments). TWOCELL software is capable of generating Pclamp compatible data files for some analysis as well as generating ASCII files for analysis by typical spreadsheet software. Some continuous data (such as single-channel data) was analyzed and/or displayed upon playback from VCR tape using Axotape software (Axon Instruments). Unless stated otherwise data were filtered upon playback from VCR tape at 0.2 x f_s using an 8 pole low-pass besel filter (Series 900, Frequency Devices, Haverhill, Massachussetts).

In a typical experiment gigaohm-seal formation (> 5 GΩ) between the pipette and cell membrane was achieved by manipulating the pipettes onto unflattened cells while under observation at 400X on an inverted phase-contrast microscope (model IM-35, Carl Zeiss, New York, NY) fitted with phase-epifluorescence optics (40X Neofluar objective, NA 0.75). Currents during gigaohm-seal formation were monitored while holding the voltage at 0 mV and supplying 25 msec 1 mV voltage pulses at 2 Hz to the pipette (ΔV_p = 1 mV). Slight mouth suction was usually necessary to obtain gigaohm-seals. Positive pressure was maintained at the back of the pipette

during entry of the pipette into the bath and during its application to the cell surface by a water-filled manometer (with pressure set at 10 to 20 cm water). After gigaohm-seal formation the whole-cell recording mode was formed by rupturing the patch of membrane in the pipette (break-in) with brief strong pulses of mouth suction. For this the capacitive current spike was monitored simultaneously in both cells while holding the pipette voltage at -30 or -50 mV and supplying 50 msec -10 mV voltage pulses at 1 Hz. Before break-in the stray capacitance was compensated using the capacitance compensation circuitry of the patch-clamp amplifiers. Break-in was evidenced by a rapid increase in capacitive current. Immediately following break-in an example of the capacitive current for many cells was stored to disk (f_s = 10 kHz) for off-line analysis using Pclamp (Axon Instruments). The capacitive current was monitored in this way periodically throughout many experiments. During double whole-cell recording of single GJ-channel activity recordings were too short (due to the brief period of time that single channels could be observed) to monitor the capacitive spike. Cell capacitance was estimated from the area of the capacitive spike (Area = charge; Q in Coulombs) by dividing the area by the change in pipette voltage. Series resistance (R_s) was estimated by dividing the change in pipette voltage (10 mV) by the peak of the capacitive current. Capacitance and series resistance compensation circuitry was not used so that R_s

Fig. II-1. Schematic of whole-cell recording

(A) Two patch-pipettes filled with pipette solution are each shown on one cell of a cell pair joined by gap junctions (cell 1 & cell 2). The patch of membrane within the pipette has ruptured thus creating the whole-cell configuration.

(B) Electrical schematic diagram showing the significant resistances during double whole-cell recording. The seal resistances (between the tip of the patch-pipette and the cell membrane) are several orders of magnitude larger than the other resistances and thus are not shown. R_{S1} and R_{S2} are the access resistances through the pipettes into cell 1 and cell 2 respectively; also called the series resistance since R_S is in series with the junctional resistance (R_J). R_{M1} and R_{M2} are the nonjunctional membrane resistances of cell 1 and cell 2 respectively.

(C) Example of the voltage protocol (V_1 & V_2) and the resulting currents (I_1 & I_2) during measurement of junctional conductance. Hyperpolarizing voltage pulses are typically applied alternately to each cell. Both cells are voltage clamped to the same holding voltage. The downward currents recorded in response to a voltage pulse applied to that cell equals the sum of the currents passing across the gap junction and the nonjunctional membrane. The upward currents recorded in response to a voltage pulse applied to the other cell represent junctional currents only.

A

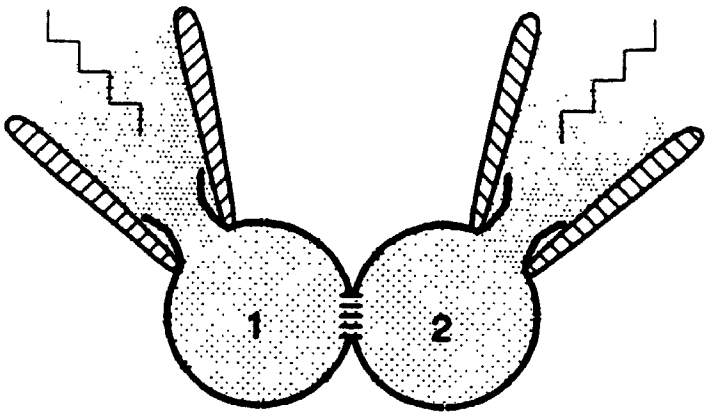

B

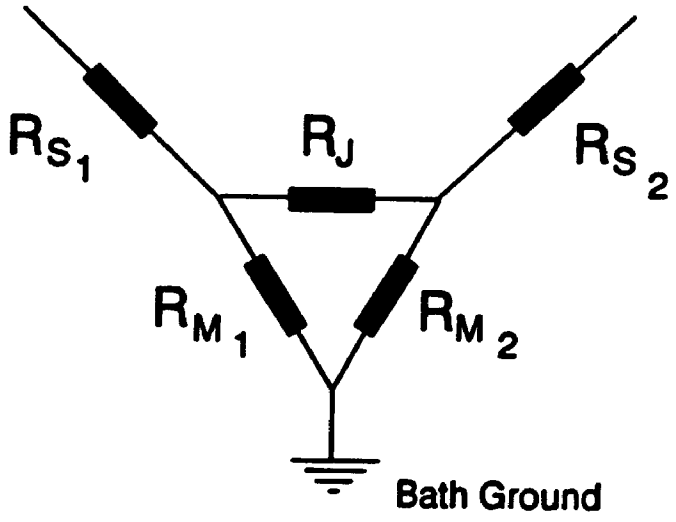

C

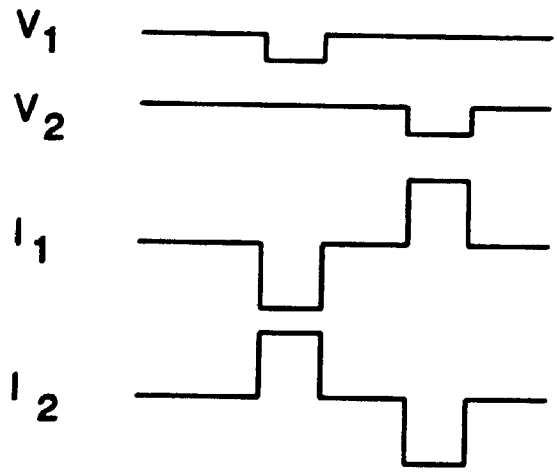

could be monitored rapidly throughout the experiment. All voltages are expressed as inside negative.

II.6 Junctional-Conductance Measurement

Measurement of macroscopic junctional currents (I_j), calculation of junctional conductance (G_j), and correction for series resistance errors have already been described in some detail (Neyton & Trautmann 1985; Rook *et al.* 1988; Veenstra & DeHaan 1988; Giaume 1991). For measurement of large junctional conductances in well-coupled cell pairs each cell was initially held at the same holding potential (-30 to -50 mV) and 1 sec -20 mV voltage pulses were supplied alternately to either cell every 3 sec (see Fig. II-1). Pulses were sent to both cells to exclude one-sided artifacts. When a pair of cells are voltage-clamped at the same holding voltage ($V_1 = V_2$), and cell 1 is stepped to another voltage, a transjunctional voltage ($V_j = V_1 - V_2$) is created. To maintain the voltage of that cell the amplifier supplies a step in current (ΔI_1) which is composed of the junctional (I_j) and nonjunctional (I_{NJ}) currents. If $I_j >> I_{NJ}$ most of ΔI_1 will enter the second cell and that amplifier will supply a step change in current (ΔI_2) that is equal in magnitude but opposite in sign to I_j. The junctional conductance (G_j) is estimated directly by dividing I_j (*i.e.* $-\Delta I_2$) by V_j (in experiments in which G_j was not corrected for R_s errors). For experiments in which R_s correction was used G_j was calculated with the equation:

$$G_J = \frac{I_J}{V_J - (R_{S_1} \cdot I_1 - R_{S_2} \cdot I_2)}$$

where R_{S1} and R_{S2} are the R_S's for cell 1 and cell 2 respectively. R_S in 14 pharate pupal epidermal (PPE) cell pairs changed an average of 56% in 20 min during voltage-dependence experiments. R_S in 90 newly-moulted epidermal (NME) cell pairs changed an average of 48% in 20 min during uncoupling kinetics experiments.

In order to minimize errors due to voltage-clamping the junctional and nonjunctional resistances, the electrode resistance (*i.e.* R_S) must be 10 to 20 times smaller than each of these other resistances (discussed in Fischmeister *et al.* 1986; Veenstra & DeHaan 1988; Veenstra 1990; Giaume 1991). In experiments with PPE cells, R_S was typically 20 ± 1 MΩ (n = 54) and junctional and nonjunctional resistances in well-coupled cell pairs were 94 ± 12 MΩ (n = 258) and 14 ± 3 GΩ (n = 29) respectively. For NME cells R_S was typically 14 ± 1 MΩ (n = 30) and junctional and nonjunctional resistances were 6 ± 1 MΩ (n = 88) and 3 ± 1 MΩ (n = 31) respectively. Therefore, errors due to R_S, especially in well-coupled NME cell pairs are significant and have been corrected where necessary.

II.7 Single GJ-channel Recording and Analysis

Open-close events of single-GJ channels in poorly-coupled cell pairs (G_J < 1.5 nS) were recognized as spontaneous step-like transitions in the current signals of both cells which

were equal in magnitude but opposite in polarity. For these measurements V_j was held constant. Single-channel conductances (γ_j) were measured for the trace with the higher signal-to-noise ratio. The magnitude of the single-channel current (Δi_j) was measured by visually averaging the plateau of the current transitions using the vertical cursors of Axotape (Axon Instruments). Frequency histograms of these events were constructed by grouping the calculated conductances ($\gamma_j = \Delta i_j / V_j$) of all step-like transitions from one cell pair into bins. These distributions were fitted to single Gaussian curves using the Gaussian-Newton approximation algorithm of Pclamp (Axon Instruments). The equation for a single Gaussian curve is:

$$F(\gamma_J) = \frac{1}{SD/2\pi} \cdot e^{-\frac{1}{2} \cdot \left(\frac{\gamma_J - \overline{\gamma}_J}{SD}\right)^2}$$

where SD is the standard deviation and $\overline{\gamma}_j$ is the mean of the distribution. Data were acquired from tape to disk for analysis by sampling at 500 Hz and filtering at 100 Hz.

II.8 Dye-Coupling Techniques

The fluorescent dye carboxyfluorescein (CF) was dissolved with vortexing for 1 min in TPS at a concentration of 10 mM. Patch-pipettes were backfilled with this solution while filtering with a 0.2μm syringe filter. Standard whole-cell recording techniques were then used to apply the pipette to one cell of a pair. The recording chamber was constantly

perfused to remove CF leaking from the pipette before gigaohm-seal formation. CF was excited by light from a mercury vapour lamp (HBO 50 W) using a BP485 excitation filter, a BP520 barrier filter and dichroic mirror FT510 (Carl Zeiss, Toronto) on a inverted microscope (model IM-35, Carl Zeiss, New York) fitted with phase-epifluorescence optics (40X Neofluar objective, NA 0.75). A modified RCA silicon-intensified target (SIT) television camera (TC1030/H: RCA Electro-Optics & Devices, Lancaster, Pennsylvania) set on automatic gain was used to monitor passage of CF between cells. The camera was attached to VCR (SL-330, Sony) and a television (TV) monitor (EVM-1220, Electrohome Inc, Kitchener, Ontario). Photographs were taken of the TV image during playback from VCR using a 35 mm camera set on a tripod with automatic exposure and Tek Pan 2415 film (Eastman, Kodak, Rochester, New York).

III PREPARATION OF ISOLATED EPIDERMAL CELLS AND PRELIMINARY CHARACTERIZATION OF JUNCTIONAL AND NONJUNCTIONAL CURRENTS

III.1 Introduction

An examination of single GJ-channel activity using double whole-cell recording is subject to certain limitations (Veenstra & DeHaan 1986; Giaume 1991). Input resistance of the cells must be high; that is the holding currents necessary to voltage clamp the cells must be small (<< 100 pA). Otherwise single-channel currents measuring 1 to 10 pA are too small to be distinguished from the background current through nonjunctional channels or from the current noise associated with many simultaneously-active GJ channels. Consequently small spheroid cells of < 20 μm diameter (and typically > 5 GΩ input resistance) are favoured (Hamill *et al.* 1981). A second limitation is that cell pairs should have an inherently low junctional conductance (< 2 nS) or a junctional conductance that can be artificially reduced (the number of active GJ channels must be low (< 5)). Two methods have been used to reduce junctional conductance in vertebrate cell pairs. Conductance has been reduced with volatile anaesthetics such as halothane or octanol (Burt 1991), or by taking advantage of the spontaneous uncoupling that sometimes occurs when the pipette solution dilutes out soluble cytoplasmic components necessary for normal coupling (Somogyi & Kolb 1988). Also, in preparing cells for whole-cell recording it is necessary that the plasma membrane be free of connective tissue so that

gigaohm-seals can be formed directly between the patch-pipette tip and plasma membrane (Hamill *et al.* 1981).

The insect epidermis is a monolayer of tightly-interconnected columnar cells (each ~10 to 15 μm in width). On its apical surface the epidermis is attached tightly to the cuticle it produces. On its basal surface it is bordered by a thick basement membrane, the basal lamina. The challenge in isolating single cells and cell pairs in this tissue is to interrupt each of these connections; cell-cell, cell-cuticle and cell-basal lamina.

This chapter describes two techniques that were developed to isolate *Tenebrio* epidermal cells. By using pharate pupal epidermal (PPE) cells the first method takes advantage of a natural process. The pharate pupal stage begins when the epidermis of the last larval instar detaches naturally from the old larval cuticle, a process called apolysis. During this stage the epidermis remains free of cuticle until it starts to synthesize a pupal cuticle 4 to 5 days later. The pharate pupal stage ends at pupation. In addition to the loss of cell-cuticle attachments, cell-cell attachments also loosen as the epidermal cells divide and rearrange themselves during metamorphosis to the pupa. The basal lamina is then removed with proteolytic enzymes. Isolation of PPE cells has been described in Churchill & Caveney (1993c).

The second method does not require that cell-cuticle and cell-cell attachments be loose. Epidermis from any insect

stage is suitable, although newly-moulted epidermal (NME) cells were used here. Following proteolytic digestion of the basal lamina a patch-pipette was used to scrape the epidermis and kill selected patches of cells to create islands of living cells. Single cells, cell pairs and cell groups of any size could be obtained with this method.

This chapter describes these two isolation methods. It also explores the electrical properties of single PPE and NME cells and whether isolated cell pairs are electrically- and dye-coupled by gap junctions. This must be done to demonstrate that isolated epidermal cells are suitable for electrophysiological studies and that functional gap junctions survive the isolation procedures. The junctional effects of volatile anaesthetics were investigated to rule out the possiblility that junctional currents were due to cytoplasmic bridges instead of gap junctions (Bukauskas *et al.* 1992). The particular advantages of the two isolation methods and the cell stages used for different types of experiments are discussed.

III.2 Materials and Methods

III.2.1 Beetle Culture and Staging

Larvae of the yellow mealworm (=flour beetle) *Tenebrio molitor* (L.) were reared on a whole wheat flour-bran-yeast mixture maintained at 27°C in a 12 h light/dark cycle.

Last instar larvae were collected immediately after ecdysis (weight > 0.1 g). Those used within 4 to 6 h are

termed newly-moulted larvae; those kept a further 6 days in 50 mm Petri dishes were termed intermoult or mid-instar larvae.

Pharate pupae (*i.e.* last instar larvae immediately following apolysis) were collected and staged just before dissection. Selection of pharate pupae involved three steps. First, only larvae that rested on top of the flour were selected (larvae at other stages usually burrow). These larvae lay mostly on their sides although they could be probed to right themselves and move slowly. Second, from these selected insects larvae at eye stages 7 to 11 (staged according to Stellwaag-Kittler, 1954) were chosen. Third, during dissection, only naked apolysed epidermis before new pupal cuticle production were accepted. Tissue prior to apolysis or tissue secreting pupal cuticle were discarded.

III.2.2 Dissection

Dissection is similar to that previously described (Caveney & Blennerhassett 1980). Just before dissection the insects were anaesthetized by submersion in 70% ethanol for 4 min. Ventral sternites from segments II to VII were excised from 6 to 10 pharate *Tenebrio* pupae or from single newly-moulted or mid-instar *Tenebrio* larva and placed into TBS in a 35 mm Petri dish. The fat body was teased away from the epidermis with fine forceps. In pharate pupae the epidermis remains loosely attached to the cuticle by muscle attachments. In newly-moulted and mid-instar larvae the epidermis remains firmly attached to the cuticle and skeletal muscle was

removed. The segments, now consisting only of epidermis plus cuticle, were transferred to fresh TBS. Tissue was kept at 24 to 28°C (room temperature) in TBS for the duration of the experiment.

III.2.3 Enzyme Solutions

Enzyme solutions were made by diluting 1% stocks of proteolytic enzyme in TBS to a concentration of 0.1 to 0.4%. Enzyme stock solutions were made up in TBS and stored at -20°C. Elastase (type IIA), crude collagenase (type IA), trypsin (type III), pronase E (type XXV), dispase (P3417), hyaluronidase (type IV) or pancreatin (P3292) were purchased from Sigma (St Louis, Missouri).

III.2.4 Isolation of Cuticle-Free Cells from Pharate Pupal Epidermis

Following dissection, squares of cuticle to which the pharate pupal epidermis was loosely-attached were incubated in 1 ml of enzyme solution, either in 0.2 to 0.4% collagenase for 10 to 20 min or in 0.1% pronase for 1 to 5 min, in a 15 ml Falcon tissue culture tube that was shortened to the 7 ml graduation mark so that forceps could be used to transfer the tissue segments directly into the solution. Following incubation with enzyme, the enzyme solution containing tissue was diluted to 6 ml with TBS, gently triturated 1 to 3 times with a siliconized (Sigmacote; Sigma) Pasteur pipette (4 mm diameter opening) and then transferred to a fresh 15 ml Falcon tube and further diluted to 15 ml and centrifuged at 100 g for

5 min. The pellet was resuspended in 15 ml TBS, centrifuged again, resuspended in 1 ml TBS and plated onto the glass coverslip base of the Plexiglas superfusion chamber (described in Chapter II). The cuticle, now cell-free, was removed from the chamber with forceps and discarded. Cells were allowed to adhere to the glass for 30 to 60 min and were used within 8 to 10 h.

III.2.5 Isolation of Cuticle-Attached Single Cells, Cell Pairs and Cell Groups in Newly-Moulted Epidermis

Following dissection, segments of cuticle with well-attached newly-moulted epidermis were incubated in 1 ml of 0.1% pronase in TBS for 1 to 2 min. Following the enzyme digestion tissue was placed in fresh TBS in a 35 mm Petri dish. This procedure removed the basal lamina while leaving the layer of epidermis intact and attached to the cuticle. Each segment of integument was then clamped epidermis side up in the recording chamber and viewed in phase-contrast. The epidermal monolayer was then scraped with a typical patch-pipette used for whole-cell recording with the tip broken back to 2 to 7 μm in diameter. The pipette was lowered through the epidermis until it just touched the cuticle and then it was drawn through the sheet of epidermal cells by moving the microscope stage. By repeating this process a grid pattern of damaged epidermal cells was created in which the centres of the grid squares contained undamaged cells.

The dimensions of the grid squares could be altered to

leave live groups of cells of any size or even cell pairs and single cells. Following the scraping procedure the tissue was left for at least 1 h and up to 6 h. This allowed the damaged cells to die and disintegrate. Just before whole-cell recording the preparation was cleaned up by sucking up the cellular debris through a broken patch-pipette (tip 2 to 7 μm) leaving only the remaining live cells. Whole-cell recording from these cells proceeded immediately.

III.2.6 Volatile Anaesthetics

2-bromo-2-chloro-1,1,1-trifluoro-ethane (halothane), 1-heptanol, and 1-octanol were purchased from Sigma (St. Louis, Missouri). These were prepared by adding directly to saline immediately before use, shaking violently for 1 min and keeping in a sealed bottle until added to the reservoir for bath perfusion.

III.3 Results

III.3.1 Efficacy of Various Enzymes

A series of proteolytic enzymes was tested on the epidermis to select the best enzyme for gigaohm-seal formation and cell isolation. Mid-instar epidermis were used for these experiments. At this stage the epidermis is firmly attached apically to the cuticle and basally to the basal lamina. Following dissection, segments were placed into various dissociation solutions of 0.1 to 0.4% elastase, collagenase, trypsin, pronase E, dispase, hyaluronidase or pancreatin and then incubated for 1 to 60 min. The presence of basal lamina

was assessed by scraping the cuticle-attached epidermis with patch-pipettes while observing the cells using phase-contrast on the inverted microscope (scrape-test) and by attempting to form gigaohm-seals on the basal plasma membranes of the epidermal cells. Scraping only damaged a narrow lane of cells in tissue treated with at least 0.4% collagenase for 10 to 20 min or 0.1% pronase for 1 to 5 min. However, scraping damaged large regions of cells (presumably still attached to an intact basal lamina) in tissue treated with the other enzymes even with incubation times of up to 60 min. Gigaohm-seals could be formed only on epidermal basal plasma membranes treated with pronase or collagenase.

Elastase did not remove the basal lamina, as demonstrated by the scrape-test or gigaohm-seal-tests. Instead, long incubations (0.2% for 30 min) loosened the epidermis from the cuticle to such an extent that sheets of cells detached from the clamped cuticle when the epidermis was scraped.

III.3.2 Isolation of Cuticle-Free Pharate Pupal Epidermal Cells

Initial attempts to isolate mid-instar cells using combinations of elastase (to loosen cell-cuticle attachments), collagenase (to remove the basal lamina), and low [Ca^{++}] and mechanical agitation (to disrupt intercellular contacts) were unsuccessful. Although small groups of cells could be freed, the harsh treatment (long incubations and mechanical agitation) damaged the small number of cells isolated in this

fashion.

Subsequent attempts to isolate epidermal cells used pharate pupal epidermis treated with pronase or collagenase since both intercellular and epidermal-cuticular contacts are reduced naturally. Small numbers (10 to 50) of single cells, pairs of cells and larger groups of spherical, phase-bright cells were isolated (Fig. III-1). Pronase was used for whole-cell voltage-clamp experiments instead of collagenase because it yielded larger numbers of cells. Most cells remained morphologically unchanged for several hours in primary culture; however, some cells extended fine cellular processes and others flattened. Although these fine cellular processes were not seen in the light microscope, cell pairs clearly separated by a small space were often electrically-coupled.

III.3.3 Isolation of Cuticle-Attached Newly-Moulted Epidermal Single Cells, Cell Pairs and Cell Groups

Practically unlimited numbers of singles, pairs and groups of epidermal cells could be created using the scrape technique. These cells were morphologically indistinguishable from isolated PPE cells (Fig. III-2). The cells remained attached to the cuticle and were not observed to flatten. Isolated single cells were never close enough to neighbouring cells to determine if electrical-coupling via filopodia was present.

Fig. III-1. Isolated PPE cells in phase-contrast

Most cells are phase-bright and spherical with large round nuclei. A few cells flatten (note cell in top left corner). Two patch-pipettes are shown on a cell pair. Scale bar, 10 μm.

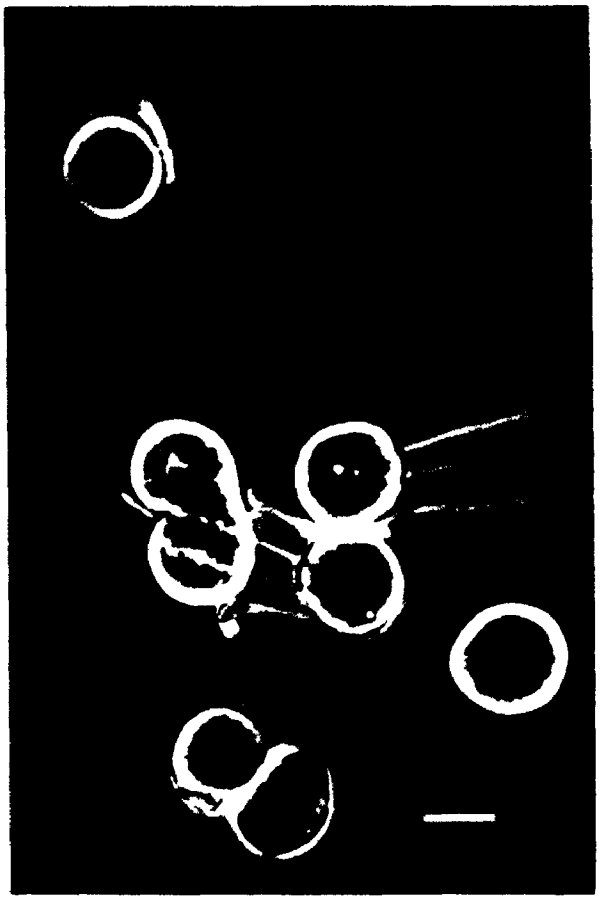

Fig. III-2. Isolated cuticle-attached NME cells

Phase-contrast micrographs looking through the cuticle at NME cells before (a) and after (b) cell isolation by scraping the tissue with a broken patch-pipette. Scale bar, 10 μm.

(a) Basal lamina has been removed in (a) with pronase treatment. Individual cells are partially outlined by phase bright 'swollen' intercellular spaces. The nuclei are the less bright white 'balls' roughly in the centre of the cells.

(b) 1 hour following scraping of the epidermis. Scarring of the cuticle can be seen as diagonal lines extending from lower left to upper right. A 'checkerboard' pattern of live cells in small groups, pairs (arrowhead) and single cells can be seen. Much of the debris from dead cells has been sucked away through a broken patch-pipette.

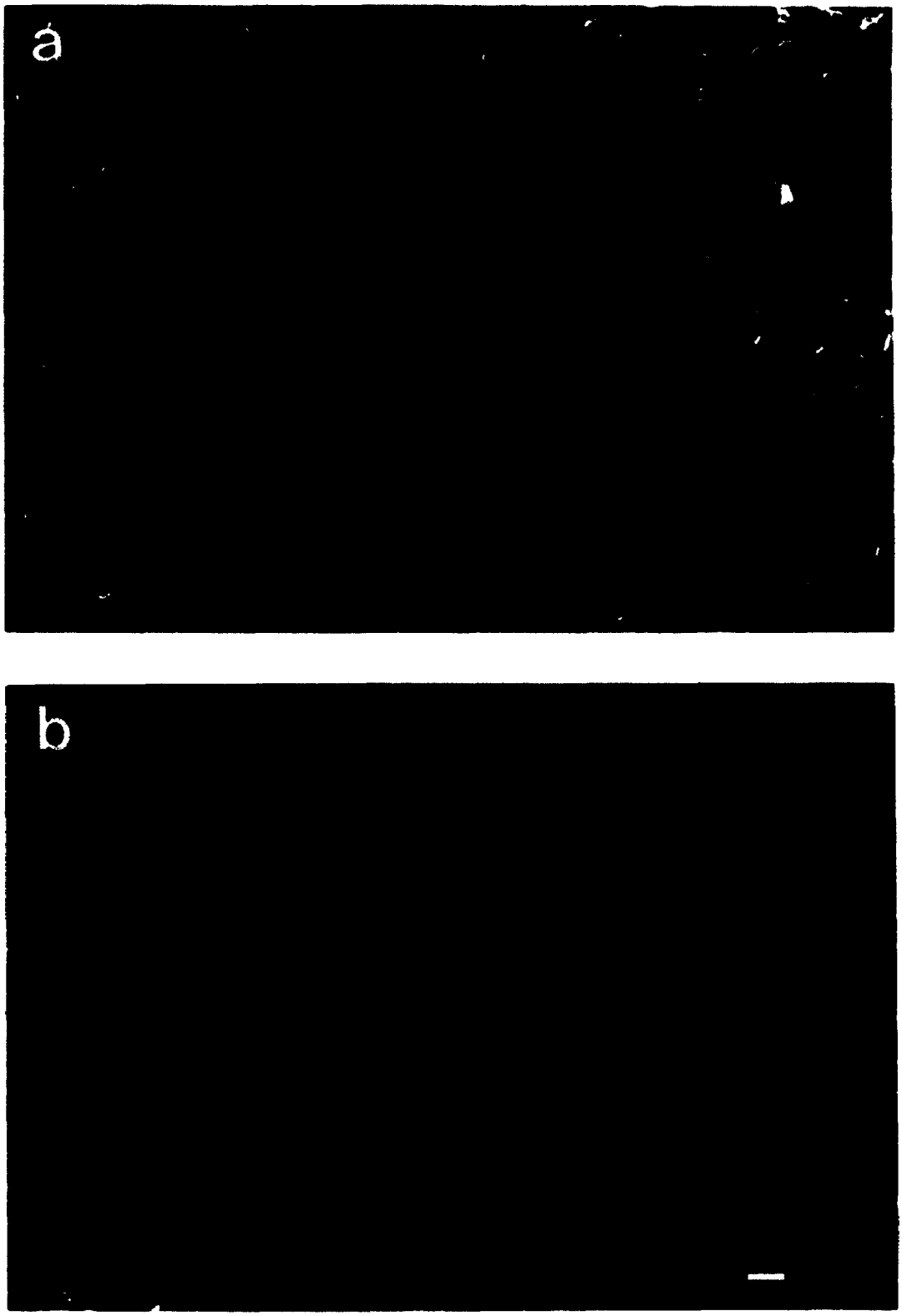
a
b

III.3.4 Gigaohm-Seal Formation, Series Resistances and Passive Electrical Properties of Single Cells

High-resistance gigaohm-seals (> 5 GΩ) were easily obtained on the isolated PPE cells (success rate > 90%; n > 200) and NME cells (success rate > 70%; n > 800) and could often be maintained for up to 1 h. The lower success rate for gigaohm-seals on NME cells was probably due to the presence of debris from scrape-killed cells.

The average series resistances (R_S) in 108 PPE cells and 60 NME cells were 19 ± 1 MΩ and 14 ± 1 MΩ, respectively.

The values of whole-cell capacitance and membrane potential just after break-in in 54 PPE cell pairs (n = 108 cells) and in 30 NME cell pairs (n = 60 cells) were 9.8 ± 0.5 pF and -22 ± 2 mV (range: -3 to -60 mV) and 12.6 ± 0.4 pF and -5 ± 2 mV (range: 0 to -23 mV), respectively.

III.3.5 Nonjunctional Currents in Pharate Pupal Epidermal Cells

The response of single PPE cells to voltage pulses of ± 100 mV was ohmic (Fig. III-3). The input resistance in 29 single cells was 14 ± 2 GΩ. These data demonstrate that the nonjunctional membrane (under the conditions used) has a very high input resistance and lacks voltage-gated channel activity, and therefore would not interfere with the measurement of junctional currents.

Fig. III-3. Whole-cell currents in single PPE cell pairs

(A) Single whole-cell current traces in response to 1000 msec voltage jumps (-100 to 100 mV, in 10 mV increments) applied from V_H = -40 mV. The arrowhead denotes the zero current level.

(B) The current-voltage relationship measured through the midpoint of the traces was linear with V_M = -25 mV and input resistance of 11 GΩ.

A

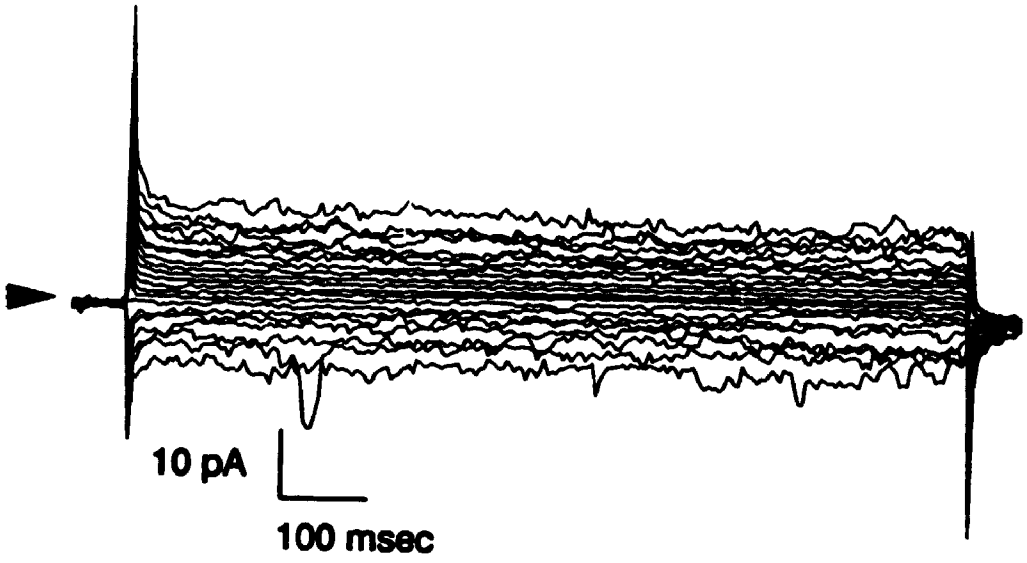

B

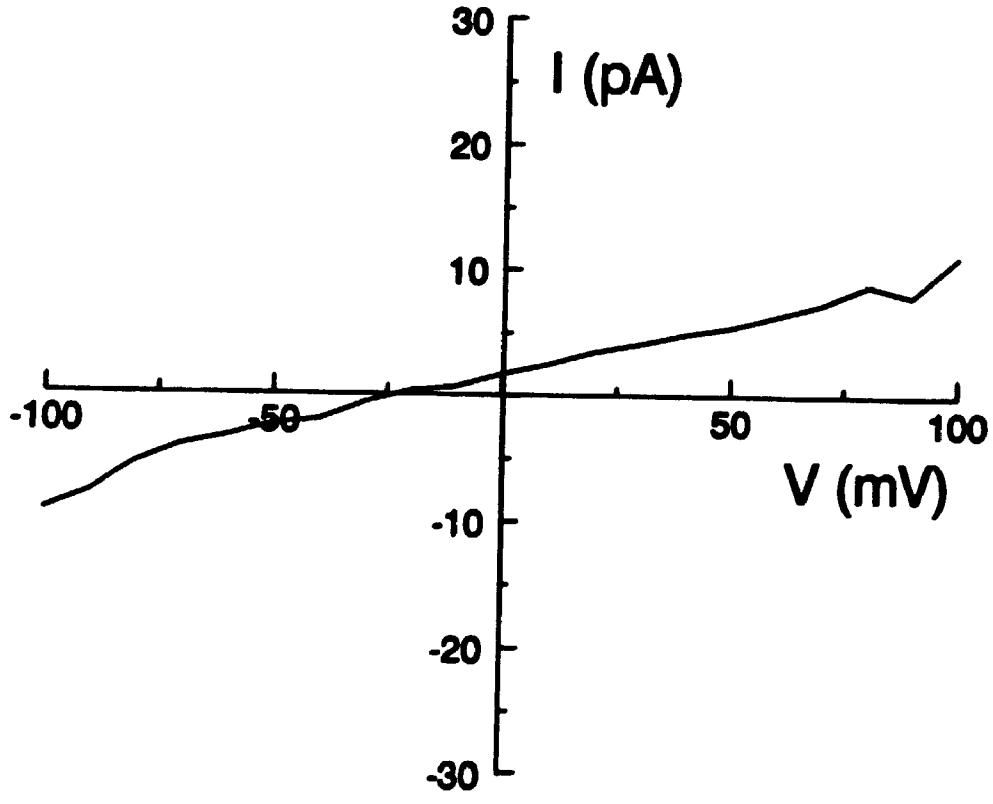

Fig. III-4. Whole-cell currents from a single cuticle-attached NME cell

(A) Single whole-cell current traces in response to 2250 msec voltage jumps (-100 to +70 mV in 10 mV increments) applied from V_H = -30 mV. The arrowhead denotes the zero current level. The currents activated with hyperpolarization are time-dependent taking 2000 msec to reach steady-state. The holding current between pulses was -29 pA. The maximum steady-state current with a -100 mV voltage pulse was -931 pA. The current-voltage relationship for these traces is shown in the upper right. The instantaneous current-voltage relationship (dotted line) was linear. The steady-state (solid line) was non-linear with V_M = 20 mV. The current turns on at about -25 mV in this example. The membrane resistance calculated from the linear portion of the curve (0 to +50 mV) was 1016 MΩ.

(B) Single whole-cell current in response to a voltage ramp (-80 to +80 mV, 1500 msec duration) applied from V_H = -30 mV. The arrowhead denotes the zero current level. The V_M was -12 mV, the holding current between ramps was -33 pA and the maximum activated current was -402 pA. The membrane resistance calculated from the linear portion of the curve at positive voltage was 1960 MΩ. This is the same cell as in **(A)**.

(C) Time-dependent activation of the current following break-in. Currents in response to voltage ramps (as in **(B)**) are shown for 10 sec, 2 min and 5 min following break-in (same cell as in **(A)** and **(B)**. The current was maximal at 5 min and remained at that level for the remaining 15 min of the experiment.

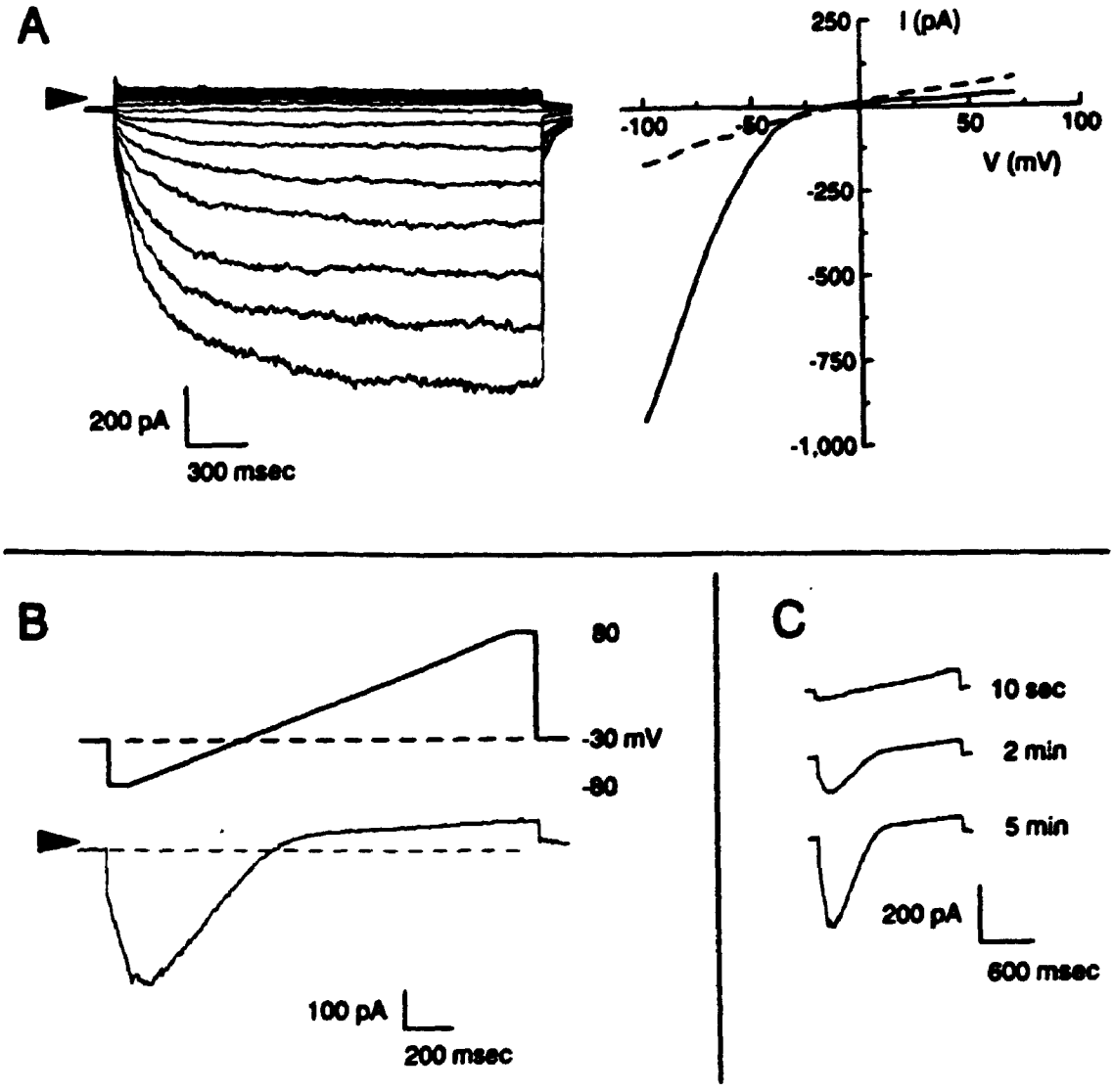
A
250
I (pA)
-100
-50
50
100
V (mV)
-250
-500
-750
-1,000
200 pA
300 msec
B
80
-30 mV
-80
100 pA
200 msec
C
10 sec
2 min
5 min
200 pA
600 msec

III.3.6 Nonjunctional Currents in Newly-Moulted Epidermal Cells

Single NME cells, in contrast to PPE cells, had a nonohmic response to voltage pulses (Fig. III-4A). Large currents (200 to 1000 pA at -100 mV) were activated at voltages less than -13 to -40 mV and were inactive at more depolarizing voltages (Fig. III-4A). During voltage pulses the current turned on in a time-dependent fashion taking ~2 sec to reach steady-state. The response to voltage ramps is shown in Fig. III-4B and the whole-cell recording induction of the current in Fig. III-4C. Upon first whole-cell recording from single NME cells the input resistance was high and the response ohmic (Fig. III-4D). However, within 2.5 to 5 min of break-in a hyperpolarization-activated current began to appear and usually persisted for the duration of the experiment (< 30 min). This suggests that a cytoplasmic component necessary for regulating the current is lost during whole-cell recording, or alternatively the current is activated by differences in osmotic pressure between the pipette and bath solution. The average input resistance calculated from cells before the current activated was 3 ± 1 GΩ (n = 31).

III.3.7 Isolated Cell Pairs are Both Electrically- and Dye-Coupled

In addition to having negative membrane potentials, the presence of functional gap junctions is indicative of live cells with minimal damage since membrane potential, $[Ca^{++}]_i$ and

$[ATP]_i$ affect the gating of gap junctions in the cells of this (see Chapters IV and VI) and other tissues (review: Bennett *et al.* 1991).

Isolated PPE cell pairs were both electrically- and dye-coupled, confirming that functional intercellular junctions survive the dissociation procedure. Carboxyfluorescein transfer (Fig. III-5) was detected between 44% of PPE cell pairs studied (n = 34) and junctional currents (Fig. III-6A) were detected in 70% of the successful recordings. The mean initial junctional conductance (G_j) in PPE cell pairs (calculated by dividing the junctional current by the transjunctional voltage, I_j / V_j) was 11 ± 1 nS (n = 258). A wide range of initial conductances between 0 to 95 nS were found in these cells. In contrast NME cell pairs were very strongly electrically-coupled (Fig. III-6B). Junctional conductances were detected in 100% of NME cell pairs examined with conductances ranging from 31 to 818 nS (n = 88) with a mean of 161 ± 13 nS. Frequency histograms of the initial junctional conductances are shown for PPE and NME cell pairs in Fig. III-6C & D.

Occasionally PPE cell pairs that did not appear to be touching (as seen in the light microscope) were electrically-coupled. It is plausible that the cells were in contact via fine cellular extensions or filopodia as this condition could be simulated by gently pulling the cells apart, while whole-cell recording the junctional currents.

Fig. III-5 Dye-coupling in PPE cell pairs

Phase contrast (a) and epifluorescent (b & c) micrographs of dye-transfer in a PPE cell pair. Carboxyfluorescein (10 mM) was applied through a single patch-pipette (extending from the left in (a). (b) was taken 2 sec and (c) 45 sec following rupture of the patch of membrane in the pipette. Scale bar, 10 μm.

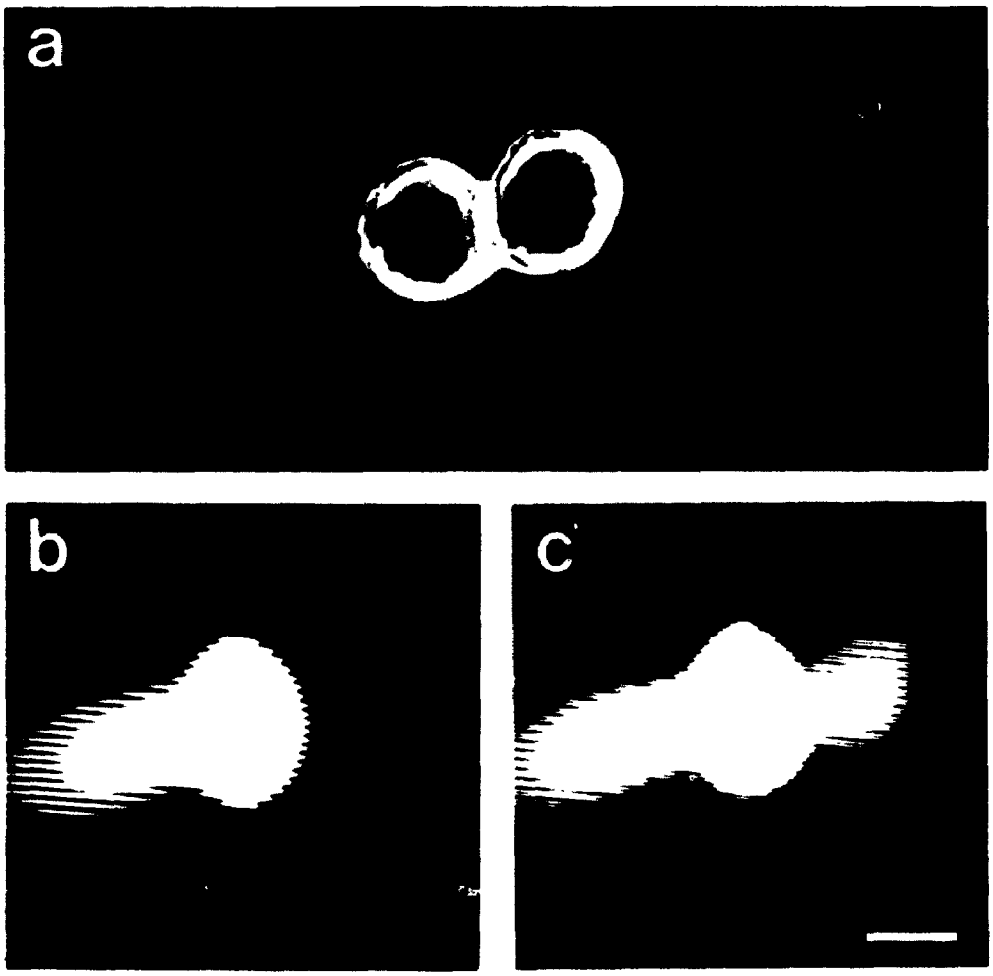
a
b
c

Fig. III-6. Junctional currents in PPE and NME cell pairs

(A) & **(B)** Examples of junctional currents just after break-in in **(A)** PPE and **(B)** NME cell pairs. Voltage (V_1 & V_2) and current (I_1 & I_2) traces for both cells are shown. Junctional currents were generated by applying 1 sec 20 mV transjunctional voltage pulses at 0.5 Hz in alternating fashion to both cells. Holding voltages are -50 mV in **(A)** and -30 mV in **(B)**. Lower holding voltages were used in NME cell pairs to reduce the contribution of nonjunctional currents.

(C) & **(D)** Distribution of the initial junctional conductances in PPE **(C)** and NME **(D)** cell pairs. These data show that nearly all NME cell pairs are extremely well coupled ranging from 31 to 818 nS; (mean: 161 ± 13 nS; n = 88) relative to PPE cells which display a range of initial junctional conductances from 0 to 95 nS (mean: 11 ± 1 nS; n = 258).

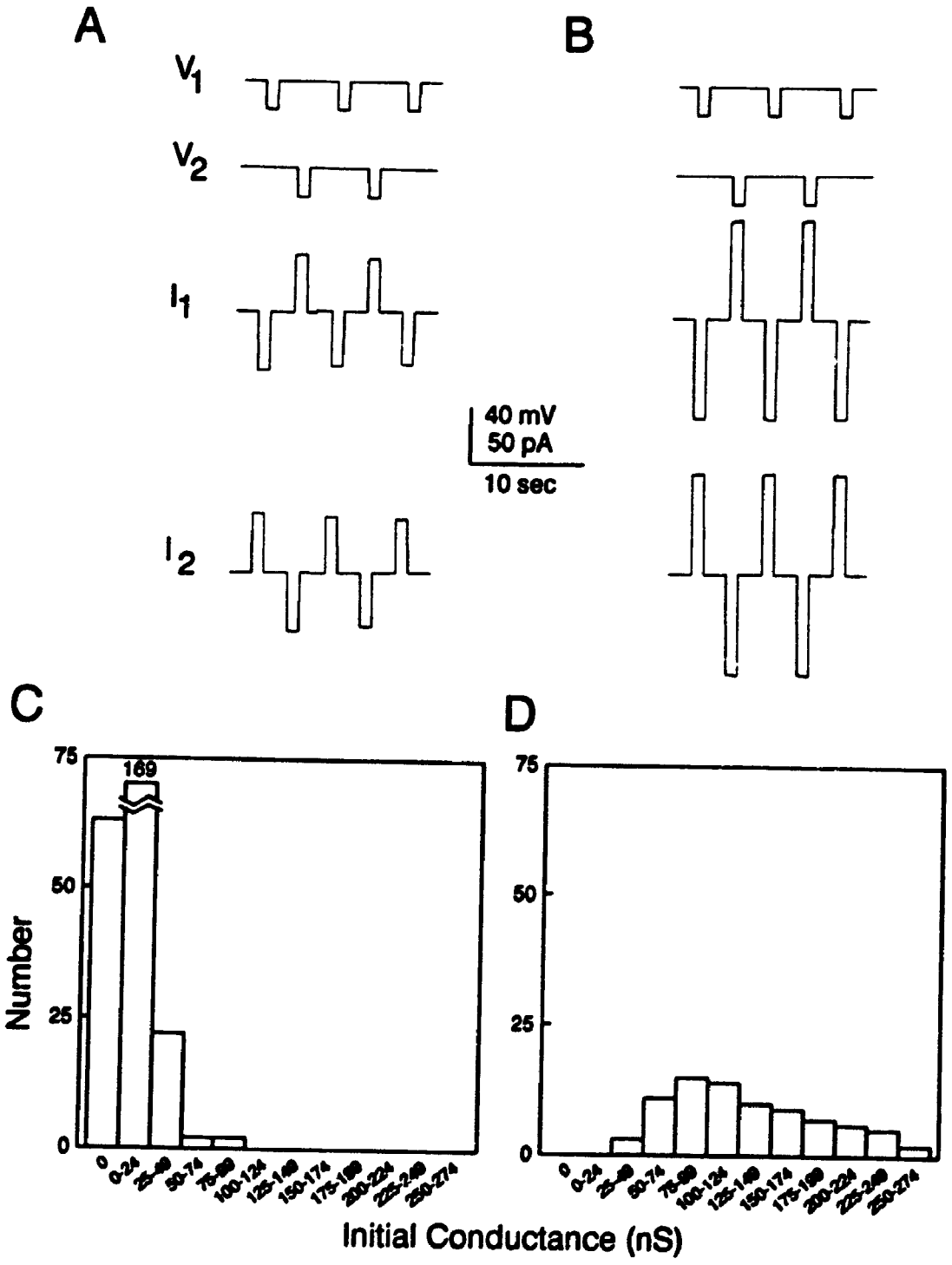
A
B
V1
V2
I1
I2
40 mV
50 pA
10 sec
C
D
75
50
25
0
169
Number
0
0-24
25-49
50-74
75-99
100-124
125-149
150-174
175-199
200-224
225-249
250-274
Initial Conductance (nS)

III.3.8 Sensitivity of Junctional Currents to Volatile Anaesthetics

Several volatile anaesthetics, lipophilic compounds known to close gap junctions in many cells (Johnston *et al.* 1980; Burt & Spray 1989; Burt 1991), were used to demonstrate that these junctional currents were indeed passing through gap junctions and not cytoplasmic bridges, which are unaffected by these compounds (Bukauskas *et al.* 1992). 1-Octanol (1 mM), 1-heptanol (2 mM) and halothane (10 mM) (Sigma) (added directly to TBS and shaken vigorously for 1 min just prior to use) rapidly and reversibly-uncoupled PPE cell pairs when perfused into the bath (Fig. III-7A). The rates of uncoupling were the same for all compounds (at these concentrations) with lower concentrations failing to uncouple the cells. Octanol and heptanol but not halothane sometimes harmed the cells after repeated or prolonged exposure.

III.3.9 Sensitivity of the Hyperpolarization-Activated Nonjunctional Current in Newly-Moulted Cells to a Volatile Anaesthetics

Since this large nonjunctional current was activated by voltages at which GJ channels are most active (Chapter VI), a means of blocking this current is necessary if these cells are to be used for single GJ-channel studies. Since many nonjunctional-ion channels are inhibited by halothane (Johnston *et al.* 1980; Burt & Spray 1989; Burt 1991) and since junctional currents in NME cell pairs are so large, the

Fig. III-7. Inhibition of junctional and nonjunctional currents with volatile anaesthetics

(A) Inhibition of junctional currents in PPE cell pairs. Voltage (V_1 & V_2) and current (I_1 & I_2) traces for a PPE cell pair are shown. The pulsing protocol is as described for Fig. III-6 with the holding voltage at -50 mV. When the bath was perfused continuously (4 to 6 ml/min) with 1 mM octanol (OCT) during the horizontal bar, complete uncoupling occurred in 1 min, leaving only a small downward nonjunctional current in the pulsed cell (arrowhead). Coupling was completely restored in 2 min upon washout of octanol.

(B) Inhibition of the hyperpolarization-induced nonjunctional current of NME cells with halothane. A train of voltage ramps (-100 to +80 mV) were applied every 10 sec. When the bath was perfused continuously (4 to 6 ml/min) with 10 mM halothane (HAL) during the horizontal bar, the hyperpolarization-gated current (arrowheads) was inhibited. The current was blocked and fully recovered each within 1 min.

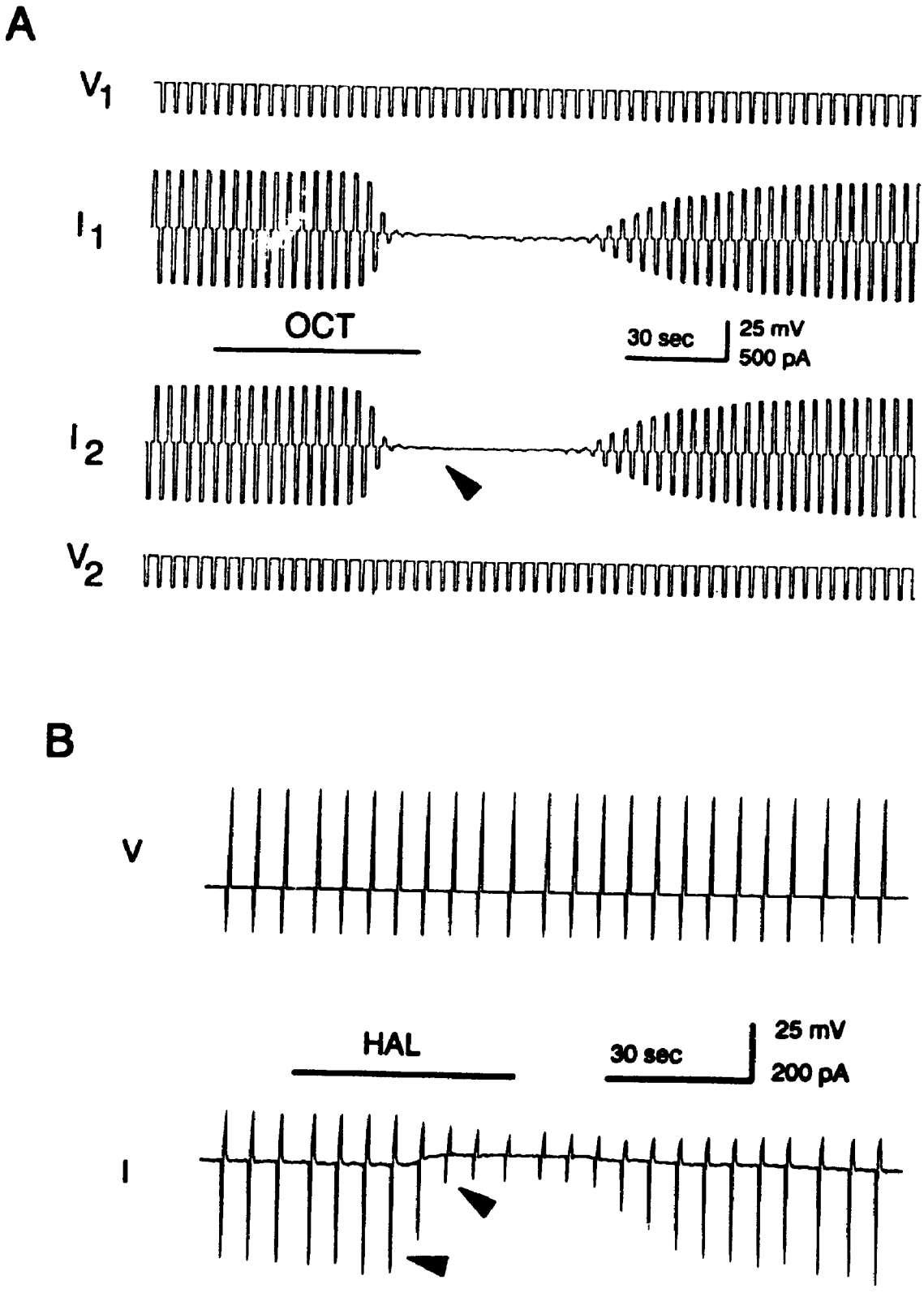
A
V1
I1
OCT
30 sec
25 mV
500 pA
I2
V2
B
V
HAL
30 sec
25 mV
200 pA
I

possibility was explored that halothane inhibition of the nonjunctional current in NME cells might both reduce junctional currents to that of a few channels and eliminate the background noise created by the nonjunctional current. Fig. III-7B shows that the hyperpolarization-activated nonjunctional current in NME cells is indeed reversibly blocked by halothane at the concentrations that are effective at reducing junctional currents in PPE cells (10 mM). The time course of block and recovery are similar to those for gap junctional currents.

III.4 Discussion

This chapter describes two techniques that were developed to isolate epidermal cells suitable for whole-cell voltage-clamp recording. These cells are suitable for whole-cell recording and have functional gap junctions.

III.4.1 Cell Isolation

The results of digestion of basal lamina with collagenase differs from earlier enzymatic studies of other insect tissues in which elastase was used to remove the basal lamina (Levinson & Bradley 1984; Koefoed 1987). It would appear that collagen and not elastin is the major component of the basal lamina in *Tenebrio* epidermis. Though elastase had little effect on the epidermal basal lamina, prolonged incubation loosened the epidermal sheet from the cuticle, suggesting the presence of elastin or elastin-like components in the connective tissue between the epidermis and cuticle.

Completely isolated PPE cells sometimes underwent changes in morphology within several hours after isolation, including a change from a spheroid to a flattened shape. In addition, epidermal cells were often electrically-coupled even though they did not appear to be touching suggesting that the cells were linked by fine cytoplasmic processes. Coupling via filopodia has been described in *Xenopus* embryos (Loewenstein *et al.* 1978) and neonatal rat heart cells (Rook *et al.* 1988). This isolated PPE cell preparation may be useful for studying epidermal cell behaviour *in vitro* since spreading and the formation of cellular processes have been observed for epidermal cells in undissociated epidermis from *Rhodnius* during wounding (Wigglesworth 1937), in the epidermal cell-assisted migration of tracheoles (Wigglesworth 1959; Wigglesworth 1977) and after enzymatic digestion of the basal lamina (Locke 1987). In *Calpodes* epidermis, enzymatic dissociation of cell-to-cell contacts induces filopodia formation (Locke 1987). It is possible that GJ formation at the end of filopodia is a significant form of communication between separated cells.

III.4.2 Isolated Cells Meet the Criteria for Whole-Cell Recording

In the introduction to this chapter several limitations to recording single-channel activity from whole cells were outlined. The average input resistance in PPE cell pairs is 14 GΩ. This translates into a maximal holding current of a few

pA, suggesting that single-channel currents should be easily resolved. In addition to a high input resistance, PPE cells responded ohmically to voltage pulses indicating that the pipette solutions and recording techniques used in this study did not activate voltage-gated currents. This condition is useful in studies of macroscopic junctional voltage dependence since there is little doubt that the observed voltage-dependent currents are junctional. In a variety of cell types pharmacological means have been necessary to reduce or eliminate large nonjunctional conductances (McMahon *et al.* 1989; Rüdisüli & Weingart 1989; Moore *et al.* 1991). This treatment may introduce undesirable side effects. In contrast to PPE cells, NME cells had a similar high input resistance (1 to 8 GΩ) however, soon after the start of recording a large hyperpolarization-activated current developed. The presence of this current would increase background current noise for single GJ-channel recording besides complicating V_M-dependence studies on gap junctions.

For single-channel activity to be recorded only a few channels should be active between cell pairs. This condition is met in PPE cells as many cell pairs were poorly-coupled at the start of recording (probably due to the harshness of the isolation method). Two other methods that can be used to reduce junctional conductance in PPE cell pairs include exposure to volatile anaesthetics (discussed below) and spontaneous uncoupling (Chapter IV). In NME cells all isolated

cells were very well-coupled, thus it is impossible to detect single-channel currents without using harsh methods to artificially reduce conductance. Conveniently, the hyperpolarization-activated nonjunctional current in these cells is blocked by halothane therefore 10 mM halothane treatment could be used in these cells to reduce the current contributions from both junctional and nonjunctional sources. Spontaneous uncoupling does reduce junctional currents in these cells (Chapter IV), however, not to levels where single-channel currents can be observed.

III.4.3 Benefit of Isolating Cells From Different Epidermal Stages

The initial intention in isolating cells from different stages in the moult cycle was not to carry out developmental studies. Tissue from the different stages were selected for technical reasons; PPE cells were naturally free of cuticle and their reduced intercellular contacts made it easier to completely isolate cells, and NME cells were well-attached to the cuticle (necessary for scraping). However, these isolated cell preparations would be useful for examining developmental changes in both junctional and nonjunctional electrical properties of epidermal cells. It is possible to use the scrape technique to isolate cells from any larval instar or stage in the moult cycle. Indeed the results presented here suggest that the hyperpolarization-activated nonjunctional current in NME cells was not present in PPE cells and thus may

be regulated during development.

In subsequent chapters of this thesis PPE and NME cells were used for different studies. Often this was because each preparation had particular advantages. PPE cell pairs were best for studying single GJ-channel properties because single-channel activity was easier to obtain under a variety of conditions. Furthermore, since PPE cells lack the hyperpolarization-activated nonjunctional currents found in NME cells these were best used for studying junctional voltage dependence. However, because of the variable nature of the extent of coupling in PPE cells and the small numbers of cell pairs that could be isolated on any given day, PPE cells were not suitable for studying the effects of modulators of gap-junctional conductance. NME cell pairs, however, were ideal for this since unlimited numbers of well-coupled cell pairs were isolated. This was probably due in part to the less disruptive isolation technique.

III.4.4 Volatile Anaesthetics

Volatile anaesthetics uncouple epidermal cell pairs and also knock out the hyperpolarization-activated nonjunctional current. These compounds have been shown to uncouple all gap junctions studied (*e.g.* Johnston *et al.* 1980; Terrar & Victory 1988; Burt & Spray 1989; Nakahiro *et al.* 1989; Niggli *et al.* 1989) and have been used by many investigators to reduce junctional coupling so that single GJ-channel activity may be revealed (*e.g.* Burt & Spray 1988b; Somogyi & Kolb 1988;

Rüdisüli & Weingart 1989; Spray *et al*. 1991b). These compounds are presumed to act by reducing channel activity by disrupting normal channel-lipid interaction (Burt & Spray 1989; Burt 1991; Takens-Kwak *et al*. 1992) although other mechanisms are under investigation (Peracchia 1991). These anaesthetics also block (*e.g*. Nakahiro *et al*. 1989) or activate (*e.g*. Yang *et al*. 1992) a variety of nonjunctional-ion channels.

Although the volatile anaesthetic concentrations used in this study cannot be precisely determined, consistent results were obtained by adding the compound at the stated concentrations directly to the bath saline immediately before use. It was likely that the effective concentrations used in this study are comparable to those used in other studies on gap junctions where concentrations less than 10 mM were shown to be effective. Halothane appeared to be the best choice for use on the epidermis since it did not harm the cells after prolonged or repeated exposure.

In summary, new methods have been developed for isolating epidermal cells from different stages in the larval moult cycle. These preparations are suitable for whole-cell voltage clamping of single cells and cell pairs. Functional gap junctions that are sensitive to volatile anesthetics survive the isolation procedure. PPE and NME cells have large input resistances and negative membrane potentials. During recording a hyperpolarization-activated and time-dependent current develops in NME cells that reduced their suitability for

voltage-dependence and single GJ-channel studies. PPE cells are especially useful for studying single GJ-channels and NME cells for studying gap junction modulation at the macroscopic level since many well-coupled cells can be isolated.

IV SPONTANEOUS UNCOUPLING AND ATP-DEPENDENT MODULATION OF MACROSCOPIC JUNCTIONAL CONDUCTANCE

IV.1 Introduction

A condition necessary for whole-cell recording of single GJ-channel activity (discussed in Chapter III) is that junctional conductance be reduced to very low levels. This has been accomplished in some vertebrate cell types by taking advantage of an artifact induced by whole-cell recording (Neyton & Trautmann 1986a; Somogyi & Kolb 1988; Cooper *et al.* 1989; Paschke *et al.* 1992). During whole-cell recording a low resistance hole is created in the plasma membrane that connects the pipette solution with the cytoplasm. The pipette solution diffuses into the cell and soluble cytoplasmic constituents diffuse out into the pipette (Pusch & Neher 1988). Under these conditions junctional conductance in some cell types declines to undetectable levels over a period of 20 to 60 min (Somogyi & Kolb 1988; Cooper *et al.* 1989; Paschke *et al.* 1992) and is called 'spontaneous uncoupling' by Somogyi & Kolb (1988).

Spontaneous uncoupling is reduced in several vertebrate cell types by adding ATP to the pipette solution (Somogyi & Kolb 1988; Cooper *et al.* 1989; Sugiura *et al.* 1990; Paschke *et al.* 1992). This finding inspired investigators to examine whether junctional conductance in whole-cell clamped cell pairs could be modulated by a variety of phosphorylating agents. Phosphorylation is known to alter the activity of a

diverse selection of ion channels (review: Levitan 1985). Activators and inhibitors of protein kinase C increased junctional coupling in corpus cavernosum cell pairs (Moreno *et al.* 1993) and decreased it (resp.) in a variety of other vertebrate cells (Chanson *et al.* 1988; Randriamampita *et al.* 1988; Reynhout *et al.* 1992; Münster & Weingart 1993). Agents that increase intracellular cAMP levels generally increased junctional coupling in vertebrate cells (Lasater & Dowling 1985; Burt & Spray 1988a; Somogyi & Kolb 1988; Cooper *et al.* 1989; De Mello 1991; Xiao & De Mello 1991; Paschke *et al.* 1992; Moreno *et al.* 1993), although in some types, it decreased (Laufer *et al.* 1989; Moore *et al.* 1991; Sakai *et al.* 1992). Agents affecting cGMP levels decreased junctional conductance in neonatal rat cell pairs (Burt & Spray 1988a; Takens-Kwak & Jongsma 1992).

Direct phosphorylation of vertebrate gap junction proteins by protein kinases has been described in rat hepatocytes (Saez *et al.* 1986; Traub *et al.* 1987), and for connexin43 (Musil *et al.* 1990; Laird *et al.* 1991; Musil & Goodenough 1991; Lau *et al.* 1992; and reviews: Loewenstein 1986; Musil & Goodenough 1990; Stagg & Fletcher 1990).

Another possible mode of action of ATP on coupling is by direct binding to junctional channels. Activation or inactivation of nonjunctional-ion channels by direct binding of ATP or cyclic nucleotide monophosphates to channels is widely reported (reviews: Latorre *et al.* 1991; Nichols &

Lederer 1991; Standen 1992). One study on guinea pig cardiac cell pairs suggests that ATP acts directly on GJ channels and not via an intermediate enzymatic step (Sugiura *et al*. 1990).

In this chapter, spontaneous uncoupling in insect epidermal cells is investigated as a possible tool for studying GJ-channel activity. In addition, an examination of uncoupling kinetics provides additional insight into epidermal GJ-channel gating. ATP partially inhibits spontaneous uncoupling between epidermal cells as reported in vertebrate cells. The role of ATP in this action was probed using nonhydrolysable ATP analogues to test whether ATP acts via an enzyme-dependent or independent mechanism. An enzymatic mechanism was supported, therefore, ATP may be required to maintain functional coupling by acting as a substrate for phosphorylation of gap junctions. Since many inhibitors have become available for common second messenger operated kinases a rapid screening method was developed to detect the presence of electrical coupling within small groups of NME cells exposed to a variety of inhibitors (the 'capacitance measuring technique'). This technique may be used to easily test the uncoupling effects of many compounds (*e.g.* anti-gap junction monoclonal antibodies). Several possible mechanisms of ATP action in maintaining open gap-junctional channels are discussed.

IV.2 Materials and Methods

IV.2.1 Chemicals and Solutions

The chemicals used in this chapter obtained from Sigma (St. Louis, Missouri) were: adenosine 5'-triphosphate, disodium salt, (ATP; A2383); 5'-adenylylimidodiphosphate, monolithium salt (AMP-PNP; A2647); alkaline phosphatase (type VII-NLA, P0655); apyrase (A7646); chlorpromazine (C8138); guanosine 5'-triphosphate, monosodium salt (GTP; G8877); iodoacetate (I2512); N-ethylmaleimide (E3876); polymyxin B sulfate (P1004); staurosporin (S4400); Walsh Inhibitor (P5015).

The chemicals obtained from Boehringer Mannheim (Montreal, Quebec) were: acid phosphatase (108219); adenosine 5'-O-(3-thiotriphosphate), tetralithium salt (ATPγS; 102342).

The chemicals obtained from Calbiochem (La Jolla, California) were: bisindolylmaleimide (203290); calmidazolium (208665); D-erythr-sphingosine (567725); genistein (345834); H-7 (371955); H-89, (371963); KN-62 (422706); KT-5823 (420316).

Dimethylsulfoxide (DMSO) was obtained from Aldrich (27585-5, Milwaukee, Wisconsin).

All compounds were made up in ATP-free TPS to the indicated concentrations (before pH adjustment) except for calmidazolium, KN-62, staurosporin, bisindolylmaleimide, D-erythrosphingosine, genistein and KT-5823 which were first dissolved in DMSO and then diluted to the final

concentrations. The final concentration of DMSO ranged from 1 to 5% (vol/vol). Up to 5% DMSO did not uncouple cell groups as measured with the capacitance technique.

TPS with raised Ca^{++} or Mg^{++} concentrations was made by adding additional $CaCl_2$ or $MgCl_2$ to TPS before adjusting the pH. Therefore, 2 mM and 5 mM extra $CaCl_2$ was added to make the 0.7 μM and 2.6 μM free Ca^{++} solutions respectively. A public domain computer program (CaBuffer) that was written by Dr. Jochen Kleinschmidt and obtained from Dr. Stephen Sims (Dept. Physiology, U.W.O.) was used to calculate the free $[Ca^{++}]$ in the solutions. These calculations adjusted for pH, temperature and ionic strength. The values used for each of these were pH 6.7, 25°C and 0.4 mol/L, respectively.

IV.2.2 Capacitance Monitoring In Cell Groups

Groups of cuticle-attached NME cells were prepared using the scrape technique (Chapter III). One cell in the middle of the group was voltage clamped using standard whole-cell recording. A train of hyperpolarizing 10 mV voltage pulses were applied (0.05 Hz) and the capacitive spike monitored on the computer screen. For this the TWOCELL program (Appendix 3) was used to deliver pulses and then automatically store a capacitive spike to a Pclamp compatible file every three minutes for off-line analysis. The length of the pulse was varied from 25 to 150 msec so that the capacitive current reached steady-state. Complete uncoupling was recognized as the development of a smaller rapidly decaying capacitive spike

Fig. IV-1. Capacitance technique for monitoring conductance in small groups

A capacitive spike is shown from a cell group having ~30 cells before (**A**) and after (**B**) complete uncoupling. I_L represents the leak current (*i.e.* steady-state holding current during the pulse), and I_P the peak current of the capacitive spike. In coupled cell groups the area of the capacitive spike is large: 493 pF in this example, consistent with a cell group of ~37 cells calculated using the single cell capacitance of 13.2 pF from the trace in (**B**). Upon complete uncoupling the capacitive spike has a reduced area, I_P, I_L and a fast decay reflecting the capacitance of a single cell. (this example was taken from a cell group uncoupled with 11 mM ATPγS, the traces are from 30 sec (**A**) and 30 min (**B**) following break-in.

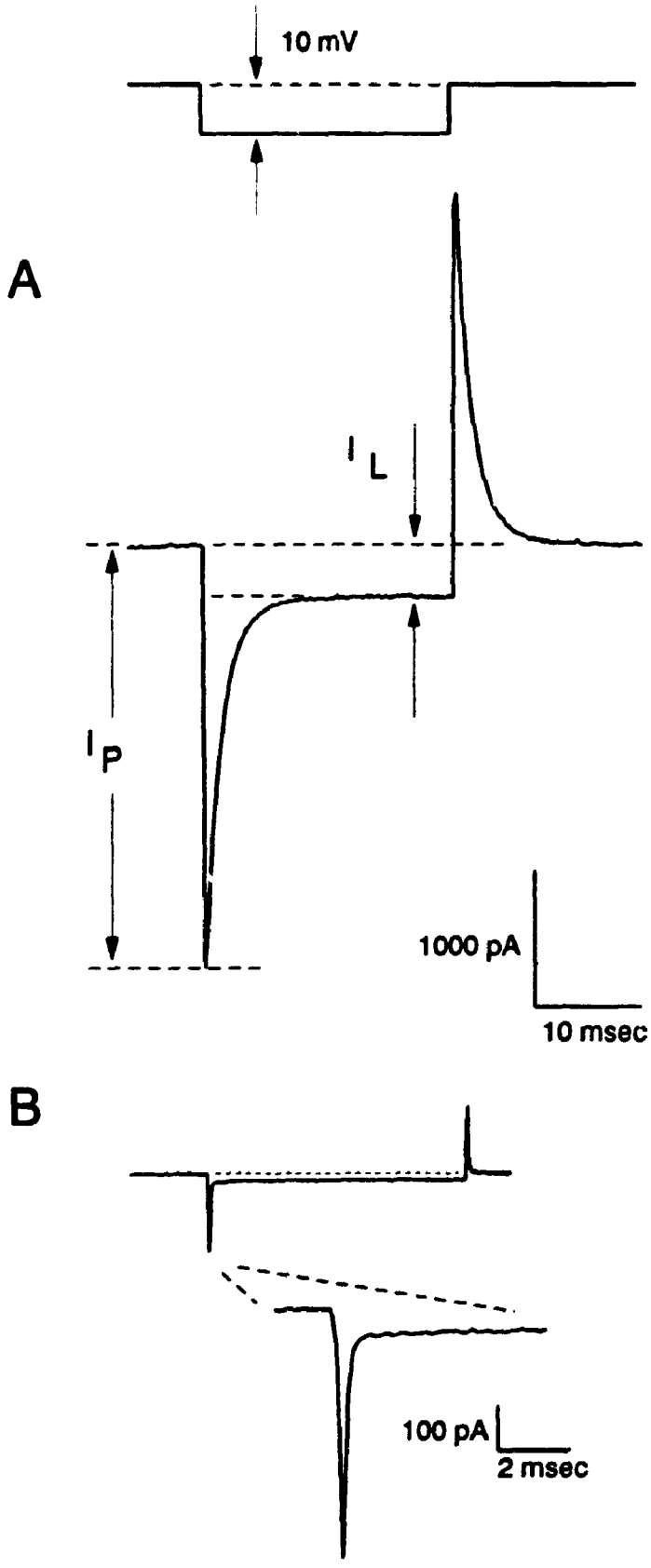
10 mV
A
I_L
I_P
1000 pA
10 msec
B
100 pA
2 msec

that corresponded to the capacitance of a single cell (Fig. IV-1). Sudden drops in the peak of the capacitive spike usually indicated pipette clogging and mouth suction was applied to improve series resistance. The holding voltage was maintained at the zero current level (*i.e.* the membrane potential) by switching the amplifier to search mode. The time constant of the search response was slow enough not to affect the capacitive spike while maintaining the holding voltage at zero current. Data were filtered at 10 to 20 kHz.

IV.3 Results

IV.3.1 Spontaneous Uncoupling in PPE Cell Pairs

The mean initial G_j in 258 cell pairs was 10 ± 1 nS ranging from 0 to 95 nS (Chapter III). Single-channel activity was observed immediately after break-in in 4% of these cell pairs, while 24% of the pairs were completely uncoupled. For these measurements the potentials of both cells were held at -50 mV (*i.e.* V_H = -50 mV) and depolarizing 20 mV pulses were applied to one cell or hyperpolarizing 20 mV pulses were applied alternately to both cells. Well-coupled cell pairs rapidly uncoupled following break-in when ATP-free pipette solution was used (Fig. IV-2A). As I_j dropped and the amplifier gains were increased, open-close events of single GJ-channels were detectable as spontaneous and quantal changes in the recorded currents (I_1 and I_2) that were equal in magnitude but opposite in sign (Fig. IV-2A). To observe single-channel activity, the pulsing was stopped and V_j set at

Fig. IV-2. Spontaneous uncoupling in PPE cell pairs and inhibition of spontaneous uncoupling by ATP

(A) An example of spontaneous uncoupling. Current (I_1 & I_2) and voltage (V_1 & V_2) traces are shown (compressed time scale) from a cell pair without ATP in the pipette solution. Voltage pulses (1 sec, 20 mV, 0.3 Hz) were applied to cell 1 with V_H = -50 mV for both cells. Bars between the current traces indicate changes in amplifier gain. Initial I_j = 180 pA (G_j = 9 nS) declined to the 5 pA current (γ_j = 250 pS) representative of single channels within 10 min. A constant V_j with a reversed polarity of 20 mV (V_1 = -50 mV, V_2 = -30 mV) was used to monitor the spontaneous and quantal behaviour of the single-channel events at the end of the current traces. The data for the figure were sampled from tape at 15 Hz.

(B) Stabilization of junctional conductance in PPE cell pairs by 5 mM ATP in the pipette solution. G_j (I_j / V_j) from 12 cell pairs without ATP in the pipette were normalized to the initial G_j and graphed against time after break-in (■). Data points at one min intervals are shown. Cell pairs rapidly uncoupled with a time after break-in to a 50% loss of G_j (G_{j50}) of 7.5 min. When 5 mM ATP was added to the pipette solution spontaneous uncoupling was inhibited (●). G_j gradually decreased with time (G_{j50} = 37 min) but never to the conductance level at which single-channel events were observed (n = 8 cell pairs). The initial G_j was > 10 nS in all cell pairs used in this graph.

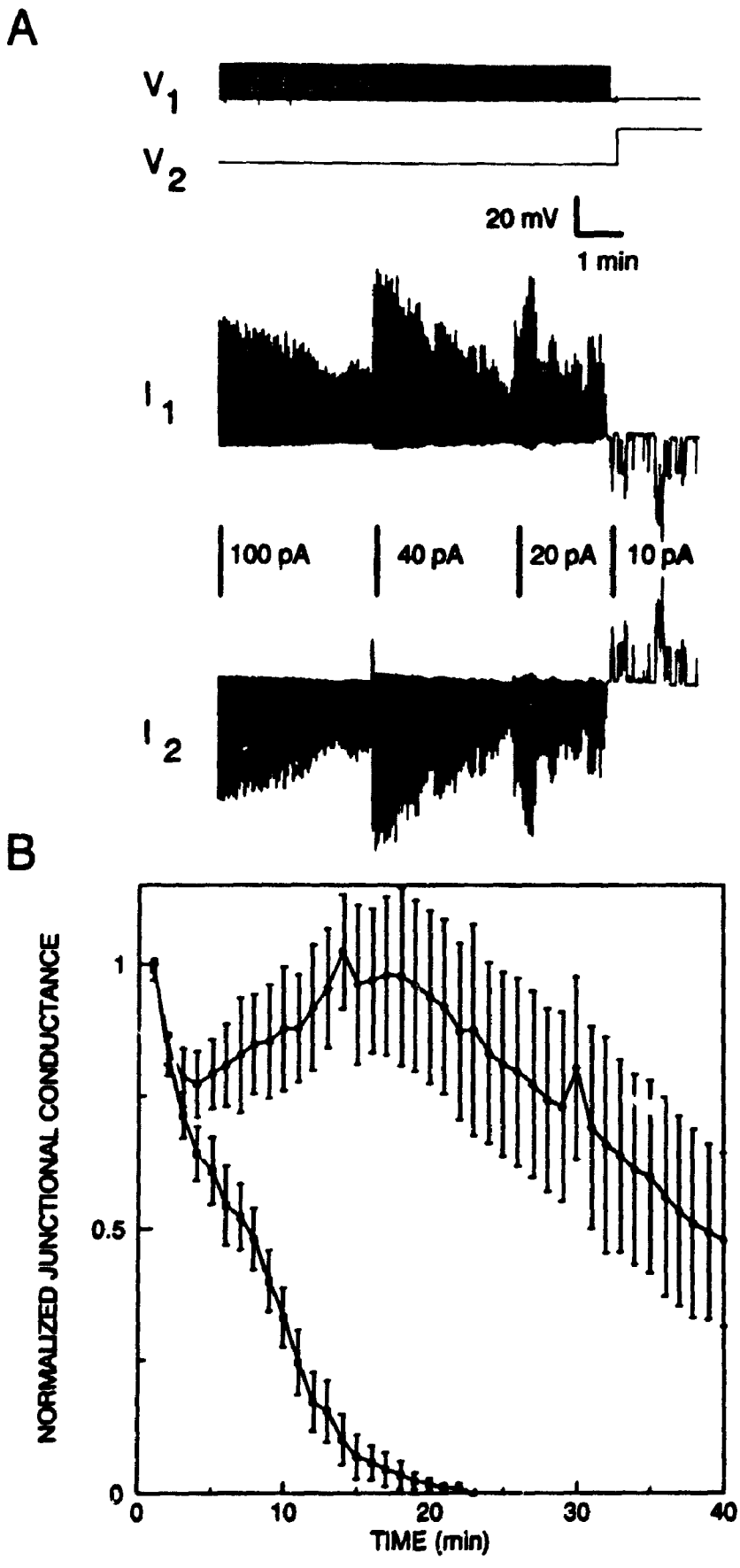
A
V1
V2
20 mV
1 min
I1
100 pA
40 pA
20 pA
10 pA
I2
B
NORMALIZED JUNCTIONAL CONDUCTANCE
1
0.5
0
0
10
20
30
40
TIME (min)

a constant level. Channel activity lasted < 10 min once detected. The mean half-time to complete uncoupling (to the level of observing single-channel events) for 12 cell pairs (with initial G_j > 10 nS) was 7.5 min (Fig. IV-2B). Another way to express this is as 7.5 min after break-in to a 50% loss in junctional conductance (*i.e.* G_{j50}).

IV.3.2 Inhibition of Spontaneous Uncoupling in PPE Cell Pairs by ATP

Since 'rundown' of G_j (*i.e.* spontaneous uncoupling) has been explained in some vertebrate cell types to be due to washout (Neyton & Trautmann 1986a; Somogyi & Kolb 1988), the effect on G_j of ATP in the pipette solution was tested. 5 mM ATP (with 2 mM added $MgCl_2$) in the pipette solution substantially inhibited rundown with G_j slowly decreasing to a little less than 50% in 30 min (Fig. IV-2B). The G_{j50} for the average curve was 37 min. G_j often increased within minutes of break-in suggesting that 5 mM ATP may have been higher than endogenous levels in those cells. G_j in well-coupled ATP-loaded cell pairs never dropped to the single-channel level. In four cell pairs with ATP in the pipette solution the initial G_j was < 2 nS and single-channel events were observable immediately after break-in. These were used in Chapter V to study single-channel properties.

IV.3.3 Spontaneous Uncoupling in NME Cell Pairs

When monitoring the kinetics of uncoupling in PPE cell pairs the between experiment variation was high (note the size

of the standard error bars of the ATP curve Fig. IV-2B). To reduce the effects of this variability NME cell pairs were used. Many more well-coupled NME cells can be isolated compared to PPE cells, thus increasing the sample size. In addition, series resistance was monitored throughout the experiment and junctional conductance measurements corrected for these errors.

Junctional conductance was found to decline following break-in as seen in PPE cell pairs (Fig. IV-3A). The G_{J50} was 4 min. Single-channel activity was not observed in NME cell pairs as in PPE cell pairs since the cells remained coupled more than 30 min. This is probably due to the higher initial levels of coupling in NME *vs* PPE cell pairs since the rates of uncoupling (G_{J50} = 4 and 7.5 min respectively) were similar. A few recordings in NME cell pairs lasted long enough (> 35 min) to reach about 2 nS junctional conductance; the background current noise was too large, however, to clearly discern GJ-channel activity. This is possibly due to a hyperpolarization-activated current in NME cells (Chapter III). Also, with long experiments the gigaohm-seals may start to degenerate and series resistances increase (due to pipette clogging or manipulator drift) thus increasing background noise or prematurely ending the experiment.

IV.3.4 ATP Analogues Do Not Mimic ATP Effects

The presence of 5 mM ATP in the pipette solution significantly slowed spontaneous uncoupling in NME cell pairs

Fig. IV-3. Mechanism of ATP inhibition of uncoupling involves enzymatic hydrolysis of ATP

Data for these results were generated and analysed as for the results in Fig. IV-4 except that alternating transjunctional voltage pulses were used and data for 5 min intervals are shown.

(A) Spontaneous uncoupling in NME cell pairs and stabilization of G_j by 5 mM ATP added to the pipette solution. NME cell pairs rapidly uncoupled with G_{j50} = 4 min (n = 10) when ATP was not present in the pipette solution (CON, ■). Although the rate of uncoupling was faster than in PPE cells (G_{j50} = 7.5 min) single-channel events were never observed. Conductance remained above 2 nS for up to 40 min after break-in these cells whereas single-channel events were observed by 15 to 20 min in PPE cells and complete uncoupling was observed soon after. When 5 mM ATP was added to the pipette solution spontaneous uncoupling was inhibited (●). G_j declined more slowly than in the absence of ATP with G_{j50} = 8.5 min (n = 7 cell pairs). The initial G_j was > 31 nS in all cell pairs used in this graph. The difference between these two curves is statistically significant ($p > 0.05$).

(B) AMP-PNP (●) and ATPγS (■) do not mimic the effect of ATP. When 10 mM of either of these compounds were added to the pipette solution instead of ATP the uncoupling curves were statistically insignificant from the control solution without ATP (▲). The G_{j50} for both AMP-PNP (n = 8) and ATPγS (n = 8) was 3.5 min. The difference between each of these curves and the 5 mM ATP curves is statistically significant ($p > 0.05$).

(C) ATP does not act by chelating intracellular free Ca^{++}. When the calculated [Ca^{++}] in the pipette solution was elevated to 0.2 μM (■) the rate of uncoupling in NME cell pairs did not change compared to CON (G_{j50} = 3.5 min). When the calculated [Ca^{++}] was elevated to 2.6 μM (▲) NME cell pairs rapidly uncoupled with a G_{j50} of 1.5 min. To test whether ATP reduced the rate of uncoupling by reducing the free [Ca^{++}]i, 10 mM $MgCl_2$ (●) was added to the pipette solution thus reducing the free ATP levels available for Ca^{++} binding to negligible levels. The added Mg^{++} did not prevent the ATP effect which had a G_{j50} of 8.5 min (n = 6 for each of these curves).

(D) Alkaline phosphatase does not prevent ATP action. The addition of 125 U/ml alkaline phosphatase to the pipette solution in the presence of 5 mM ATP did not increase the rate of uncoupling compared to ATP alone (n = 8).

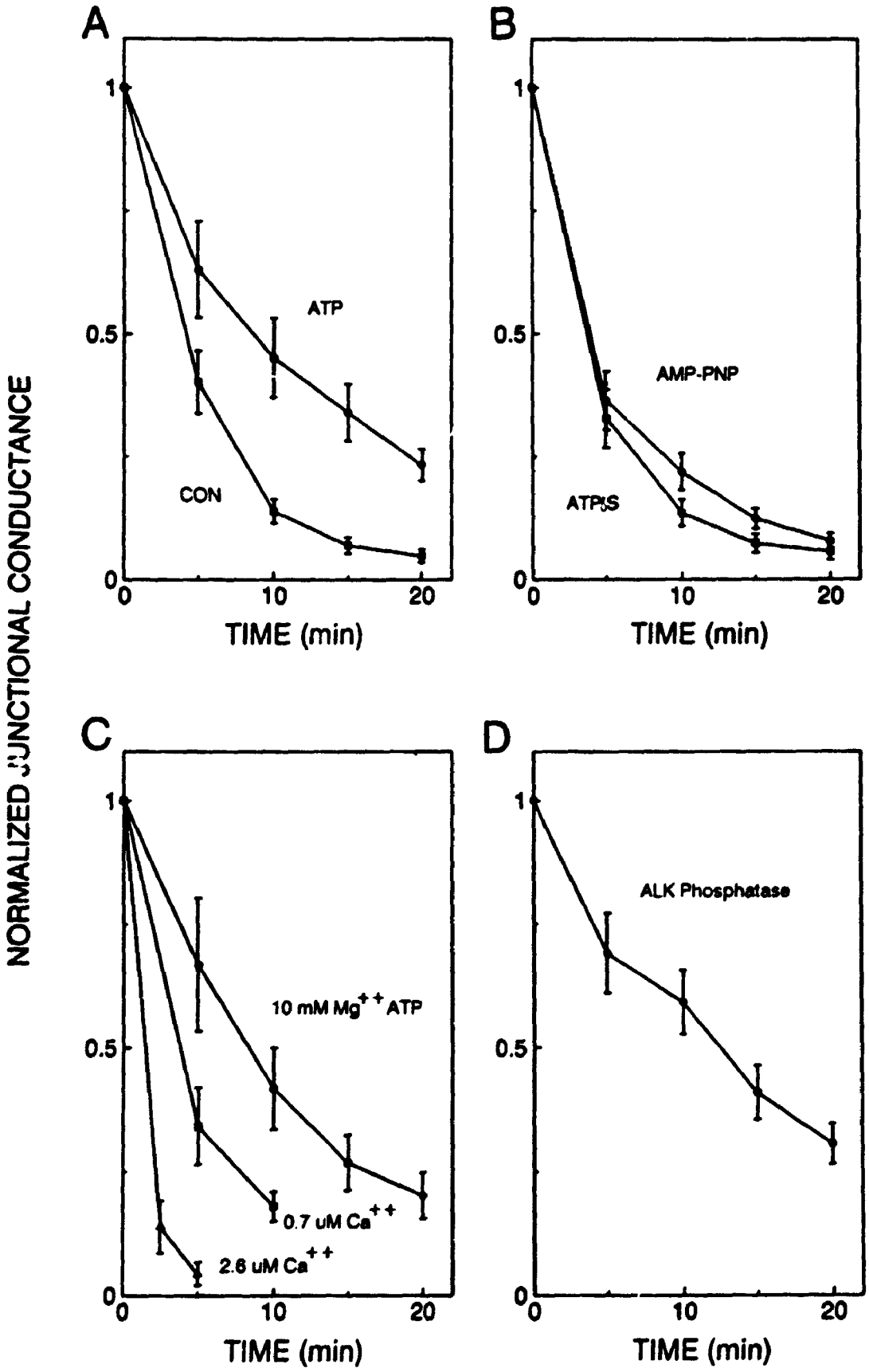
A
B
C
D
NORMALIZED JUNCTIONAL CONDUCTANCE
1
0.5
0
0
10
20
TIME (min)
ATP
CON
AMP-PNP
ATPγS
10 mM Mg++ ATP
0.7 uM Ca++
2.6 uM Ca++
ALK Phosphatase

as seen in PPE cell pairs (Fig. V-3A). The G_{J50} was 8.5 min. This was 4 times less than in PPE cell pairs (G_{J50} 37 min) and may be due to the initial increase in PPE cell pair junctional conductance that occurred prior to its decline or to the difference in the size of the initial conductance.

There are two general mechanisms whereby ATP can act: via direct ATP binding without hydrolysis and/or via an enzymatic step requiring ATP hydrolysis. A direct way to distinguish between ATP-binding and ATP-hydrolysing mechanisms is to test whether nonhydrolysable ATP analogues mimic the action of ATP. Fig. IV-3B shows results obtained by replacing 5 mM ATP with 10 mM ATPγS, a poorly-hydrolysable ATP analogue, and 10 mM AMP-PNP, a nonhydrolysable analogue. With either compound the rate of uncoupling was statistically indistinguishable from ATP-free solution (same effect with 5 mM solutions of each compound). These results suggest that ATP is used in an enzymatic process that maintains coupling.

IV.3.5 ATP Does Not Act by Chelating Intracellular Free Calcium

While attempting to examine the Mg^{++}-dependence of the ATP effect it was accidentally found that subphysiological $[Ca^{++}]_i$ slowed spontaneous uncoupling in a manner similar to ATP (data not shown). Although the mechanism is unknown it is possible that ATP might act by chelating excess free Ca^{++} in the normal pipette solution and resulting in an error in data interpretation that has been uncovered for a Ca^{++}-activated K^+

channel (Klöckner & Isenberg 1992). Fig. IV-3C shows that increasing $[Ca^{++}]_i$ to 2.6 μM rapidly uncouples NME cell pairs. To exclude the possibility that ATP chelates Ca^{++}_i, 10 mM $MgCl_2$ was added to the 5 mM ATP pipette solution, thus reducing the calculated free noncation-bound [ATP] to negligible levels (300 μM). 5 mM ATP + 10 mM $MgCl_2$ prevented uncoupling as did 5 mM ATP + 2 mM $MgCl_2$, suggesting that ATP does not act by chelating Ca^{++}_i. Since reducing $[Ca^{++}]_i$ changes the rate of spontaneous uncoupling, the Mg^{++}-dependence of the ATP effect was not examined, as it is technically difficult to reduce $[Mg^{++}]_i$ without affecting $[Ca^{++}]_i$. These experiments should be done by measuring the actual free Ca^{++} and Mg^{++} concentrations at least in the pipette and bath solutions if not directly in cytoplasm.

IV.3.6 Alkaline Phosphatase Does not Inhibit ATP Action

The possibility that ATP is a substrate for phosphorylation was explored by adding alkaline phosphatase to the pipette solution. Coupling may be maintained in normal cells by the phosphorylation of gap junctions themselves or of a nonjunctional protein in any cellular process that may in turn affect gap junctions. Alkaline phosphatase (125 U/ml) did not uncouple NME cell pairs since the rate of spontaneous uncoupling was not increased when it was added to the pipette solution together with the ATP (Fig. IV-3D).

IV.3.7 Capacitance Monitoring In Cell Groups

The NME cell pair isolation method had yet to be

developed when the ability of ATP to delay spontaneous uncoupling was first discovered. To test if ATP acted via phosphorylation a rapid screening technique was developed for monitoring the presence of coupling in cell groups (Fig. IV-1). Basically, groups of 10 to 50 NME cells were created using the scrape technique (Chapter III) and standard whole-cell recording techniques were used to record from one of the cells in the middle of the group (Chapter II). The capacitance was monitored for 30 to 60 min with a train of voltage pulses. In a well-coupled group of cells the capacitance is very large and when the recording cell uncouples from the group the capacitance drops to a value corresponding to that of a single cell. The pipette solution included inhibitors of protein kinases or other compounds which were tested for their ability to uncouple completely the cell under study from its neighbours.

Capacitance traces from a group of cells that completely uncoupled is shown in Fig. IV-4. Agents known to uncouple insect gap junctions such as octanol (Chapter III), iodoacetate (Lees-Miller & Caveney 1982) and N-ethylmaleimide (Politoff *et al.* 1969) were used as positive controls. A result with iodoacetate is shown in Fig. IV-4. The capacitance at the start of recording is large (376 pF). At 6 min capacitance is still large (302 pF) but by 18 min the capacitance in the iodoacetate-treated cell group reduced to 10.4 pF, typical of a single cell. Similar results were

Fig. IV-4. Use of the capacitance measurement technique to monitor uncoupling by an agent known to uncouple epidermal cells.

Iodoacetate (IAA), an agent known to uncouple insect epidermis from previous studies was used to demonstrate the usefulness of the capacitance measuring technique for detecting complete uncoupling. Voltage pulses (-10 mV, 25 msec) were used to generate these currents from an NME cell group with 40 to 45 cells. IAA was added to the bath just after recording was begun. At 30 sec post break-in the capacitance was 375 pF. By 18 min following break-in the cells were completely uncoupled with a capacitance of 10.4 pF. The effect of IAA is not reversible.

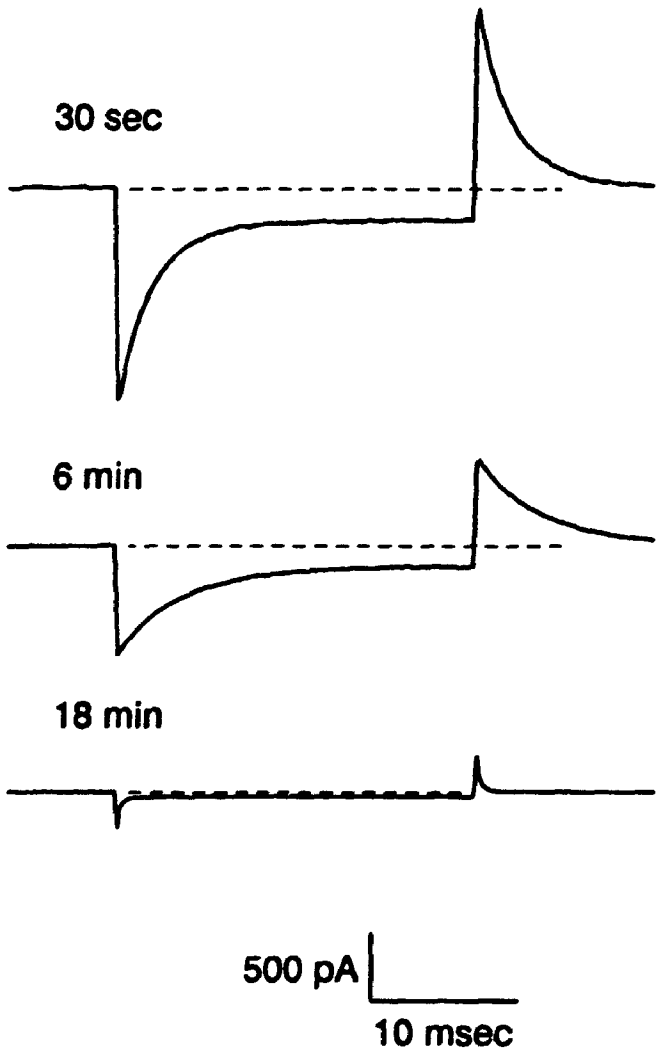
30 sec
6 min
18 min
500 pA
10 msec

Table 1. Summary of results using capacitance measuring technique on cell groups

Effects of a variety of protein kinase inhibitors and other agents on the presence of electrical coupling in NME cell groups recorded using the capacitance measurement technique for detecting the presence of coupling.

Compound	Concentration	Complete Uncoupling	n
Known uncouplers of insect gap junctions			
iodoacetate	1, 5 mM	yes, 20 - 40 min	5b
1-octanol	1 mM	yes, 1-2 min, reversible	3b
N-ethylmaleimide	10 mM	yes, 35 - 40 min	3p
Nucleotides			
ATP-free TPS		no	> 30
apyrase	50, 100 U/ml	no	4p
ATP	5 mM	no	3p
ATPγS	1, 5, 10 mM	yes, 20 - 30 min	11p
AMP-PNP	10 mM	no	14p
GTP	5 mM	no	7p
Phosphatases			
alkaline phosphatase	25, 50, 250 mg/ml	no	11p
acid phosphatase	1 mg/ml	no	3p
Protein kinase A inhibitors			
Walsh inhibitor	1 mg/ml	no	7p
H-89	100, 250 μM	no	6p
Protein kinase C inhibitors			
H-7	1 mM	no	4p
staurosporin*	1 μM	no	4p
bisindolylmaleimide*	120 μM	no	2p, 3pb
D-erythro-sphingosine*	1 mM	no	5p
polymyxin B sulfate	200 μM	sometimes, 15 - 20 min	8p
	2 mM	sometimes, 10 - 30 min	5p
Tyrosine kinase inhibitor			
Genistein*	148 μM	no	6p
cGMP-dependent protein kinase inhibitor			
KT-5823*	100 μM	no	5p
Calmodulin and Ca^{++}/calmodulin kinase inhibitors			
chlorpromazine	200 μM, 700 μM	no	6p
calmidazolium*	146 μM	no	2p
KN-62*	100 μM	no	3p, 3b

p = compound added to pipette solution, b = compound added to bath solution, pb = added to both
* dissoved in DMSO before dilution in TPS

obtained with N-ethylmaleimide (Table 1). Octanol, as expected, reversibly reduced the measured capacitance to that of one cell within 1 to 2 min of starting bath perfusion. Thus, this technique is useful for detecting the presence or absence of coupling.

IV.3.8 Effects of Kinase Inhibitors on the Presence of Coupling in Cell Groups

The results of screening agents that induce total uncoupling are reported in Table 1. The effects of spontaneous uncoupling, as found in cell pairs, were examined on cell groups. ATP-free pipette solution did not induce complete uncoupling even in groups of only 5 cells (up to 45 to 60 min recording). This could be due to the inability to deplete the entire group of ATP (or some other component) from all the cells in the group. Apyrase, a soluble ATPase that was included in the pipette solution to reduce [ATP] in cell groups even further, did not facilitate uncoupling. ATPγS (at 1, 5 and 10 mM) uncoupled cell groups in 20 to 30 min, supporting a role for ATP in maintaining functional coupling.

Inhibitors of common second messenger regulated protein kinases were tested for their ability to uncouple cell groups (see Table 1). Each of the targeted kinases have been been shown to have possible effects on gap junctions from other tissues (see introduction to this chapter). ATP could maintain functional coupling by acting as a substrate for phosphorylation of gap junctions. Most kinase inhibitors have

a moderate specificity and can possibly inhibit a variety of kinases. In addition, both general acid and alkaline phosphatases were added to the pipette solution. Of all of the tested compounds only polymyxin B, which is generally used as a protein kinase C inhibitor, occasionally completely uncoupled the cells. Most of the compounds were added to the pipette solution although a few were added to the bath solution at the start of recording, or several hours before. Cell recordings were made for at least 30 min and often up to 40 to 45 min.

IV.4 Discussion

IV.4.1 Spontaneous Uncoupling

Just as many vertebrate cell types, insect epidermal cell pairs spontaneously uncoupled during double whole-cell recording. In PPE cell pairs the time to complete uncoupling was short enough to observe single-channel activity. While NME cell pairs did not uncouple fast enough to see single-channel events the large number of well-coupled cells that were isolated at this stage facilitated examination of the mechanism of ATP reduction of spontaneous uncoupling. A likely explanation for this difference is that PPE cell pairs were much less well-coupled after isolation and consequently junctional conductance drops to the level of single channels in a shorter time. This is supported by the finding that the average rates of uncoupling between PPE and NME cells were very similar (G_{j50} = 7.7 and 4.1, respectively).

IV.4.2 Direct ATP-Binding *vs* ATP-Hydrolysis by an Enzymatic Process

The roles of ATP in cells is so diverse that its loss could perturb any number of cellular processes that in turn could alter the activity of gap junctions. Because of this it is difficult to use whole cell experiments to dissect out the various actions of ATP. One of the simplest possible mechanisms whereby ATP could affect GJ channels (and simplest to test) is direct ATP-binding to GJ channels. ATP and a variety of cyclic nucleotides both increase or decrease the probability of opening of several nonjunctional-ion channels (reviews: Latorre *et al.* 1991; Nichols & Lederer 1991; Standen 1992). The best studied example is the ATP-gated potassium channel in heart (Standen 1992). Binding of ATP to the channel closes it and the loss of ATP opens it. In this way cardiac cell excitability is linked to the metabolic state of the cell. In cardiac cell pairs there is some evidence that ATP can act directly to open GJ channels (Sugiura *et al.* 1990). Nonhydrolysable analogues of ATP are commonly used to distinguish between ATP-binding and enzymatic processes that require hydrolysis of the terminal 5' phosphate on ATP.

Two ATP analogues, ATPγS and AMP-PNP were tested on epidermal cells to show that direct ATP-binding cannot account for the ability of ATP to reduce spontaneous uncoupling. ATP must participate in an enzymatic process that somehow affects gap junctions. Among the many possibilities are direct

phosphorylation of gap junctional proteins (or an associated protein necessary for gap junction function), maintenance of an ATP-driven metabolic process such as Ca^{++} homeostasis or ATP-dependent maintenance of plasma membrane structure. In support of an enzymatic effect ATPγS but not AMP-PNP (or GTP) uncoupled NME cell groups when added to the pipette solution (Table 1). ATPγS, unlike AMP-PNP, is not completely nonhydrolysable. ATPγS is slowly hydrolysed by some kinases and thiophosphate is not readily removed from proteins by protein phosphatases, thus it can act as an inhibitor of some ATP-dependent processes.

IV.4.3 Phosphorylation

GJ-channel proteins may need to be phosphorylated in order to open. This could be a primary phosphorylation step that allows the channels to be functional after which other mechanisms can modulate channel activity. This notion is based on the observation that voltage can modulate junctional conductance during spontaneous uncoupling (Chapter VI). Once uncoupling is completed, however, hyperpolarization of the cells cannot elicit a junctional current. In support of a priming phosphorylation step, direct phosphorylation of known vertebrate gap junction proteins occurs during post-translational processing (Saez *et al.* 1986; Traub *et al.* 1987; Musil *et al.* 1990; Laird *et al.* 1991; Musil & Goodenough 1991; Lau *et al.* 1992). For instance, connexin43 may need to be phosphorylated for its transport to the membrane (Musil *et al.*

1990) or phosphorylation may be required to maintain gap junctional plaques (Musil & Goodenough 1991).

Phosphorylations at additional sites on the protein may modulate junctional conductance, as has been demonstrated in vertebrate cell pairs with modulators of protein kinase activity. This gating could be similar to the voltage-dependent gating that affects junctional conductance only after the primary gating step has occurred.

A priming phosphorylation step has been explored in epidermal cells in two ways. First, two general protein phosphatases, acid and alkaline phosphatase, were added to the pipette solution. If the gap junction proteins were phosphorylated then phosphatase may dephosphorylate the channels and close them. Neither phosphatases uncoupled cell groups, nor did alkaline phosphatase added to both cells of a pair cause the cells to uncouple. These results do not exclude the possibility that significant phosphorylation could occur on sites inaccessible to, or not specific for, these phosphatases.

The second way this question was addressed was to treat NME cell groups with readily available protein kinase inhibitors. Again, if the primary phosphorylation was maintained by the continual activity of one of these kinases then inhibiting the kinase may uncouple the cells. A wide range of inhibitors of well known second messenger-operated kinases were tested.

Only polymyxin B uncoupled the cells completely. This inhibitor is generally used as a protein kinase C inhibitor (Mazzei *et al.* 1982). This result could indicate an involvement of protein kinase C. Several other more potent and specific protein kinase C inhibitors were without effect, however (see Table 1). Furthermore, the concentration of polymyxin B was rather high (200 μM to 2 mM) suggesting that it may have acted through another mechanism. Polymyxin B is a member of a loosely-related group of membrane-active peptides (all components of antibiotics or venoms) that associate with, disrupt and sometimes form pores in cellular membranes (review: Cserháti & Szögyi 1993). This suggests that polymyxin B may act on gap junctions by disrupting the plasma membrane. Membrane-active peptides may prove to be useful tools for examining mechanisms of GJ-channel gating as the mode of action of these peptides is becoming increasingly better understood.

There are a few possible problems to be aware of when interpreting the kinase inhibitor data: 1. partial uncoupling may have occurred but not detected, 2. 30 to 45 min may not have been long enough to see an effect, 3. not enough inhibitor may have entered the cell, 4. water soluble inhibitors applied via patch pipettes may not have passed through gap junctions to act on both sides of the junctions of the recording cell, and 5. the phosphate on the protein may have a long turnover time. Finally, the kinase inhibitors that

were used were those that are readily available. Although protein kinases contribute to the most ubiquitous of intracellular control mechanisms, over 200 protein kinases have been cloned (Johnson & Barford 1993) and who knows how many kinases remain to be discovered? Moreover, there are probably many kinases not activated by extracellular signals; for example the AMP-activated protein kinase (Hardie & MacKintosh 1992).

The capacitance technique for detecting the presence of coupling in cell groups was designed to screen for compounds that cause cells to uncouple completely. The cell pair technique has many advantages over this technique, including the ability to measure junctional conductance directly instead of merely the presence of coupling, and the ability to control the concentration of compounds on both sides of a gap junction more precisely. The problem with the cell pair method is that it is very time consuming in generating statistically significant data. The capacitance technique was applied primarily because it is fast and because the NME cell pair system was developed only late in the project. It would be useful to continue investigations into the ATP effect and other modulators of junctional conductance using a combination of both methods.

IV.4.4 Other Possible Mechanisms of ATP Action

ATP could be acting on junctional conductance in ways other than through phosphorylation. It has been demonstrated

here that epidermal gap junctions are Ca^{++}-dependent, as shown for *Chironomus* salivary gland cells (Loewenstein 1966; Loewenstein *et al.* 1967). This suggests that ATP could maintain coupling by acting as an energy substrate for a mechanism that maintains low $[Ca^{++}]_i$. This possibility has been suggested in previous experiments in *Tenebrio* (Lees-Miller & Caveney 1982) and *Chironomus* salivary gland cells (Politoff *et al.* 1969; Rose & Loewenstein 1976) in which metabolic inhibitors were shown to uncouple the cells. Rose and Loewenstein (1976) demonstrated directly that a reduction in ATP could increase intracellular $[Ca^{++}]$ to levels that uncoupled the cells (Rose & Loewenstein 1976). It is unlikely that this explains spontaneous uncoupling in double whole-cell recording since the pipette solution is strongly buffered with 10 mM EGTA and since the volume of pipette solution is at least 10,000 times that of the cell. To be sure of this, experiments should be done in which Ca^{++} levels are measured during whole-cell recording.

The maintenance of plasma membrane integrity could require ATP-dependent metabolic processes that might conceivably result in closure of GJ channels, if deprived of ATP. Several treatments which probably disturb plasma membrane structure have been shown to reduce junctional communication, thus supporting membrane involvement in gap junction function. Besides the effects of long chain alkanols and other volatile anaesthetics (review: Chapter III), fatty acids have been

shown to affect gap junctions (review: Burt 1991) and other nonjunctional-ion channels (review: Ordway *et al.* 1991) as well. When ATP is depleted in cultured human astroglial cells (Sun *et al.* 1993) or cultured myocardial cells (Gunn *et al.* 1985) lipid degradation has been shown to occur. This could result in destruction of specific lipids that are needed to maintain functional GJ channels (review; protein-lipid interactions within biological membranes: Vogel 1992; Cserhåti & Szögyi 1993). A classical example of the role of membrane lipids in supporting protein function is protein kinase C which must be associated with plasma membrane phosphatidylserine to be enzymatically active (review: Newton 1993).

Another ATP-dependent membrane-maintaining mechanism that has been recently discovered is the active maintenance of lipid asymmetry by a transmembrane 'lipid pump'. Recently, evidence in cardiac cells has suggested that the activity of the cardiac sodium-calcium exchanger is enhanced in the presence of ATP (Collins *et al.* 1992). ATP is hydrolysed in this system and inhibitors of an aminophospholipid translocase, or treatments that affect phosphatidylserine on the inner face of the membrane, prevent ATP from stimulating sodium-calcium exchange current (Hilgemann & Collins 1992). Aminophospholipid translocases are transmembrane proteins which actively maintain lipid asymmetry in plasma membranes by translocating phosphatidylserine from the outer to the inner

leaflet of the plasma membrane (reviews: Devaux 1988; Devaux 1991). It is possible that phosphatidylserine or some other phospholipid must be present at certain concentrations in one or other leaflet of the plasma membrane in order for gap junctions to function properly.

In summary, epidermal cell pairs spontaneously uncoupled during double whole-cell recording. ATP in the pipette partially prevented this uncoupling. During spontaneous uncoupling in PPE cell pairs the junctional conductance dropped low enough that single GJ-channel activity was observed. ATP stabilized conductance in PPE cell pairs and allowed voltage dependence in well-coupled cells to be examined (Chapter VI). ATP probably worked by acting as a substrate for an unidentified enzymatic process as nonhydrolysable analogues did not mimic its action. The precise enzymatic process probably is a key priming step that must gate the channels before other gating mechanisms, such as voltage, can become effective. Phosphorylation by common second messenger regulated kinases was explored using a rapid screening technique that monitored the drop in capacitance among cell groups during uncoupling. This technique would be useful to screen other things (*i.e.* anti-gap junction antibodies) for their ability to uncouple epidermal cells.

V GJ-CHANNEL PROPERTIES IN EPIDERMAL CELL PAIRS

V.1 Introduction

In the previous chapter it was shown that junctional currents in PPE cell pairs decayed towards zero conductance in the absence of ATP in the pipette solution. Random and quantal fluctuations in the currents were observed just before complete uncoupling (see Fig. IV-2A). Such current patterns are typical of those seen during the opening and closing of most biological membrane channels already studied (Hille 1992).

Based on early electron-microscopic and molecular permeability data it was concluded that gap junctions probably consisted of many parallel units each providing discrete, continuous and direct intercellular passageways or channels (Loewenstein 1966; Loewenstein 1981). The first direct evidence for this 'unit hypothesis' came in 1978 when Loewenstein *et al.* measured tiny quantal increases in junctional current during the early stages of gap junction formation between two *Xenopus* blastomeres manipulated into contact. These measurements had limited time resolution and only provided an estimate of the actual conductance of the units. Double whole-cell recording allows GJ-channel conductances and activity to be measured directly with millisecond time resolution (Neyton & Trautmann 1985; Veenstra & DeHaan 1986). Using this technique it has been demonstrated that GJ channels behave like nonjunctional channels in that

Table 2. Summary of single-channel conductances found for GJ channels in other vertebrate and invertebrate double whole-cell voltage-clamped cell pairs

Tissue	Single Channel Conductance (pS)	Reference
Neonatal Rat Ventricle	53 - 60	Burt & Spray, 1988
	20 - 30, 45 - 60	Rook *et al.*, 1988
	40 - 50	Rook *et al.*, 1990
	18, 43	Rook *et al.*, 1992
	21, 40 - 45, 70	Takens-Kwak *et al.*, 1992
	40	Münster & Weingart, 1993
Neonatal Hamster Ventricle	20 - 30, 45 - 50	Wang *et al.*, 1992
Embryonic Chick Ventricle	58 - 60, 166	Veenstra & DeHaan, 1986 Veenstra & DeHaan, 1988 Veenstra, 1990
	42, 80, 119 157 & 200, 240	Chen & DeHaan, 1992
Adult Guinea Pig Ventricle	37	Rüdisüli & Weingart, 1989
Human Cx43 in SKHep1 cells	60, 90	Moreno *et al.*, 1992
Mouse Embryonic Astrocytes (Cx43)	50 - 60	Giaume *et al.*, 1991
Rat Brain Astrocytes (Cx43)	50 - 60	Dermietzel *et al.*, 1991
Human Corpus Cavernosum Smooth Muscle (Cx43)	23, 38, 57, 93, 134	Moreno *et al.*, 1993
A7r5 Rat Aorta Smooth Muscle Cell Line (Cx43)	36, 89	Moore *et al.*, 1991
WB Rat Liver Cell Line (Cx43)	20 - 30, 80 - 90	Spray *et al.*, 1991
Rabbit Sinus Nodal Cells (Cx43)	34 - 95	Anumonwo *et al.*, 1992
Neonatal Rat Heart Fibroblasts	21	Rook *et al.*, 1992
Human Cx32 in SKHep1 Cells	25 - 35, 120 - 130	Moreno *et al.*, 1991
BRL Rat Liver Cell Line	30, 60, 90	Paschke *et al.*, 1992
FL Human Amniotic Cell Line	30, 60, 90	Paschke *et al.*, 1992
Embryonic Chick Lens	286	Miller *et al.*, 1992
Frog Lens Epithelial Cells	100	Cooper *et al.*, 1989
Teleost Horizontal Cells	48 - 61	McMahon *et al.*, 1989
Pancreatic Acinar Cells	27, 130	Somogyi & Kolb, 1988
Pancreatic Beta Cells	20	Pérez-Armendariz *et al.*, 1991
Chinese Hamster Ovary Cells	22, 37, 50, 70, 120	Somogyi & Kolb, 1988
Rat Lacrimal Gland	70-180	Neyton & Trautman, 1985
Xenopus Embryonic Muscle	100	Chow & Young, 1987
Earthworm Giant Axon	30 - 40, 90 - 110	Brink & Fan, 1989
Aedes albopictus Mosquito Cell Line	166	Bukauskas & Weingart, 1991
	365	Bukauskas & Weingart, 1993

they have discrete unit conductances and are able to switch between open and closed states.

A wide range of single GJ-channel conductances have been reported in cells isolated from vertebrates ranging between 20 to 286 pS (see Table 2). In many cell types more than one unit conductance has been observed. The mechanisms accounting for these observations in gap junctions is unclear. This is because GJ channels cluster into gap-junctional plaques making it difficult to determine either the number of active channels between a cell pair or whether multiple conductances in a recording are due to the activity of different GJ-channel types with different conductances or only one active GJ channel with substates.

For nonjunctional-ion channels, however, the properties of 'single' channels can be examined directly using the cell-attached patch-clamp technique. Therefore, subconductance states and possible mechanisms accounting for them have been confidently proposed (reviews: Fox 1987; Meves & Nagy 1989). Three different channel conductance states have been described: 1. zero current through the channel (fully-closed), 2. maximal current through the channel (fully-opened), and 3. intermediate levels of current through the channel indicating subconductance state(s). Subconductances have been proposed to arise by two mechanisms. First is the 'subunit' type of gating in which multiple conducting units are envisioned each of the same or different conductance that can open in concert or

individually. In the second model subconductances are described as partially-closed or partially-open substates. A channel with a single conducting unit or pore undergoes a conformational change that reduces current through the channel. The study of substates may provide insight into the structure, regulation and ion permeation mechanisms of ion channels in general and GJ channels in particular. Moreover, substates may have specific physiological roles (Fox 1987; Meves & Nagy 1989).

In spite of the difficulties in confidently determining the presence of substates in gap junctions, both a subunit and a partially-closed model of substate gating have been proposed to account for more than one unit conductance measured in a cell type (see Neyton & Trautmann 1985; Veenstra & DeHaan 1986; Rook *et al.* 1988; Somogyi & Kolb 1988; Veenstra 1990; Moore *et al.* 1991; Chen & DeHaan 1992; Manivannan *et al.* 1992; Bukauskas & Weingart 1993; Weingart & Bukauskas 1993). Two variations of the partially-closed model proposed for GJ channels include a graded model of substate gating in which channels can open smoothly to any conductance intermediate between fully-open and fully-closed, and a stable substate model of gating in which channels open to a limited number of stable substates in addition to the fully-open state.

In this chapter double whole-cell voltage-clamp methods were applied to examine the properties of GJ channels in cell pairs from the insect epidermis. There were two reasons for

initiating this research. First, no insect GJ channels had been examined at this resolution when this work was begun. Only recently have double whole-cell voltage-clamp reports on insect gap junctions appeared in the literature (Bukauskas *et al.* 1991; Bukauskas & Weingart 1993; Churchill *et al.* 1993). Second, several questions have been raised concerning the complex regulation of gap junctional permeability in intact insect epidermis during the moult cycle (such as in response to treatment with 20-hydroxyecdysone and at compartment boundaries, as reviewed in Chapter I). High resolution recordings of single-GJ channel activity might provide more insight into these questions. I hope to convince the reader that a large-conductance GJ channel found in these cells is among the first described that is capable of existing in partially-closed substates. The possible relevance of this finding to the potential role of gap junctions in intercellular signalling in insects is discussed. Most of this work has been published (Churchill & Caveney 1993a,b,c).

V.2 Results

V.2.1 Initial Observations of Main-state and Substate Conductances

The activity of individual GJ channels (*i.e.* microscopic junctional currents) was recognized as spontaneous and quantal changes in current that were equal in magnitude but opposite in sign in the two cells of a whole-cell voltage-clamped cell pair (Fig. V-1). To obtain recordings of single-GJ channels

Fig. V-1. Single-channel currents when first clearly detectable near the end of spontaneous uncoupling

Unitary currents from single-GJ channels observed in a poorly-coupled PPE cell pair following spontaneous uncoupling. Current (I_1 & I_2) and voltage (V_1 & V_2) traces are shown on an expanded time scale from a cell pair clamped with pipettes containing an ATP-free solution. A train of voltage pulses (1 sec, 20 mV, 0.3 Hz) were initially applied to cell 1 with V_H = -50 mV for both cells. A constant V_j with a reversed polarity of 20 mV (V_1 = -60 mV, V_2 = -40 mV) was used to monitor the spontaneous and quantal behaviour of the unitary single-channel currents. Each dotted line represents 4.6 to 5 pA (230 to 250 pS) of conductance. Baseline (closed) is indicated at 'C'. 'O' indicates the direction of channel opening. The data for this figure sampled from tape at 100 Hz.

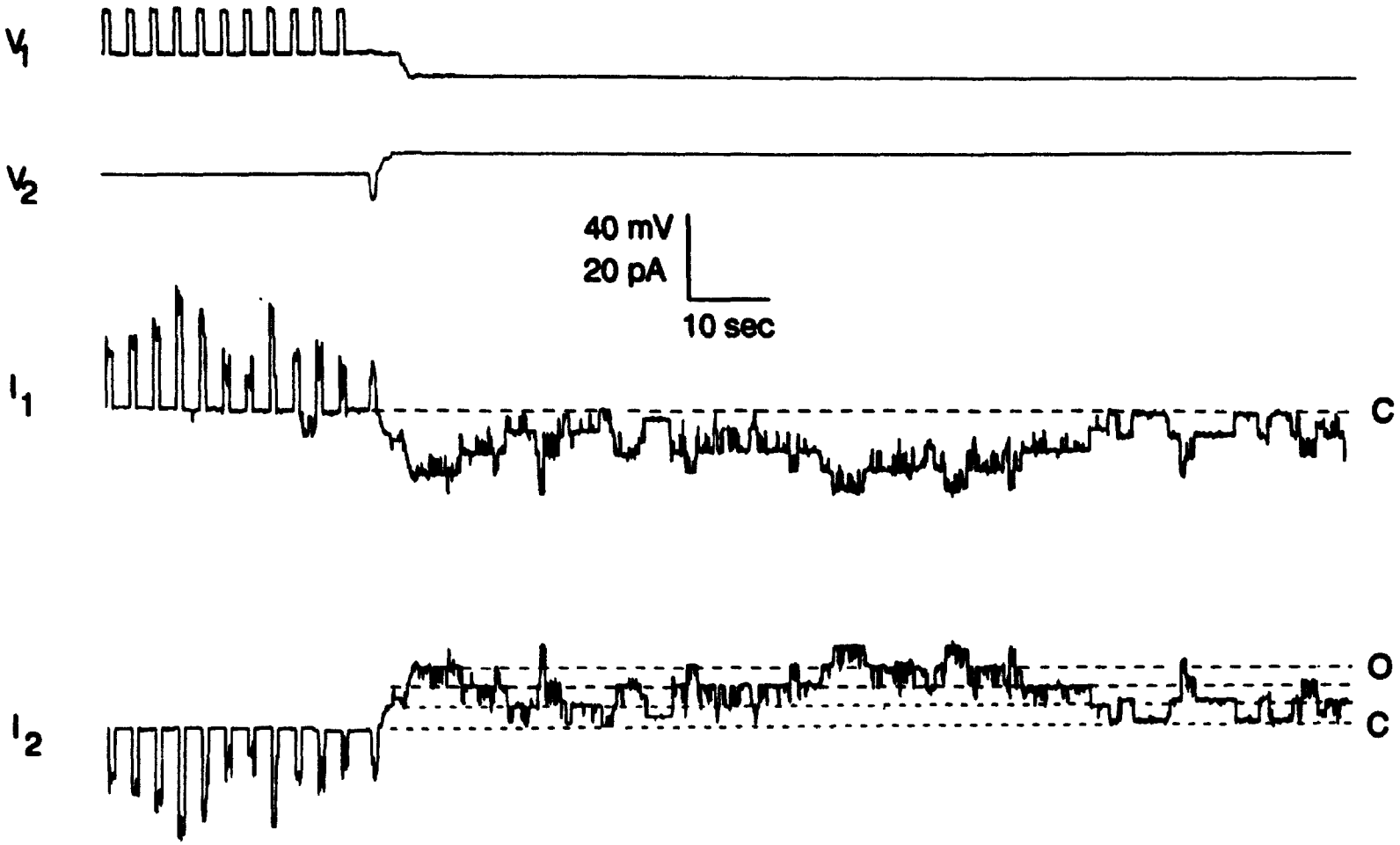
V1
V2
40 mV
20 pA
10 sec
I1
C
I2
O
C

the level of coupling in a cell pair had to be reduced to less than 2 nS (*i.e.* poorly-coupled) such that only a small number of GJ channels were active. This condition was met during spontaneous uncoupling in PPE cell pairs (Chapter IV), by finding ATP-loaded PPE cell pairs with reduced levels of coupling or by reducing coupling using volatile anaesthetics.

The analysis of substate conductances was performed here on data obtained from poorly-coupled ATP-loaded PPE cell pairs where more single-channel events were recorded than from non-ATP-loaded spontaneous-uncoupled cell pairs. The length of single-channel recording for ATP-loaded and nonATP-loaded cell pairs were 16 ± 1 min (n = 4 cell pairs) and 6 ± 1 min (n = 14 cell pairs), respectively.

Upon visual inspection of the spontaneous step-like current transitions (each transition is an 'event') in any poorly-coupled cell pair, it was clear that there was only one dominant step size (Fig. V-1, Fig. V-2A, Fig. V-4). Under extremely reduced coupling conditions, such as towards the end of recordings in spontaneously uncoupling PPE cell pairs, long stretches lasting seconds were observed during which junctional current was zero. This was evident as extremely low current noise levels, the absence of typical open channel noise, and correspondence of this current level with the end of spontaneous uncoupling when all channels were completely closed (*i.e.* transjunctional voltage pulses could no longer elicit junctional currents). The fully-closed current level

Fig. V-2. Main-state conductance

(A) Frequency histogram of 492 single-channel events from one PPE cell pair with ATP in the pipettes. Events were grouped into 7 pS bins and fit with a single Gaussian curve with mean ± SD of 197 ± 13 pS. V_j was maintained at 20 mV with the cells being held at a range of V_H's from -30 to +10 mV. The V_H's were shifted twice to more depolarized potentials in order to reduce nonjunctional noise and keep channel activity on scale.

(B) Dependence of unitary current (i_j) on V_j. One cell of the pair was clamped at 0 mV and the other at a range of voltages between 0 to -60 mV. Channels were not active at depolarized voltages (Fig. VI-4) therefore the reversal of the single-channel current was obtained by alternating the cell maintained at 0 mV. Averaged i_j from 6 cell pairs are graphed against V_j. 1 to 10 single-channel events were recorded at each V_j. Measurements were made only on single level events. Standard error bars are obscured by data symbols. Results were fit with a regression line with slope 271 pS ($r^2 = 0.99$) using a linear least-squares method.

(C) Typical single-channel currents are shown for V_j = -40 to +40 mV. Arrowheads denote baseline. Data for figure sampled from tape at 500 Hz.

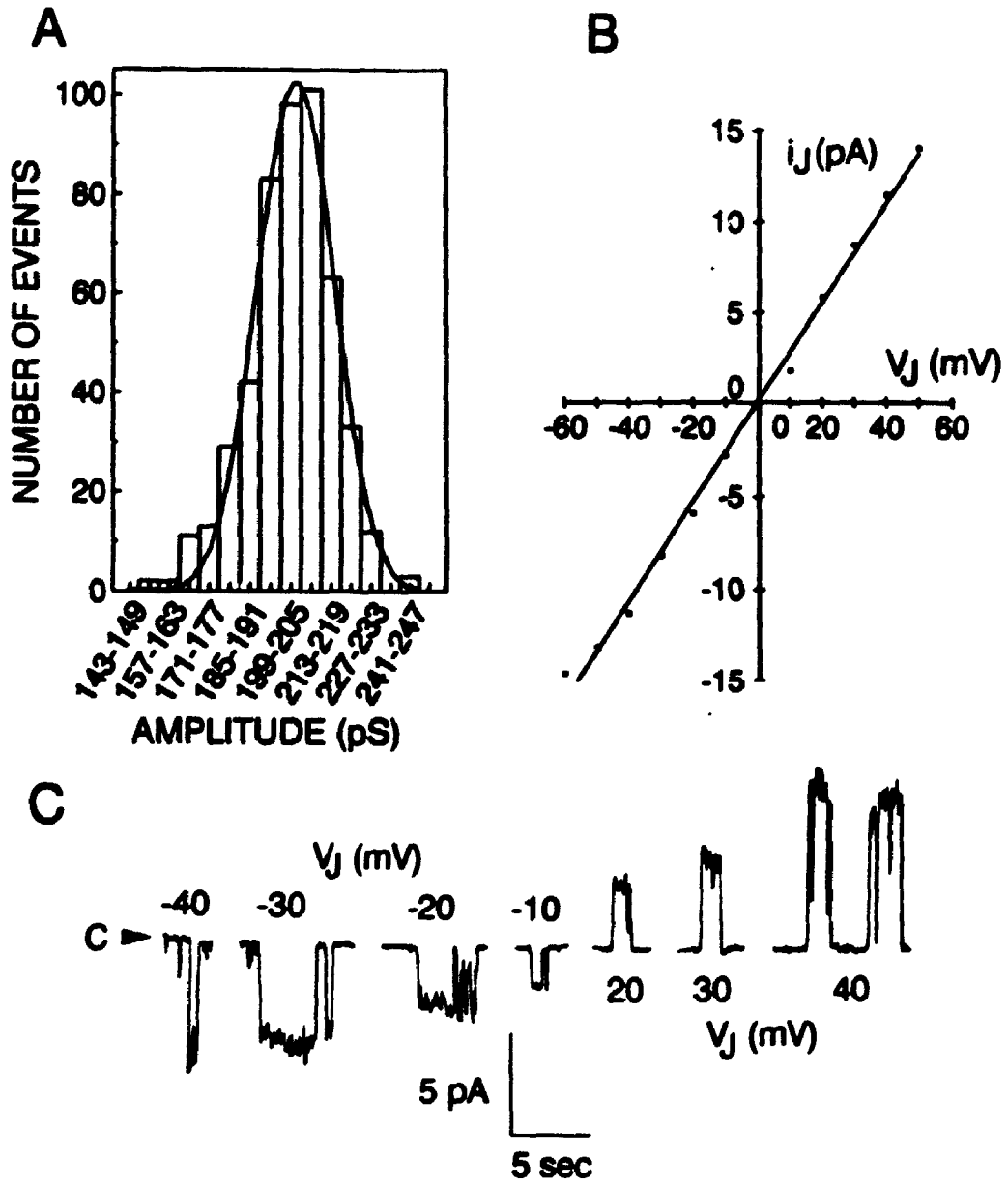
A
NUMBER OF EVENTS
100
80
60
40
20
0
143-149
157-163
171-177
185-191
199-205
213-219
227-233
241-247
AMPLITUDE (pS)
B
15
10
5
0
-5
-10
-15
iJ(pA)
VJ (mV)
-60 -40 -20 0 20 40 60
C
VJ (mV)
-40 -30 -20 -10
C
20 30 40
VJ (mV)
5 pA
5 sec

was interrupted by spontaneous and rapid (msec) discrete increases in junctional current that would remain for 10's of msec to several sec and then drop back to the fully-closed level. All such events in one cell pair were the same size and are assumed to represent the openings of individual GJ channels (and thus are deemed the fully-open main-state conductance).

Frequently during fully-open periods of a single main-state channel event, the current level would drop suddenly and only briefly to a lower current level just part way to the fully-closed level before returning to the fully-open level (Fig. V-3A a & d). These brief transitions are thought to represent partial closures or 'substates' of the fully-open main-state of a single channel. Main-state and substate conductances were analyzed separately.

V.2.2 Main-State Conductance

To analyze the main-state conductance all step-like transitions representing main-state events were measured from one cell pair and grouped into 7 or 10 pS bins on a frequency histogram. If insufficient data were available to construct a distribution histogram all measurable events from each cell pair were averaged.

The distribution of single-channel events in Fig. V-2A from a poorly-coupled ATP-loaded PPE cell pair approximated a normal distribution and was fit with a single Gaussian curve with a mean ± SD of 197 ± 13 pS (n = 492 events). From two

Fig. V-3. Substate conductances

(A) Examples of single-channel events are shown in **a-d**, each from a different cell pair. Current traces from both cells of the pair are shown. Horizontal arrows (C) mark the baseline (closed). For **a-c**, V_j = 20 mV; for **d**, V_j = -10 mV. Arrows denote examples of substate events. Substate conductances at the arrows in **a** and **d** were 43 and 235 pS, respectively. Main-state conductances for **a-d** were 286, 211, 257, and 305 pS, respectively. **b** is an example of a noisy transition between baseline and main-state. Sometimes distinct steps were discerned. **c** is an example of substate behaviour that stopped when the channel opened to main-state. The data for this figure were sampled from tape at 300 Hz.

(B) Frequency histogram of substate events occurring within main-state events (*i.e.* as in Fig. 4A **a** & **d**). Each event was normalized as a percent of the main-state in which it was observed. 544 events from 4 cell pairs with ATP in the pipette were pooled and grouped into 6 pS bins. The arithmetic mean of substate events was 37 ± 1% of the main-state ranging from 4 to 86% of the main-state.

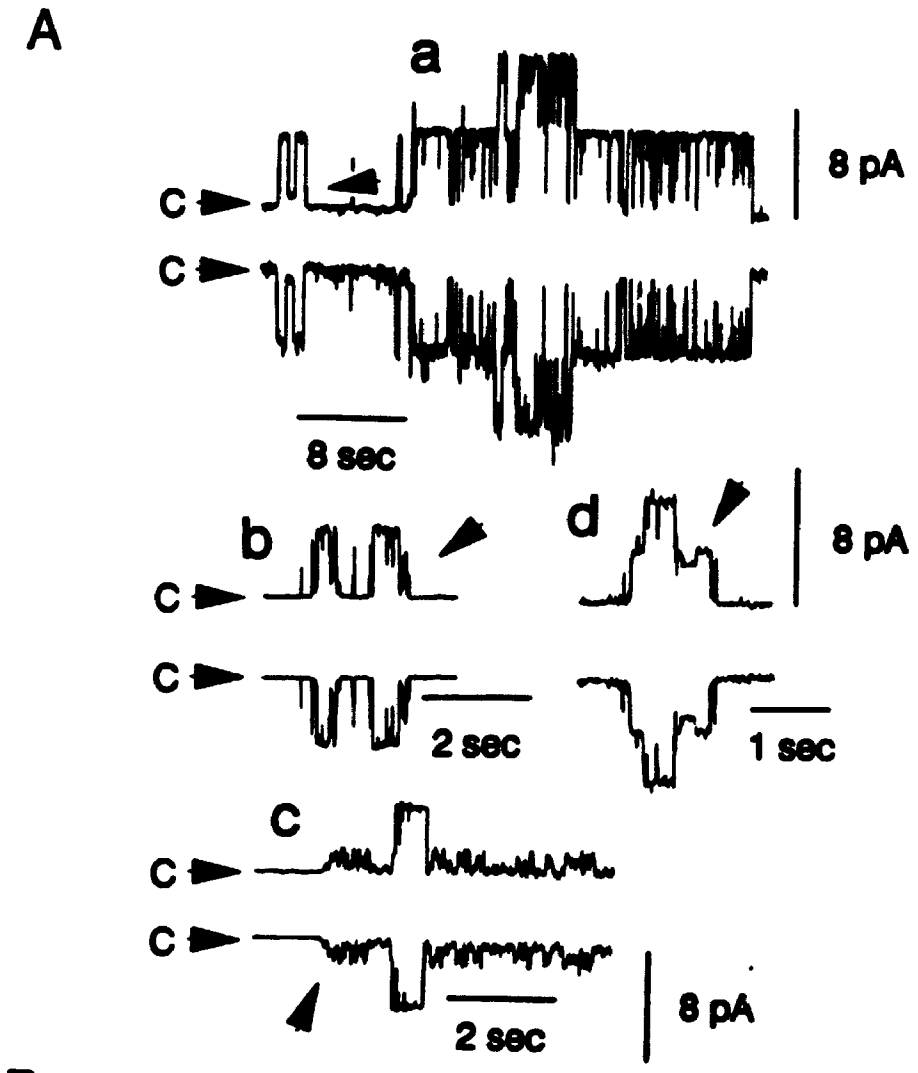
A
a
8 pA
c
c
8 sec
b
d
8 pA
c
c
2 sec
1 sec
c
c
c
2 sec
8 pA

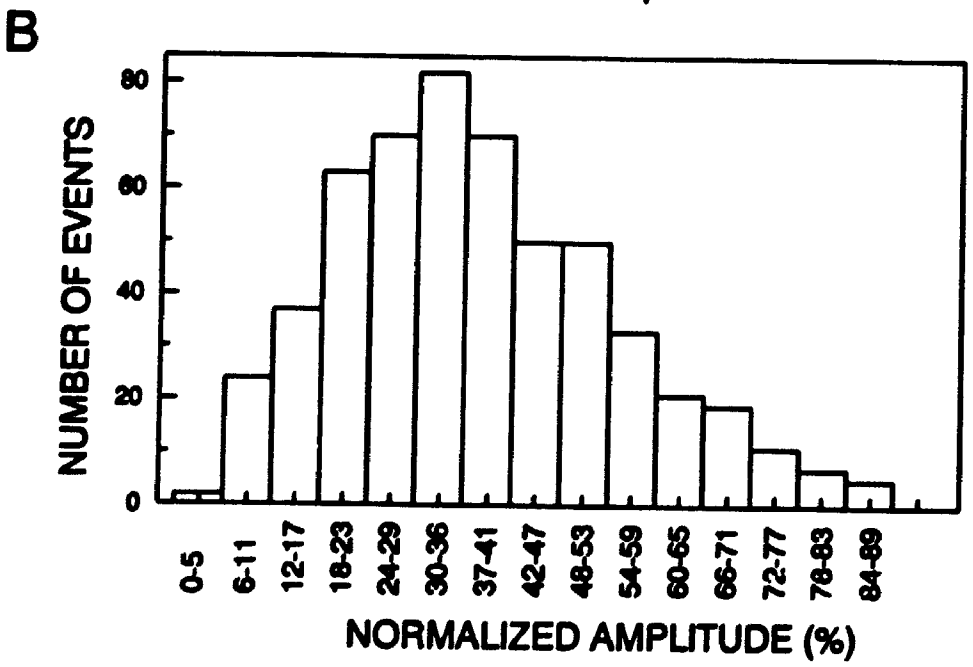
B
NUMBER OF EVENTS
0
20
40
60
80
0-5
6-11
12-17
18-23
24-29
30-36
37-41
42-47
48-53
54-59
60-65
66-71
72-77
78-83
84-89
NORMALIZED AMPLITUDE (%)

other cell pairs (with n > 100) the mean ± SD for a best fit single Gaussian curve were 214 ± 42 pS (n = 287 events) and 293 ± 24 pS (n = 166 events).

In four octanol-uncoupled ATP-loaded PPE cell pairs all measurable main-state step-like transitions were grouped into 10 pS bins and fit with a single Gaussian curve (*e.g.* Fig. V-4B). Curves with best fit mean ± SD were: 198 ± 22 pS (n = 366 events); 211 ± 24 pS (n = 383); 303 ± 16 pS (n = 333); 402 ± 26 pS (n = 209).

The arithmetic mean conductance for 169 single level channel events from 13 spontaneously-uncoupled PPE cell pairs was 288 ± 2 pS (mean ± SEM) ranging from individual cell pair means of 260 ± 9 pS (n = 9 events) to 347 ± 4 pS (n = 4 events).

The V_j-dependence of the single-channel current (i_j) was determined using spontaneously-uncoupled PPE cells (ATP-free pipette) since it was easier to obtain data from several cell pairs. One cell was clamped at 0 mV and the other at a range of voltages between 0 to -60 mV. Reversal of i_j was obtained by alternating the cell clamped at 0 mV. The single-channel I-V relationship is shown in Fig. V-2B for data obtained from 6 cell pairs. This was fit with a regression line of slope 271 pS (r^2 = 0.99) using a linear least-squares method. Typical single-channel events from which these measurements were made are shown in Fig. V-2C for V_j = +40 to -40 mV. From these results it is concluded that over the voltage range tested and

Fig. V-4. Single-channel currents in octanol-uncoupled PPE cell pairs

Voltages in both cells were held steady between +10 to -60 mV to create transjunctional voltages of 20 mV.

(A) Example of typical single-channel events. Currents from both cells are shown (I_1 & I_2). The fully-closed state is denoted at C. The dashed lines represent a single-channel conductance of 320 pS. Channel flickering often occurred during channel opening or closing (right arrowhead) or between fully-open events (left arrowhead). Data for this figure were sampled at 500 Hz.

(B) Frequency histogram of single-channel events from one cell pair best fitted with a single Gaussian distribution (mean 211 ± 24 pS, SD; n = 383 events).

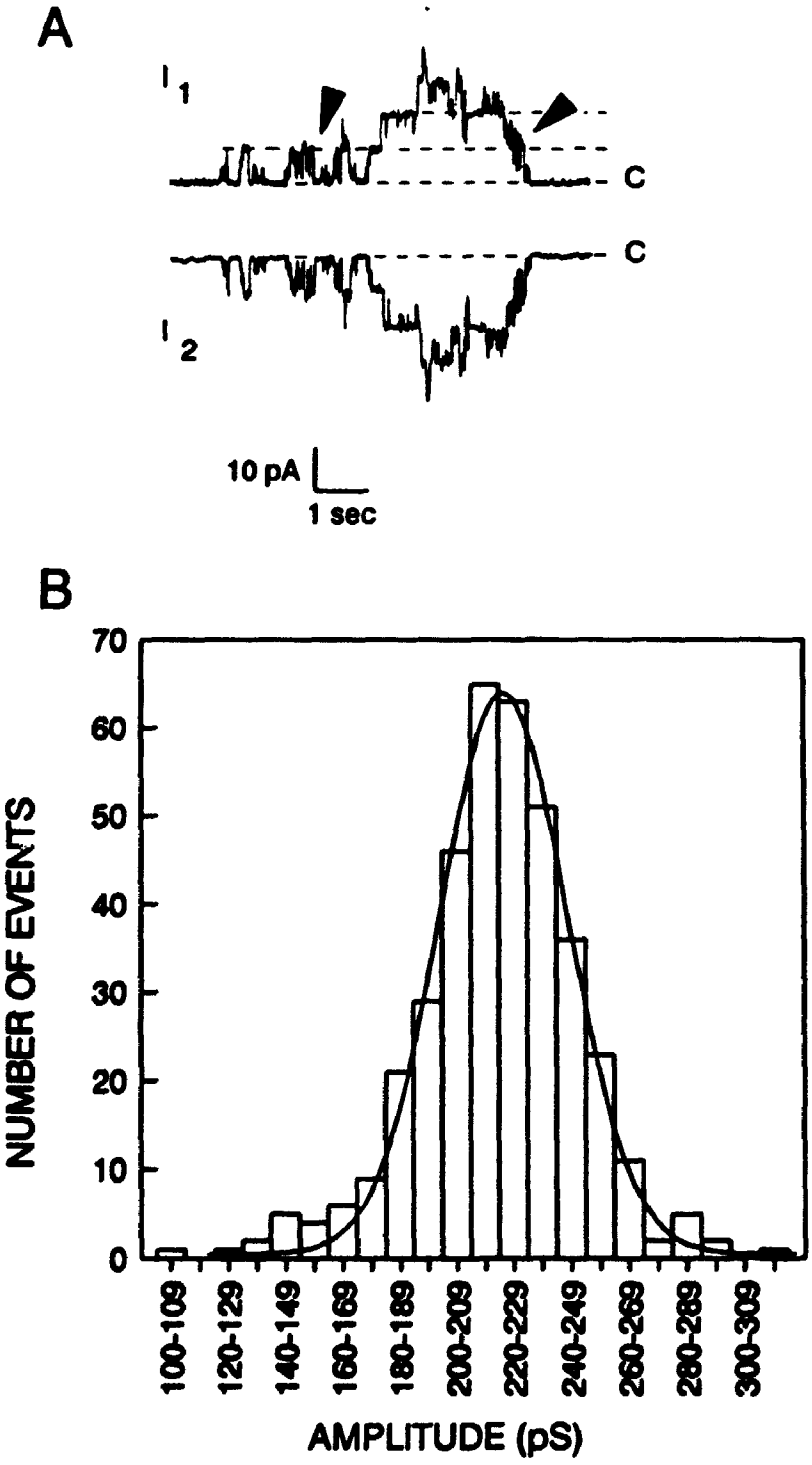
A
I 1
C
C
I 2
10 pA
1 sec
B
NUMBER OF EVENTS
70
60
50
40
30
20
10
0
100-109
120-129
140-149
160-169
180-189
200-209
220-229
240-249
260-269
280-289
300-309
AMPLITUDE (pS)

for the periods of time that channel activity was observed at each V_j (~1 min), that the main-state i_j *vs* V_j is ohmic.

The open duration of main-state events were measured in four ATP-loaded poorly-coupled PPE cell pairs. Only single-channel events characterized by a direct opening from the fully-closed state to the main-state and uninterrupted by openings of other channels were selected for these measurements. Open durations ranged from 14 to 13300 msec for a mean of 753 ± 101 msec (n = 189 events).

In one typical poorly-coupled ATP-loaded cell pair the transition times between the fully-open and fully-closed state were measured (52 smooth transitions; sample frequency = 5 kHz). Transition times ranged from 1 to 29 msec with a mean of 5 ± 1 msec. The mean transition rate was 3 pA/msec. Similar numbers were obtained from 79 smooth transitions in one typical octanol-uncoupled PPE cell pair. Transition times ranged from 2 to 23 msec with a mean of 8 ± 1 msec.

Single-channel activity was sometimes observed to occur within cell pairs that, observed in phase-contrast in the light microscope, did not appear to be in contact. Whether the fine filopodia (with gap junctions at their tips) occurred before whole-cell recording or only formed when the cells were pulled apart (due to manipulator drift) is unknown. On several occasions cells of a pair were purposely manipulated several cell diameters apart yet still maintained junctional communication.

V.2.3 Substate Conductances

Substates of the main-state single-channel conductance occurred in PPE cell pairs as momentary shifts in channel conductance during main-state events (arrowheads Fig. V-3A a & d). In addition to this, substates occasionally appeared as steps or flickering during transitional periods of channel opening or closing (arrowheads Fig. V-3A c), or as separate channel events of smaller than main-state single-channel conductance (arrowhead Fig. V-3A b).

Substates occurring within main-state events as shown in Fig. V-3A a & d were analyzed by calculating each substate as a percent of the main-state single-channel conductance within which it was observed. All substate events were pooled from four ATP-loaded PPE cell pairs and grouped into 6 pS bins on a frequency histogram (Fig. V-3B). The substate frequency distribution was very broad. Events ranged from 4 to 86% of the main-state with an arithmetic mean 37 ± 1% (n = 544 events). The nonnormalized arithmetic mean was 90 ± 2 pS (n = 545 events). The mean duration of substate events measured within single level main-state events was 42 ± 2 msec (n = 536 events) ranging from 4 to 480 msec. These represent 6 ± 1% of the total open time of all 238 main-state events in which main-state duration could be estimated. 145 (or 60%) of the main-state events, often lasting many seconds in duration, did not display substates. If these are removed from the calculation of substate open time then substates represented

14 ± 2% (n = 93 events) of the main-state open time.

The other substate behaviour of these channels appeared, upon initial visual inspection of the data records, as a smaller conductance channel. This was observed in 1 recording of short duration in ATP-loaded, 1 recording in nonATP-loaded and in 4 recordings in octanol-uncoupled PPE cell pairs. Upon closer visual inspection in the two recordings on cell pairs not uncoupled with octanol it was observed that the smaller flickering channel activity was not present whenever the larger conductance channel opened (note the very quiet plateau of the large open channel in Fig V-3A c). This suggests that only one channel with large main-state single-channel conductance was present. The channel flickered between baseline and substate levels and only occasionally opened to the main-state. As multiple main-state channel openings (concurrent openings) were not observed in these 2 recordings, it is therefore likely that only one channel was active. In cell pairs not treated with octanol in which multiple channels were clearly active this smaller conductance flickering behaviour was never observed suggesting that this may just be a property of channels in destabilized junctions in very poorly-coupled cell pairs. In a 1 min recording from one already poorly-coupled ATP-loaded cell pair the small conductance activity had a mean conductance of 77 ± 3 pS (n = 118 events) representing 22% of the 348 ± 6 pS (n = 22 events) main-state.

In octanol-uncoupled ATP-loaded PPE cell pairs, in addition to partially-closed substates, flickering partially-opened behaviour was very prominent (Fig. V-4A). This flickering behaviour occurred much more frequently in the presence of octanol and occurred over a broader range of conductances between the fully-closed and fully-open level. No attempt was made to quantify this difference and only visual inspection was made of the data. Since these flickering transitions rarely reached a current plateau for longer than a few msec and often occurred during the opening or closing of the main-state events (see Fig. V-2B), they may represent a gating behaviour of the main channel (*i.e.* incomplete openings) which is enhanced in the presence of octanol.

V.2.4 Estimated Effect of Series Resistance on Single-Channel Conductance Measurement

The time course in series resistance changes was not monitored during single-channel experiments (since the recordings were so short). However, these data were collected during experiments where uncoupling kinetics were monitored (Chapter IV). From these data a reasonable range of error can be calculated. For example at 20 min post-break-in the maximum and minimum series resistances were 103 and 12 MΩ respectively (average initial R_s in 90 cell pairs was 14.3 ± 0.4 MΩ and at 20 min after break-in was 29.6 ± 1.5 MΩ). Even if R_s was 100 MΩ for each cell of the pair the calculated error in the measurement of a single-channel current (of about 5 pA) using

the equation in Chapter II section II.6 would be 5%.

V.3 Discussion

V.3.1 The Epidermal Single GJ-Channel Conductance is Large

The single-channel conductances measured for insect epidermal cells are among the largest that have been recorded. In vertebrates single-channel conductances range from 20 to 286 pS (see Table 2 for references). In mammalian heart values of 20 to 240 pS have been recorded with 100 pS or less being most common. In mammalian liver values range from 20 to 130 pS, 90 to 130 pS is most common. Of the remaining conductances that have been measured for vertebrates all are under 130 pS except for 286 pS measured in embryonic chick lens cell pairs.

In insects two other large conductance channels have recently been reported. These include the 345 pS GJ channel in cockroach hemocytes (Churchill *et al.* 1993, and Chapter VII) and the 365 pS channel in the *Aedes albopictus* mosquito cell line (Bukauskas & Weingart 1993). Previously, the mosquito channel was reported to be 166 pS (Bukauskas *et al.* 1991). This difference is probably due to different recording conditions as the larger conductance was measured during formation of gap junctions (Bukauskas & Weingart 1993) and the smaller conductance was measured in poorly-coupled cells that had already made contacts *in vitro* (Bukauskas *et al.* 1991).

A large single-channel conductance for insects is consistent with previous experiments using tracer molecules of

assorted sizes to estimate the limiting pore size(s) of the channels. The pore size in *Chironomus* salivary gland junctions was estimated to be 2 to 3 nm (Flagg-Newton *et al.* 1979; Schwarzmann *et al.* 1981; Zimmerman & Rose 1985) in contrast to a pore size in a variety of cultured mammalian cells of 1.6 to 2 nm (Flagg-Newton *et al.* 1979; Schwarzmann *et al.* 1981). In *Tenebrio*, techniques similar to those used by Zimmerman and Rose (1985) estimated pore size to be 2.4 to 3.4 nm (Safranyos 1985).

If it is assumed that the GJ channel has a uniform diameter along the length of the pore and the absence of electrostatic charges within or at the openings of the channel, the conductance of the channel can be calculated using the equation: $\gamma_j = \pi r^2 / (\rho \cdot L)$, where r is the pore radius, L is channel length, and ρ (Ωcm) is the resistivity of the pore fluid (Berdan & Caveney 1985). If channel length is taken as 20 nm (measured from thin section electron micrographs; Berdan & Caveney 1985), resistivity as 100 Ωcm (slightly greater than epidermal cytoplasm at 65 Ωcm; Caveney & Blennerhassett 1980) and channel radius as 1.5 nm (Safranyos 1985) then single-channel conductance would be about 350 pS. This value is in agreement with that measured in this study.

Previous estimations of single-channel conductance in *Tenebrio* using morphometric and whole-tissue electrophysiological data by Berdan & Caveney (1985) yielded a single-channel conductance of between 94 to 213 pS. This

suggests that their assumption that all the particles within gap junctional plaques were open GJ channels may not have been valid. This implies that channels in mature gap junctional plaques open and close under steady-state conditions in a manner similar to that seen in these recordings.

V.3.2 Smaller-Than-Main Conductance Activity Probably Fits a Partially-Closed Substate Model of Channel Gating

In addition to a large main conductance level, three distinctly different observations of lower conductance behaviour were observed.

The first of these appeared as a broad range of lower conductance states that interrupted main-state events (see Fig. V-3A a & d). In very poorly-coupled PPE cells, just before the end of complete spontaneous uncoupling, junctional current was zero much of the time interrupted with occasional discrete steps to the main conductance. During main-state openings the conductance often dropped briefly to lower conductance levels before returning to the main conductance level. The simplest interpretation of this observation is that a single large-conductance GJ channel opened to the fully-opened main-state and occasionally closed partially. Partially-closed states are stable since they remained at the lower conductances for up to 480 msec.

Criteria for defining channel substates has been outlined by Fox (1987). According to such criteria these would be

substates of the main-state of the channel, since substates occurred infrequently and interconverted directly with the main-state, were always observed in the presence of main-state activity, and could not be attributed to concurrent openings of 2 or more channels of small conductance that could sum to give the main-state conductance.

The second lower-than-main-state conductance activity involved flickering between the fully-closed state and lower conductance states interrupted by occasional complete openings to the main conductance level (see Fig. V-3A c). This behaviour would appear to fit the first two of the three criteria for substates since flickering occurred close to but never at the same time as main-state events. This is consistent with a single active channel that transits frequently between the fully-closed state and partially-open states and occasionally opens to the fully-open state. The term flickering is used here because this lower conductance activity was not stable. It did not plateau at one conductance and the peaks of each flickering event had a wide range of conductances.

The last lower-than-main-state conductance activity observed was flickering or distinct steps that occurred during opening and closing transitional periods of main-state events (see Fig. V-3A b and Fig. V-4A). In addition to this observation, smooth transitions for opening and closing between fully-open and closed states were normally slow (1 to

29 msec). Although it was difficult to measure transition times at sample frequencies faster than 5 kHz because of increases in background noise, transitions > 15 msec would still represent slow (msec) transitions at faster sample frequencies. Most nonjunctional ion channels and some GJ channels (Veenstra & DeHaan 1988) have fast transition times (μsec) reflecting the instability of the channel in any other but the opened and closed conformations. The slow transition times of epidermal and some other GJ channels (Neyton & Trautmann 1985; Chow & Young 1987; Rook *et al.* 1988; Rüdisüli & Weingart 1989) suggest that these may have multiple stable conformations and hence can transit through those states more slowly.

The observation of slow transition times, coupled with the multiplicity of partially-closed substate conductances and flickering transitional gating properties in epidermal channels, support a substate model of gating which states that GJ channels can open to any conductance between fully-open and fully-closed but usually have two or more preferential conducting states (Neyton & Trautmann 1985; Young *et al.* 1987; Rook *et al.* 1988). In support of this finding unstable flickering to less-than-main-state conductances and flickering during transitional periods of main-state channel openings, seemed to be increased during treatment with octanol. Although this was not determined quantitatively the differences were quite striking on visual examination of the data (compare Fig.

V-1 & V-2A to Fig. V-4A). Octanol most likely disturbs either directly or indirectly channel-lipid interactions (review: Burt 1991). Support for this view is the observation that alkanols such as octanol and other volatile anaesthetics can alter the activity of a broad range of junctional and nonjunctional channels (Johnston *et al.* 1980; Terrar & Victory 1988; Burt & Spray 1989; Nakahiro *et al.* 1989; Niggli *et al.* 1989) and other membrane associated proteins (*e.g.* protein kinase C; Slater *et al.* 1993). If octanol acts on membranes then the observation of increased flickering would support the substate model of gating since membrane perturbing agents could conceivably hinder conformational changes in gap junction proteins responsible for substate conductances.

V.3.3 Substate Gating is a Common Feature of Insect GJ Channels

The ability of a GJ channel to exhibit various substates may be a common feature of insect GJ channels. Recently, Bukauskas and Weingart (1993) have reported two distinct substates that are 1/5th and 1/7th of the 365 pS main-state channel in an *Aedes albopictus* cell line. The channel recordings from these cells appeared very much like those from the epidermis in having stable partially-closed interruptions during main-state events. These investigators examined single GJ-channel conductances during GJ formation. At the early stages of GJ formation there probably exists a short period of time when only one GJ channel is active. This condition is

attained in epidermal cells at the very end of spontaneous uncoupling. This greatly reduces the likelihood that multiple step conductances are due to the activity of separate channel populations with different conductances. In most cell preparations with multiple step conductances, however, it has proven difficult to distinguish between a substate model of gating or the presence of distinct channel classes.

V.3.4 Other Possible Models of Substate Gating

Although the partially-closed model of substate gating is favoured two other models must be considered. These are that multiple channel classes with different conductances or a cooperating subunit model of gating could be present. The first is unlikely since channel activity can be observed in epidermal cells when one or only a few channels are active. Also, only one main-state conductance was observed in any one cell pair. Independent channel classes with distinct conductances would rarely open in tandem to give main-state events with partially-closed states as observed here. Alternatively, multiple channels organized into small collectives with similar or different conductances could act cooperatively by opening in concert and occasionally closing individually. Six channels each with a 20 pS conductance would yield conductance states in 20 pS increments. Three units of 20, 35 and 90 pS would yield conductance states of 20, 35, 90, 55, 110, 125 and 145 pS. Observations of 6 and 4 equally spaced single-channel conductances have been made in chick

embryo cell pairs (Chen & DeHaan 1992) and in purified lens gap junctions (Zampighi *et al.* 1985). A possible argument against cooperative gating in the epidermis is the presence of a broad range of subconductance states rather than certain preferred discrete subconductances. Also, independent channel events with small conductances were never observed (excepting the flickering behaviour) which might be expected if there were subunits with different conductance.

V.3.5 Possible Functions of GJ-channel Substates in the Developing Insect Epidermis

It is possible that the behaviour of single-GJ channels during whole-cell recording is not representative of the properties of GJ channels in normal gap junctions where most of the channels are open and collected into plaques. It is possible that channels interact cooperatively (in a manner distinct from substate gating). For instance, in large plaques of tightly-packed gap junctions— ~2000 particles / μm^2 in *Tenebrio* epidermis (Berdan & Caveney 1985)—the conformational states of the channels may be stabilized. Changes in the state of a small number of the proteins may result in a concerted change in state of all the proteins. Destabilization may thus result in the substate gating observed in this study. Cooperativity has been proposed in the gating of patch-clamped septal membranes containing gap junctions from crayfish giant axons (Manivannan *et al.* 1992) and in antibody perturbation experiments in cardiac myocytes (Lal *et al.* 1993).

In spite of concerns that substate behaviour is an artifact of whole-cell recording it is conceivable that the permeability properties of an entire gap junction reflects the properties of the individual channels. Substates could be a physiologically modifiable behaviour of epidermal GJ channels. In the intact epidermis several observations have led to the hypothesis that epidermal GJ channels regulate the passage of different size classes of molecules (reviewed in Chapter I). These observations include the increase in electrical coupling with 20HE treatment without a concurrent increase in fluorescent tracer permeability, the nonsynchronous changes in electrical and tracer permeability during the insect moult cycle, and the selective permeability of gap junctions at segment borders where there is the maintenance of electrical coupling in the absence of tracer permeability.

Two models proposed to explain these observations include the existence of multiple channel classes with distinct conductances and permeabilities that undergo distinct regulation, and one class of channel that can be regulated to exhibit distinct permeabilities. The results in this chapter support the latter model. (Caution is advised, however. It is possible that other channel classes exist that do not survive cell isolation or 'shut down' earlier during spontaneous uncoupling). The substate model suggests that electrical coupling could increase without affecting tracer coupling if a closed population of channels opened to a substate that was

permeable to small inorganic ions but not larger molecules and, tracer movement between cells could be reduced or lost without a loss of electrical coupling if some or all the channels were shifted to a substate with reduced permeability to the larger molecules.

It is conceivable that subconductance states could also represent reduced permeability states to larger molecules provided that substates arise when a conformational change in a channel results in partial occlusion of a channel pore or the movement of charges within the pore. The conductance of a channel need not correspond to its permeability to larger molecules, however. Many nonjunctional-ion channels, the maxi-K^+ channel for instance, have a large conductance with a tiny selectivity filter that allows only the K^+ ion through (Jan & Jan 1989; Hille 1992) Present technology available for insects does not allow conductance and permeability to larger molecules to be determined simultaneously in a single population of GJ channels. However, the availability of specific connexin RNAs in vertebrates along with their transfection into communication incompetent exogenous expression systems (*i.e.* SKHep1 or N2A cells) may allow questions of this sort to be addressed.

V.3.6 Between-Experiment Variation in Main-State Single-Channel Conductance

In any one cell pair only one main-state conductance was found. However, between experiments the mean main-state

conductance varied from 197 to 403 pS. The source for this variation is unknown. It could reflect the expression of different populations of channel with different conductances in epidermal cells from different regions of the tissue. When using PPE cells, the region of the epidermal segment that any particular cell pair came from is not known. Another likely possibility is that the variation may be due to recording errors or to a single channel class that can exist at different apparent main-states. The evidence for only one channel class instead of multiple channels with distinct conductances includes: 1. all channels are closed with spontaneous uncoupling, 2. all channels are V_M dependent (Chapter VI), 3. all channels have similar transition times, open times, substate behaviour and overall patterns of activity, and that 4. treatment with octanol did not reveal multiple main-state single-channel conductance levels in individual cell pairs. The possible errors that could be expected due to series resistance were calculated to be only as large as 5%, thus it is unlikely that this alone can account for the variation.

In summary, at least one large-conductance GJ channel has been found in insect epidermal cell pairs. This channel had a variety of substates that under normal physiological regulation may account for the selectivity of gap junctional permeability that has been observed in intact epidermis. A partially-closed model explaining substate gating is favoured

although a cooperating subunit-type of substate gating cannot be ruled out.

VI VOLTAGE DEPENDENCE OF JUNCTIONAL CONDUCTANCE

VI.1 Introduction

This chapter describes the characterization of voltage dependence in epidermal cell pairs. GJ channels are distinct from nonjunctional-ion channels in that there are two instead of only one possible voltage axes across the structure (Fig. VI-1). The single voltage axis affecting nonjunctional-ion channels is the membrane potential or inside-outside voltage (called V_M or V_{I-O}). It is parallel to the long axis of nonjunctional-channel pores and extends from the inside to the outside of the cell. The two voltages across GJ channels are the transjunctional voltage (V_j) which is parallel to the long axis of the channel pore extending between the insides of neighbouring cells, and the membrane potential which is perpendicular to the long axis of the channel pore extending from the inside to the outside of the channel (or cell).

There are two main reasons for characterizing the voltage dependence of a gap junction. First, voltage dependence may be physiologically significant in the tissue. This may be determined by examining junctional sensitivity and the kinetic response to changes in voltage. Second, a careful biophysical characterization of a gap junction facilitates comparisons of these channels with those from other classes of organism and other insects.

Transjunctional (V_j) and membrane-potential dependent (V_M) gating has been described for gap junctions from a variety of

Fig. VI-1. Schematic diagram of two possible types of voltage dependence in gap junctions

Diagram shows segments of two closely apposed plasma membranes with a single GJ channel joining the cytoplasms of the adjacent cells (cell 1 & cell 2). V_j denotes the transjunctional voltage which extends parallel to the channel pore and V_M denotes the membrane potential or inside-outside voltage that probably exerts an effect perpendicular to the channel pore. A nonjunctional-ion channel is shown in cell 2. Only V_M affects these channels.

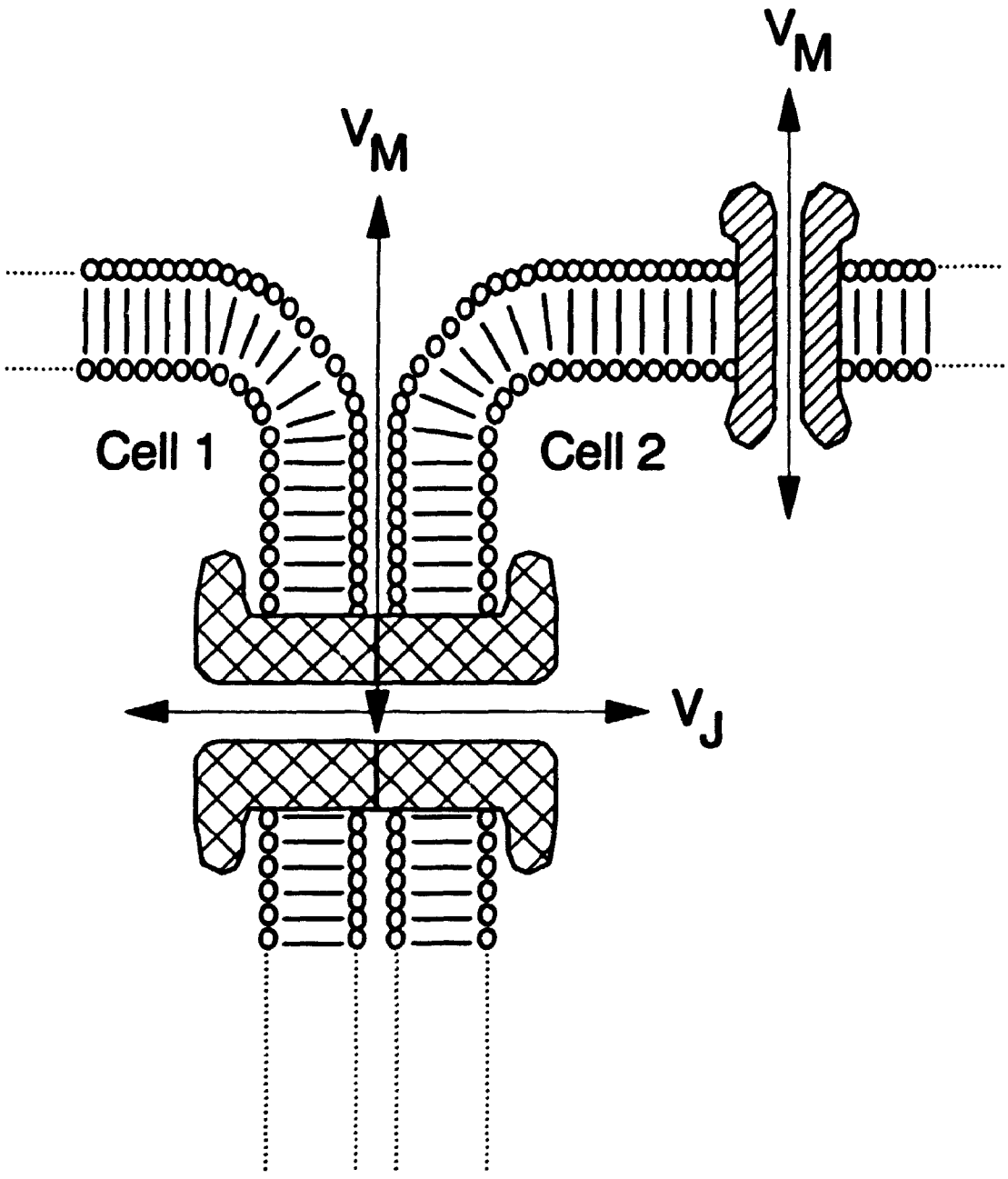
V_M
V_M
Cell 1
Cell 2
V_J

organisms (reviews: Spray *et al.* 1984; Spray & Bennett 1985; Spray *et al.* 1985; Neyton & Trautmann 1986b; Spray 1990; Spray *et al.* 1991a). V_j-dependent gating is the most common and is found in a variety of vertebrates and invertebrates. In contrast, V_M-dependent gap junctional gating has only been described in a few tissues. Voltage-dependent gating is absent in many preparations, including earthworm giant axon (Verselis & Brink 1984), adult mammalian ventricular cells (White *et al.* 1985), adult mammalian hepatocytes (Spray *et al.* 1986), pancreatic acinar cells (Somogyi & Kolb 1988), pancreatic β-cells (Pérez-Armendariz *et al.* 1991), frog lens epithelial cells (Cooper *et al.* 1989) and embryonic chick lens (Miller *et al.* 1992).

V_j-dependence can be either symmetric or asymmetric such that junctional conductance declines for either both or only one polarity of V_j (review: Spray *et al.* 1991a). The rectifying synapse of crayfish giant axons was the first voltage-dependent gap junction to be described in detail (Furshpan & Potter 1959). Depolarizing current only flows from the giant axon to the motor axon since V_j-dependence is asymmetric and since junctional conductance decreases rapidly (1 msec) to changes in transjunctional voltage (V_j) of the appropriate polarity (Giaume *et al.* 1987). Although many electrical synapses do not express V_j-dependence (*e.g.* Johnston & Ramon 1982; Verselis & Brink 1984) several examples of rectifying synapses have been identified in a variety of

invertebrates (Arvanitaki & Chalazonitis 1959; Auerbach & Bennett 1969; Smith & Bauman 1969; Nicholls & Purves 1972; Ringham 1975).

The earliest and most detailed description of a symmetrically V_j-dependent junction was in amphibian blastomeres (Spray *et al.* 1979; Harris *et al.* 1981; Spray *et al.* 1981). In this system junctional conductance is maximal at V_j = 0 mV (*i.e.* when both cells are held at the same voltage) and declines sigmoidally towards zero conductance when V_j's of either polarity are applied (*i.e.* irrespective of which cell is hyperpolarized or depolarized). These gap junctions exhibit the most sensitive steady-state response to changes in V_j of known gap junctions. Other V_j-dependent gap junctions with this type of voltage dependence include those in fish embryos (White *et al.* 1982), Rohon Beard neurons in *Xenopus* embryos (Spitzer 1982), and in poorly-coupled rat lacrimal gland cell pairs (Neyton & Trautmann 1985).

Some recent studies in mammalian heart (connexin43 based) and liver (connexin32 based) gap junctions are contradicting earlier reports that voltage dependence is absent in these tissues. Current to voltage relationships were linear in adult mammalian hepatocyte pairs (Spray *et al.* 1986; Spray *et al.* 1986; Reverdin & Weingart 1988), isolated connexin32 based gap junctions in bilayers in pipette tips (Spray *et al.* 1986) and connexin32 expressed in *Xenopus* oocytes (Dahl *et al.* 1987; Swenson *et al.* 1989). However, recent work in adult mammalian

hepatocyte cell pairs (Moreno *et al.* 1991a; Spray *et al.* 1991a), isolated gap junctions in bilayers (Young *et al.* 1987), isolated gap junctions in liposomes (Mazet *et al.* 1992), and in hepatoma cells transfected with connexin32 (Moreno *et al.* 1991a; Moreno *et al.* 1991b; Moreno *et al.* 1991c; Spray *et al.* 1992) supports the presence of V_j-dependence in liver gap junctions.

The literature on mammalian heart gap junctions is similar. Early studies on ventricular cell pairs from adult rat (Kameyama 1983; Metzger & Weingart 1985; White *et al.* 1985; Weingart 1986; De Mello 1991), adult guinea pig (Noma & Tsuboi 1987) and adult dog (Wu *et al.* 1993) failed to show voltage dependence. More recently, however, symmetrical V_j-dependence has been found in embryonic chick heart (Veenstra 1990), poorly-coupled neonatal cardiac cell pairs only at high voltages (Rook *et al.* 1988) and neonatal hamster cardiac cells at high voltage (Wang *et al.* 1992). Moreover, V_j-dependence, usually at V_j's > 40 to 50 mV, has been identified in other cell-types expressing connexin43, including mammalian astrocytes (Dermietzel *et al.* 1991; Giaume *et al.* 1991), corpus cavernosum smooth muscle (Moreno *et al.* 1993), adult mammalian SA nodal cells (Anumonwo *et al.* 1992), and hepatoma cells transfected with human Cx43 (Spray *et al.* 1992; Spray *et al.* 1993).

The reasons for these conflicting results in liver and heart gap junctions is unclear. Initially, before examples of

voltage dependence in adult (*e.g.* liver) or later embryonic tissues (*e.g.* neonatal heart) were known, it was suspected that embryonic tissues expressed voltage dependence and adult tissues did not. More recent hypotheses are directed at explaining why poorly-coupled cells exhibited voltage dependence while well-coupled cells did not (Neyton & Trautmann 1985; Rook *et al.* 1988; Veenstra 1990; Giaume *et al.* 1991). These possibilities include a cytoplasmic access resistance at the mouths of channel pores that reduces the V_j 'sensed' by individual channels (Wilders & Jongsma 1992), series resistance errors in very well-coupled double whole-cell voltage-clamped cell pairs that mask voltage dependence (Spray *et al.* 1991a), channel proteins in large gap junctions that interact to prevent voltage-gate related conformational changes (Mazet *et al.* 1992), or the regulation of voltage dependence by post-translational modifications such as phosphorylation (Moreno *et al.* 1992).

All insect gap junctions examined to date exhibits V_M-dependence. These include junctions between *Chironomus* salivary gland cell pairs (Obaid *et al.* 1983), *Drosophila* salivary gland cell pairs (Verselis & Bargiello 1991; Verselis *et al.* 1991), and a cell line from a mosquito, *Aedes albopictus* (Bukauskas *et al.* 1991). In these preparations depolarizing both cells drives junctional conductance towards zero and hyperpolarization of the cells increases conductance. Except maybe for *Chironomus*, these gap junctions all show some

degree of V_J-dependence in addition to V_M-dependence. The observation of V_M-dependence has not been restricted to insects however, as a small degree of V_M-sensitivity was described for squid blastomeres upon pharmacological treatment (Spray *et al.* 1984; Bennett *et al.* 1988), and in salamander rod photoreceptors (Stern & Macleish 1985). Recently, depolarization of both cells in mammalian liver (Spray *et al.* 1991a) and connexin26 transfected *Xenopus* embryos (Barrio *et al.* 1991; Rubin *et al.* 1992) resulted in a variable increase in junctional conductance.

The purpose of this chapter is to describe the characterization of voltage dependence of gap junctions in PPE cell pairs using double whole-cell voltage-clamp recording. Both V_J- and V_M-dependence in well-coupled cell pairs and in cell pairs with only a few active GJ channels will be described. The possible function of V_M-dependence in this tissue and comparison to the V_M-dependence found in other insects will be discussed. Reports of this work have already appeared in the literature (Churchill & Caveney 1993a,b)

VI.2 Results

VI.2.1 V_M-Dependence of G_J in Pharate Pupal Epidermal Cell Pairs

The effects of V_M on G_J was examined using the following protocol (Fig. VI-2A). V_H was held at -50 mV for both cells of a PPE cell pair and conditioning pulses of the same magnitude (+40 to -90 mV) and duration were supplied to both cells. G_J

Fig. VI-2. Macroscopic V_M-dependence of G_j

(A) Voltage (V_1 & V_2) and current (I_1 & I_2) traces are shown from an ATP-loaded PPE cell pair. V_H was -50 mV for both cells and conditioning pulses of -90 to +40 mV were applied simultaneously to both cells (conditioning pulses of 40, -50, -10, -50 and 10 mV are shown here). Conditioning pulse order was random. The duration of conditioning pulses were long enough to reach steady-state I_j. Test pulses (1 sec, 20 mV, 0.3 Hz) were supperimposed on the conditioning pulses and were applied alternately to both cells to monitor I_j. I_j was strongly dependent on V_M with I_j approaching 0 pA at V_M = +40 mV and increasing with hyperpolarization. Decay and recovery of steady-state I_j was faster and slower respectively with greater depolarization. The data for this figure were sampled from tape at 15 Hz.

(B) Average steady-state G_j / G_{jmax} *vs* V_M curve for 7 cell pairs. The dotted line joins the points. This curve was fit to a two-state Boltzmann relationship describing two independent gates in series (see equation in text section VI.2.1). The voltage at which half the gates are open (V_o) was -5.5 mV and, A, the constant expressing voltage sensitivity, was 0.050 (r^2 = 0.83). These values were used to generate the solid line displayed on the graph. The gating charge (z = ART / F) was estimated from A to be 1.3. These data suggest that steady-state G_j depends strongly on V_M.

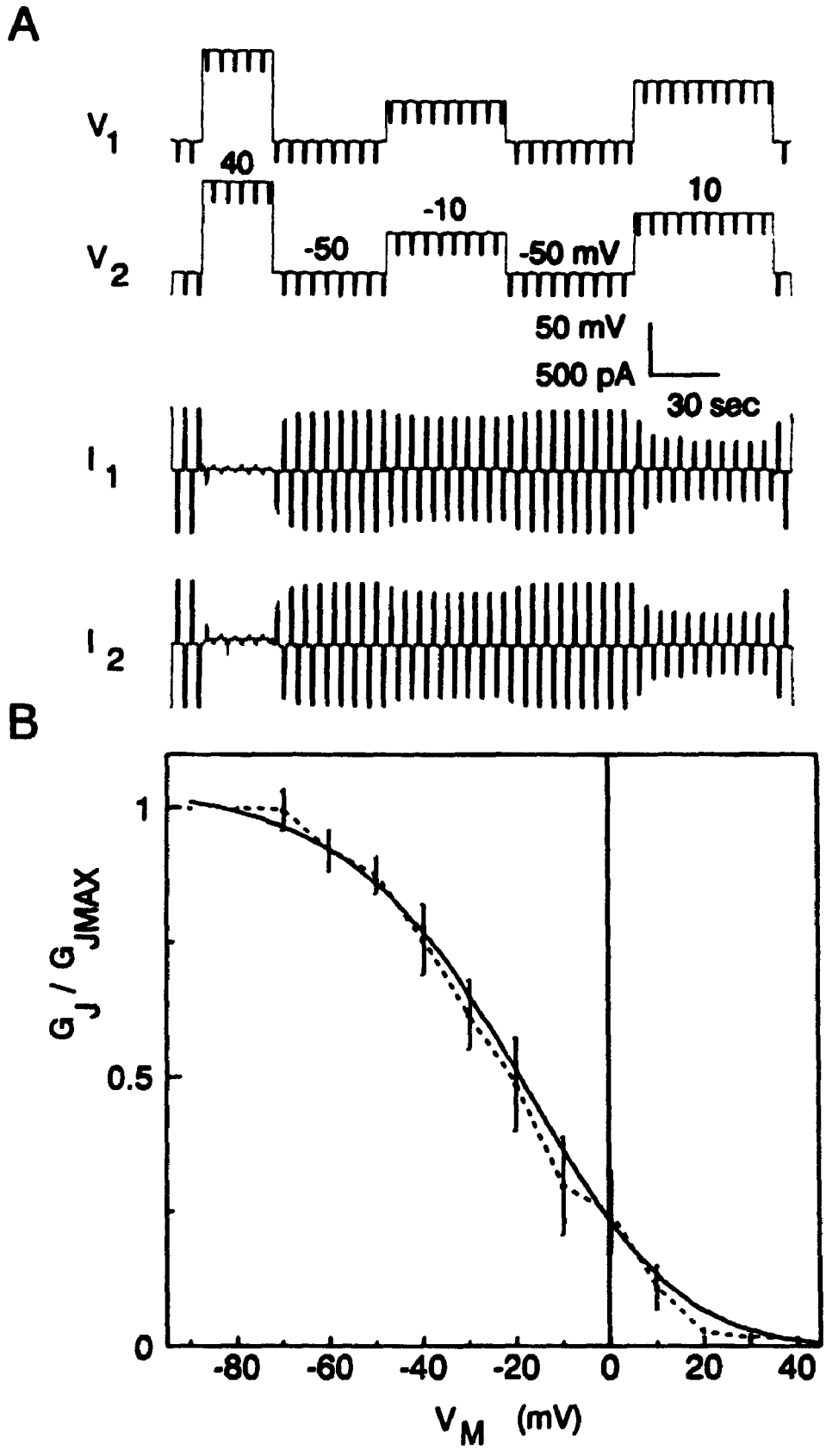
A
V1
40
V2
-50
-10
-50 mV
10
50 mV
500 pA
30 sec
I1
I2
B
1
0.5
0
GJ / GJMAX
-80
-60
-40
-20
0
20
40
VM (mV)

was monitored by superimposing hyperpolarizing 20 mV test pulses (1 sec, 0.3 Hz) on the conditioning pulses. The test pulses alternated between cells to rule out one-sided artifacts. Conditioning pulse duration was under the experimenter's control so that V_M was changed only when steady-state was reached. G_j was corrected for series resistance errors (see Chapter II) and for uncoupling by using a factor which was based on the ratio of the initial G_j at V_M = -50 mV following break-in and G_j at V_M -50 mV just before the conditioning pulse. The long time required to reach each new steady-state resulted in these experiments lasting from 15 to 30 min, during which time substantial uncoupling occurred (Fig. IV-1(B)).

Fig. VI-2B is a sample set of traces showing the effect of V_M on G_j. A conditioning pulse of +40 mV resulted in a decrease in steady-state I_j to near 0 pA with a time course of less than 6 sec. Upon restoration of V_M to -50 mV recovery of steady-state I_j was slow, taking from 18 to 24 sec. Depolarization to +10 mV in this example resulted in a 30 to 40% drop in steady-state I_j with a slower time course of 15 to 18 sec. A -10 mV conditioning pulse resulted in only a slight decrease in steady-state I_j occurring with a slow time course (9 to 12 sec). In general, the restoration of steady-state I_j upon return of V_M to -50 mV occurred more slowly than the decay with depolarization. The decay and recovery of steady-state I_j was faster and slower, respectively, with larger

depolarizing conditioning pulses. Hyperpolarizing conditioning pulses generally resulted in small increases in steady-state I_J with slow time courses (> 10 sec). The contribution of nonjunctional currents during conditioning pulses were very small, as seen by the small upward deflections in the overall holding current of both cells with changes in V_M in Fig. VI-2A. This is supported by whole-cell recordings from single unpaired PPE cells (Chapter V).

The mean steady-state G_J response for 7 cell pairs, was normalized to the maximal steady-state G_J (G_{Jmax}) and plotted on a steady-state G_J / G_{Jmax} *vs* V_M curve (Fig. VI-2B). The steady-state G_J curve approached 0 nS at V_M positive to 0 mV and increased sigmoidally at V_M < 0 mV. The mean voltage at half-maximal steady-state G_J was -26 ± 4 mV (n = 7 cell pairs) ranging from -8 to -39 mV. For comparison to similar data from other insect cell pairs, this curve was fit to a previously described two-state Boltzmann relationship for two independent gates in series (Obaid *et al.* 1983; Verselis *et al.* 1991):

$$G_J = \frac{G_{Jmax}}{\left(1 + e^{A(V_M - V_o)}\right)^2}$$

where G_{Jmax} is the maximal steady-state G_J attainable at negative membrane potentials (set to 1), V_o is the V_M at which half the gates are open and A is a constant describing the steepness of the relationship. The assumptions in Boltzmann models used to model the macroscopic steady-state behaviour of

voltage-dependent channels are: 1. channel gating is a two step (open-close) first order process, 2. all channels have equal opening and closing rate constants, and 3. the channels gate independently of one another. The data were graphed as $\log((G_{Jmax} / G_J)^{½} - 1)$ *vs* V_M and fit using a linear least-squares method in order to find the best fit values for V_o (V_M at $(G_{Jmax} / G_J)^{½} - 1 = 1$) and A (slope = A / 2.3). A curve was generated from the fit values for display (Fig. VI-2B, solid line). The fit values for the averaged curve were A = 0.05 and V_o = -5.5 mV (r^2 = 0.83). The best fit values (r^2 > 0.9) for the individual curves ranged from 0.047 to 0.083 for A (mean 0.057 ± .004) and -22.0 to +12.7 mV for V_o (mean -4.8 ± 4.5 mV). The average gating charge was z = 1.5 ± 0.1, determined from z = ART / F, where R is the ideal gas constant, T the absolute temperature in degrees Kelvin and F is Faraday's constant. These data suggest that G_J depends strongly on V_M during steady-state conditions.

VI.2.2 V_J-Dependence of G_J in Pharate Pupal Epidermal Cell Pairs

The effects of V_J on G_J was examined using a voltage protocol in which both cells of the pair were voltage-clamped at -50 mV and one of the cells was stepped through a series of voltage pulses. 30 sec randomly applied square test pulses from +50 to -100 mV in 10 mV increments were applied to one cell generating transjunctional voltages of +100 to -50 mV. Between the test pulses, which were from 30 to 60 sec apart,

the degree of coupling was monitored by applying hyperpolarizing -20 mV pulses (1 sec, 0.3 Hz) alternately to either cell as in the above experiments on V_M-dependence. This also allowed monitoring of recovery of I_j from the test pulse to the -50 mV holding potential so that the next test pulse was not applied until a new steady-state was reached. Instantaneous and steady-state G_j (at the beginning and end of the 30 sec test pulse respectively) was calculated and corrected for R_s errors and for uncoupling as described for G_j *vs* V_M experiments.

Fig. VI-3A shows sample current traces from one cell of a pair at a range of V_j with the V_H = -50 mV for both cells of the pair. The voltage of cell 1 (V_1) was changed during the test pulse. With strongly depolarizing pulses I_j decayed in a time-dependent manner. Decay was faster as depolarization increased. At V_j = ±20 mV little if any time-dependent decay was observed. At V_j < -30 mV a gradual and very small time-dependent increase in I_j occurred (15 to 30 sec; in other cells this time-dependent increase was more pronounced). In this example, even with V_j > +90 mV, there remained a substantial steady-state I_j. In one cell pair in which V_j > +120 mV, a substantial residual steady-state I_j still remained. It was found that time-dependent decay of G_j with hyperpolarizing V_j test pulses occurred when the overall holding potential (V_H) was more positive than -50 mV. In Fig. VI-3C an example of junctional currents from one cell of a

Fig. VI-3. Macroscopic V_j-dependence of G_j

(A) Current traces from one cell of a PPE cell pair with ATP in the pipette solution are shown. V_H was -50 mV for both cells and 30 sec square test pulses were applied to cell 1 (*i.e.* V_1 = +50 to -100 mV). V_1 and V_j are shown at the left. Depolarizing pulses resulted in time-dependent decay of I_j. Decay was faster the greater the depolarization. At V_j = ± 20 mV there was little time-dependent decay in I_j. At V_j < -20 mV often a very slight and gradual time-dependent increase in I_j was evident (note dotted lines on traces at V_j's of -30 and -50 mV). At V_j = +90 mV, there was still a large steady-state I_j.

(B) Average instantaneous and steady-state G_j / G_{jmax} *vs* V_j curves from 7 cell pairs. The instantaneous G_j / G_{jmax} *vs* V_j curve (•) was nearly linear with a decreasing trend in instantaneous G_j / G_{jmax} at V_j > -10 mV. Steady-state G_j (■) decreased with depolarization and increased with hyperpolarization. At V_j < -10 mV steady-state G_j / G_{jmax} again decreased suggesting that V_j has some effect on steady-state G_j. The asymmetry of the curve and the residual steady-state G_j at V_j > 0 mV suggests that V_M is the stronger determinant of steady-state G_j with changes in V_j.

(C) Effect of V_H on time-dependent decay of I_j with hyperpolarizing V_j test pulses. -40 mV V_j test pulses were applied from V_H = 0, -20 and -40 mV to ATP-loaded cell pairs. The holding voltages of each cell during the V_j test pulse, V_1 and V_2, are shown at the top of each trace. Increasing hyperpolarization of both cells resulted in the decrease of time-dependent decay in the current and an increase in steady-state I_j. These data suggest that the V_M and V_j-dependent gates interact, with V_M being the main determinant of G_j.

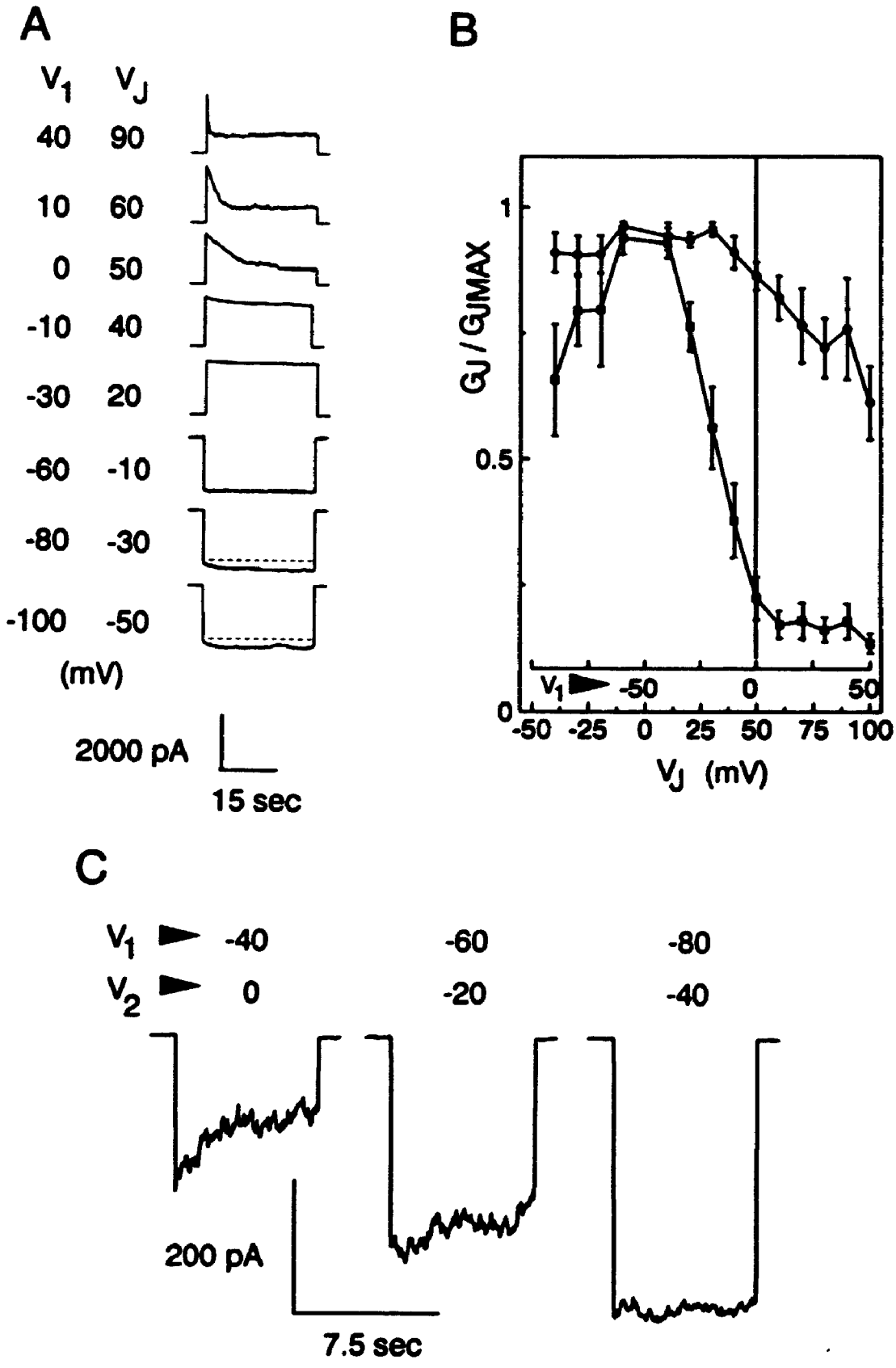
A
V1 VJ
40 90
10 60
0 50
-10 40
-30 20
-60 -10
-80 -30
-100 -50
(mV)
2000 pA
15 sec
B
GJ / GJMAX
1
0.5
0
V1
-50
0
50
-50 -25 0 25 50 75 100
VJ (mV)
C
V1
V2
-40
0
-60
-20
-80
-40
200 pA
7.5 sec

pair are shown in response to a hyperpolarizing 40 mV V_j test pulse (7.5 sec duration) applied from 3 different V_H's (0, -20, -40 mV). Time-dependent decay in I_j was dependent on the overall V_H of the two cells with increased hyperpolarization decreasing the rate of decay. The same relationship was found for depolarizing V_j test pulses as hyperpolarization of the V_H of both cells decreased the rate of time-dependent decay (data not shown).

Both the instantaneous and steady-state G_j were normalized to $G_{j_{max}}$ (instantaneous and steady-state $G_{j_{max}}$ respectively) and graphed against V_j. Fig. VI-3B plots the average instantaneous and steady-state G_j / $G_{j_{max}}$ *vs* V_j curves from 7 cell pairs. The instantaneous G_j / $G_{j_{max}}$ *vs* V_j curve (Fig. VI-3B) was mostly linear, although a decreasing trend in G_j / $G_{j_{max}}$ at V_j > -10 mV was apparent. This may be due to the difficulty of estimating instantaneous current since the multiple and very slow time constants of the decay made curve-fitting difficult. Maximum I_j was instead taken as instantaneous I_j. The steady-state G_j / $G_{j_{max}}$ *vs* V_j curve (Fig. VI-3B) shows that, as seen in the response to V_M, steady-state G_j increased upon hyperpolarization and decreased with depolarization of one cell. In this case however, $G_{j_{max}}$ was reached at about V_j = 0 mV followed by a decline at V_j < -10 mV. This decrease in steady-state G_j, coupled with the time-dependent decay of I_j with hyperpolarizing V_j test pulses when the overall V_H was less than -50 mV suggests the presence of

V_j-dependent gating. However, the asymmetry of the steady-state G_j / $G_{j_{max}}$ *vs* V_j curve, the residual steady state G_j at V_j > 0 mV, and the loss of the time-dependent decay of I_j with hyperpolarizing V_j test pulses when the overall hyperpolarization of both cells was greater than -50 mV, all suggest that V_M is the major voltage dependence determining G_j in these cells.

VI.2.3 Voltage Dependence of Single-Channel Activity in Pharate Pupal Epidermal Cell Pairs

The effects of voltage on single-channel activity was examined using a pair of voltage protocols on cell pairs which had spontaneously-uncoupled (ATP-free pipette). In the first protocol both cells of the pair were clamped at holding voltages between +20 to -20 mV creating a starting transjunctional voltage of 0 or 20 mV. The potential of only one cell was then hyperpolarized in a staircase of 10 mV steps every 20 sec thereby increasing V_j with each step. Upon completing this protocol, a second was begun in which both cells were clamped at holding voltages between +20 and -20 mV creating a transjunctional voltage of 20 mV. Both cells were then hyperpolarized in 10 mV steps maintaining a constant transjunctional voltage of 20 mV. Because the cell pairs were uncoupling during the recording, the number of active channels was slowly decreasing. Each protocol took 2 to 3 min with a 1 to 2 min break in between.

Fig. VI-4A shows sample traces from one cell pair. In the

top set, only one cell (cell 1) was hyperpolarized in staircase fashion, and in the bottom set both cells were hyperpolarized. When both cells of the pair were at more depolarized voltages there was little or no channel activity. As either one (top set of traces) or both cells (bottom set of traces) were hyperpolarized channel activity increased. The open channel probability in relation to cell voltage was estimated by graphing the average NP_o at each voltage level for 8 cell pairs (Fig. VI-4B). To determine NP_o (where N is the number of channels and P_o the probability of opening) the mean current (I) during each 20 sec voltage step was calculated by averaging the total current above baseline current and dividing it by i_j, the single-channel current level. Each NP_o value was normalized to the maximal NP_o recorded for that cell pair and graphed against the voltage of the most hyperpolarized cell of the pair (V^*). Hyperpolarization of one or both cells resulted in an increase in channel activity (Fig. VI-4B). These data also show that hyperpolarizing membrane potentials affect G_j in well-coupled cells by changing channel activity with hyperpolarization of both cells increasing channel activity more than if only one cell was hyperpolarized.

VI.3 Discussion

VI.3.1 Why Use Pharate Pupal Cells to Examine Voltage Dependence?

As discussed in earlier chapters isolated PPE cells have

Fig. VI-4. Voltage-dependence of single-channel activity

(A) Current traces from one cell of a pair without ATP in the pipette solution are shown. The voltages of each cell (V_1 & V_2) are shown at left. The top set of current traces were generated by holding both cells at 0 mV and then hyperpolarizing V_1 in staircase fashion; the voltage dropped by 10 mV with each 20 sec step. The bottom set of traces was generated following the completion of the first set. Here both cells of the pair were hyperpolarized while maintaining V_j = 20 mV. In both cases channel activity increased with hyperpolarization.

(B) Average NP_o *vs* voltage of most hyperpolarized cell of a cell pair (V^*) for 8 cell pairs (normalized to the maximal NP_o for each cell pair). Hyperpolarization of one (•) or both cells (■) of a pair increased channel activity. Pairwise hyperpolarization increased channel activity more than one-sided hyperpolarization.

A

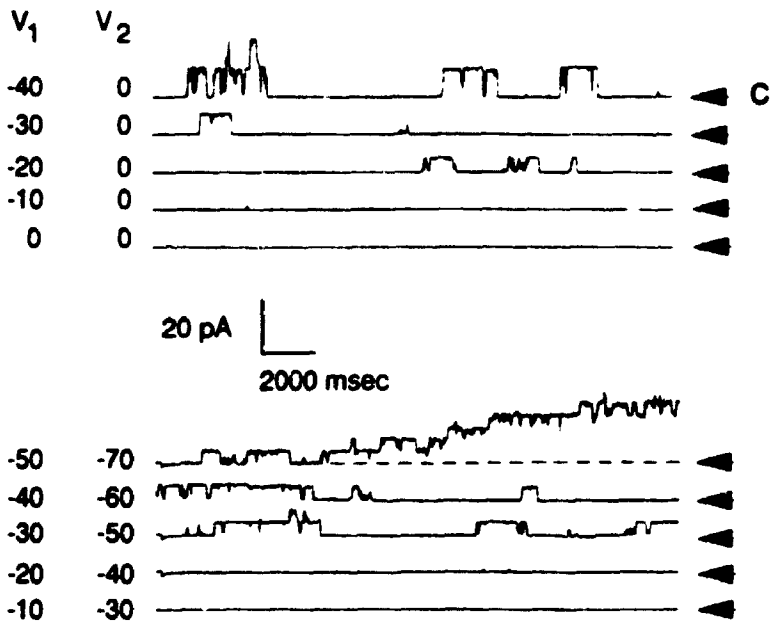
V1
V2
-40
0
-30
0
-20
0
-10
0
0
0
C
20 pA
2000 msec
-50
-70
-40
-60
-30
-50
-20
-40
-10
-30

B

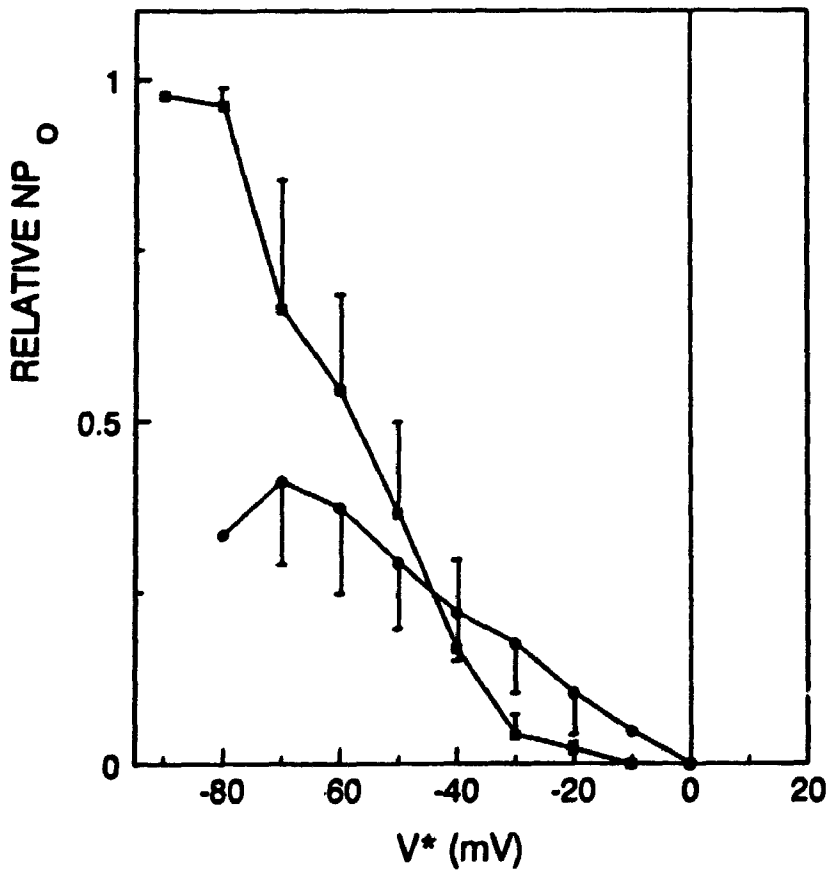
RELATIVE NP o
1
0.5
0
-80
-60
-40
-20
0
20
V* (mV)

several properties that facilitate biophysical characterization of junctional conductances (Chapter III). These include the absence of nonjunctional voltage-dependent conductances, and the relative ease that single-channel activity can be obtained during spontaneous uncoupling. Besides these reasons the relatively low junctional conductances in PPE cell pairs *vs* NME cell pairs (Chapter III) reduces the effects of series resistance errors. By example, voltage-clamp errors due to series resistance errors were so large that voltage dependence was not originally found in double whole-cell voltage-clamped hepatocytes having junctional conductances of 1 μS (Spray *et al.* 1986; Reverdin & Weingart 1988). More recent experiments on adult hepatocytes that eliminated the series resistance problems of patch-pipettes by using dual voltage clamp with four intracellular microelectrodes uncovered both V_M- and V_j-dependence (Moreno *et al.* 1991a; Spray *et al.* 1991a).

Preliminary experiments in NME cell pairs (data not shown) exhibit a similar V_M-dependence to that described for PPE cell pairs. The voltage at half-maximal conductance for the response in NME cell pairs, however, is highly variable with the V_M at half-maximal conductance often being more positive than in PPE cell pairs. Although this may be a physiological difference between PPE and NME tissue it may also be due to increased series resistance or cytoplasmic access resistance errors due to larger junctional conductances

in NME cells.

VI.3.2 Membrane-Potential Dependence Predominates in Insects

G_j in *Tenebrio* gap junctions is strongly-dependent on V_M. A similar dependence has been reported in gap junctions in three other insect tissues, *Chironomus* (Obaid *et al.* 1983) and *Drosophila* salivary gland cell pairs (Verselis & Bargiello 1991; Verselis *et al.* 1991), and cultured mosquito cells (Bukauskas *et al.* 1991). In each case G_j increased sigmoidally with hyperpolarization of both cells of a pair and approached zero with paired depolarization. These steady-state responses to V_M were essentially the same in each tissue although the A, V_o, and z obtained from the fit of a two state Boltzmann equation modelling two independent V_M-dependent gates in series were slightly different (data not available for the mosquito). In *Chironomus* and *Drosophila*, A, the constant expressing voltage sensitivity, was around 0.08 mV^{-1}. This corresponds to an equivalent gating charge ($z = ART / F$) of approximately 2 with the open probability of each hemichannel having a limiting slope of *e*-fold per ~12 mV. In epidermal tissue the response was less sensitive with A = 0.057 mV^{-1}, z = 1.5 and a limiting slope of *e*-fold change occurring every ~20 mV. All these values are comparable to nonjunctional-ion channels (Hille 1992) and are less voltage sensitive than that found in amphibian blastomeres where A = 0.2 mV^{-1} (Spray *et al.* 1981).

VI.3.3 Both Membrane-Potential and Transjunctional-Voltage Dependence are Present in these Gap Junctions

In all these insect cell pairs in which V_M-dependence has been described (*Chironomus, Drosophila, Aedes and Tenebrio*, as cited in the previous paragraph) both V_M- and V_j-dependence are present. In *Chironomus* salivary gland cell pairs V_M-dependence was suggested to be the only voltage dependence in these junctions (Obaid *et al.* 1983). In *Drosophila* salivary gland cell pairs however, these results have been re-evaluated and both V_M- and V_j-dependence was found (Verselis & Bargiello 1991; Verselis *et al.* 1991). The evidence for the presence of V_j-dependence in *Aedes*, *Drosophila* and *Tenebrio* include the observation that depolarizing and strongly hyperpolarizing V_j pulses resulted in a time-dependent decay in I_j. Furthermore, the steady-state G_j *vs* V_j curve was bell-shaped, decreasing at strongly hyperpolarizing V_j. This curve was however, asymmetric about 0 mV in all cases supporting the suggestion that although V_j-dependence is present, V_M-dependence was the major determinant of junctional conductance.

It is clear from these results that the gap junctions, in *Tenebrio*, as in *Drosophila*, are sensitive to both V_j- and V_M. If the most likely assumption is made that both V_j- and V_M-dependencies reside as physical domains within the channels (*i.e.* as 'gates'), as is the case with nonjunctional channels (Jan & Jan 1989; Hille 1992), it is interesting to speculate whether V_j- and V_M-dependent gates reside together in the same

or separate channels and whether there is interaction between them (see also discussion Verselis & Bargiello 1991; Verselis *et al.* 1991). It is probable that all channels within the gap junction possess a V_M-dependent gate since depolarization of both cells reduces conductance to zero. However, neither depolarization or hyperpolarization of only one cell during experiments on V_j-dependence reduces conductance to zero thus leaving a V_j-independent residual. The reason for this is unknown and has been found in every V_j-dependent gap junction studied to date (Spray *et al.* 1991a).

Several hypotheses for the presence of the V_j-independent residual conductance have been advanced: 1. the inability of generating large enough voltage pulses; 2. V_M-dependent gates reside in all channels but V_j-dependent gates reside in only a subpopulation of channels; 3. V_M-and V_j-dependent gates both reside in the same channel but there is the presence of a minimum V_j-independent subconductance state; 4. V_M-and V_j-dependent gates both reside in the same channel but there is the presence of a nonzero minimum open channel probability with V_j. In addition to these possibilities the situation in the insect gap junctions is further complicated by the presence of V_M-dependence. It must then be asked whether interaction between the two gates each present in the same population of channels results in the V_j-independent residual.

In the epidermis, it has been possible to provide depolarizing V_j pulses of 120 mV from a holding potential of

-50 mV with minimal damage to the cells. Thus, the possibility that large enough V_j pulses were not generated is unlikely in this tissue. At present there is very little evidence to clearly support any one of the remaining hypotheses. Although feasible, the evidence against the presence of a separate V_j-independent population of channels is that only a single channel type, as described by its single-channel conductance and overall pattern of activity, was found in each cell pair studied under either spontaneous or octanol-uncoupling conditions.

There is some evidence in epidermis and other tissues for the possibility of a V_j-independent subconductance state. With the present technology this can only be addressed by examining GJ-channel activity in poorly-coupled cells for V_j-dependent changes in conductance or channel activity. Although partially-closed substates have been described for epidermal gap junctions it has not been possible to obtain single-channel data at V_j's relevant to the V_j-independent residual since the channels remain active for short periods of time.

Very recently, the presence of substates has been demonstrated in an insect cell line from *Aedes albopictus* as well (Bukauskas & Weingart 1993). Their results, presented in two short communications, suggest that V_j does not affect the activity of the channel main-state but does affect the dwell time of various substates (Bukauskas & Weingart 1993). These substate 'residuals' (1/6th of the main-state) were present

during the initial stages of GJ formation at V_j's of 8 to 70 mV (Weingart & Bukauskas 1993). These results suggest that substates of GJ channels can exist at a range of voltages and supports the hypothesis that GJ channels do not fully close at large V_j. In support of this notion Chen and DeHaan (1992) have presented data suggesting that V_j-dependent decline of conductance in chick embryo cardiac cell pairs arises from a shift from higner to lower single-channel conductance states.

The V_j-insensitive residual could result from the interaction between the two types of voltage gate in an individual channel (influencing open probability or channel conductance). There is evidence from the epidermal cell pairs supporting gate interaction. There was a reduction of the time-dependent decay in G_j that occurred in response to large hyperpolarizing V_j test pulses when the holding potential was less than about -40 mV and an increase in decay when the holding potential was more depolarized (Fig. VI-3C). This indicates that V_j does not act alone in determining the kinetics of the response to the V_j pulse. Instead the response is influenced by the nonjunctional membrane potentials at which the cells are clamped. It is not unreasonable to expect that a conformational change occurring due to activation of one voltage gate could influence the voltage-dependent response of the other gate. Kinetic analyses have been done in *Drosophila* (Verselis & Bargiello 1991; Verselis *et al.* 1991) to support interaction between the V_j- and V_M-dependent gating

mechanisms in determining G_j.

VI.3.4 Membrane-Potential Dependence of Single GJ-Channel Activity

This has been the first study to examine V_M-dependence at the level of single-GJ channels. When poorly-coupled PPE cell pairs were hyperpolarized near the end of spontaneous uncoupling an increase in channel activity was observed. This was detected as an increase in the number of open channels. Single-channel conductance was not observed to change with changes in voltage. With the multichannel data presented here it is impossible to determine if this involved just a change in the probability of channels being open or additionally, an increase in the open time of individual channels. Therefore, channel activity was expressed as the product of the number of channels (N) and the probability of channel opening (P_o) *vs* voltage. Macroscopic junctional current (I) depends both on N, the current through a single channel (i_j) and P_o as defined in the relationship $I = N \cdot P_o \cdot i_j$.

There is the possibility in some cell types that voltage dependence acts indirectly through $[Ca^{++}]_i$ to gate channels. Changing the membrane potential could activate voltage-gated calcium channels or a membrane-potential dependent intracellular calcium release that increases $[Ca^{++}]_i$ and in turn closes channels. This mechanism probably cannot explain voltage dependence in *Tenebrio* since the intracellular pipette solution contained EGTA at 10 mM (free $[Ca^{++}] = 10^{-8}$ M).

Intracellular Ca^{++} would have been chelated by the EGTA once the membrane was broken open and the intracellular pipette solution was equilibrated with the intracellular contents.

VI.3.5 Does Voltage Dependence have a Physiological Role?

The average V_M at half-maximal conductance in *Tenebrio* was -26 mV. As this lies within the normal range of membrane potential in the intact epidermis (Caveney & Blennerhassett 1980), V_M could play a role in controlling the overall tone of junctional conductance. Any mechanism that regulates the membrane potential of the tissue could in turn control coupling. A limited amount of experimental evidence suggests that membrane potential can affect junctional resistance in intact *Tenebrio* and *Oncopeltus* epidermis (Blennerhassett 1984).

There is reason for caution in extrapolating voltage-dependence data from double whole-cell voltage-clamped cell pairs to intact tissue. First, Obaid *et al.* (1983) in *Chironomus* have demonstrated that cytoplasmic conditions affecting pH_i and pCa_i determine V_o of the V_M-dependent response. This suggests that internal perfusion of cytoplasm during whole-cell voltage clamp could affect the measurement of the V_M at half-maximal conductance. Preventing washout of cytoplasm during whole-cell recording by using the perforated patch technique would address this problem (Horn & Marty 1988).

Second, junctional conductances of 0 to 95 nS in isolated

PPE cell pairs (Chapter III) is less than the calculated values between any two cells in the intact *Tenebrio* epidermis. Berdan & Caveney (1985) estimated that there were 15,000 junctional channels between a pair of adjacent cells in intact *Tenebrio* epidermis. Assuming all of the channels to be open with a single-channel conductance of 300 pS, then a junctional conductance of 4500 nS is predicted between native cell pairs. Therefore, the gap junctions in isolated cell pairs have < 5% of this junctional conductance. In lacrimal gland, heart, and astrocytes voltage dependence was detected in poorly-coupled cells but not in well-coupled cells (Neyton & Trautmann 1985; Rook *et al.* 1988; Veenstra 1990; Giaume *et al.* 1991). This could be due to technical problems with whole-cell recording (discussed in the introduction to this Chapter). Alternatively, there could be differences in the proportion of the electric field sensed by each channel in large *vs* small gap junctions (Jongsma *et al.* 1991) or, channels in large gap junctions may interact preventing conformational changes necessary for voltage-dependent gating (Mazet *et al.* 1992). Thus, although a certain gap junction protein may be endowed with a voltage-dependent gate, it may only be a functional gate under certain circumstances.

In spite of these warnings, roles for voltage dependence in whole tissue may still be suggested. In addition to membrane potential regulating the overall level of coupling in an entire tissue, a gradient of cell-cell coupling could be

created by a gradient of membrane potential across a population of cells (review: Bennett *et al.* 1981). One possible mechanism for this is the bioelectric current fields that are generated in and around developing oocytes and embryos, such as in insect oocytes (Diehl-Jones & Huebner 1993). These transcellular fields have been proposed to play a role in establishing developmental pattern (Jaffe 1981) and one way it could do so is via the voltage dependence of gap junctions. Finally, the strong V_j-sensitivity of frog blastomere gap junctions suggests that voltage dependence may control gap junctional communication during early development (Harris *et al.* 1983). The current-voltage relationship in blastomeres includes both bistability and hysteresis thus, brief changes in nonjunctional current between neighbouring cells could shift coupling to more or less stable conductance states thereby creating communication compartments.

In conclusion, epidermal gap junctions exhibited sensitivity to both membrane potential and transjunctional voltage. The data presented in this chapter demonstrate that there are strong similarities in the complex voltage-dependent gating properties of GJ channels in several insect cell types. This strong sensitivity to membrane potential, coupled with the relatively larger single GJ-channel conductances (Chapter V) suggests that there is an insect 'family' of gap junction proteins distinct from the vertebrate class of connexin-based GJ channels. This is supported by the lack of crossreactivity

of vertebrate connexin probes with insect tissue and heterologous coupling between hemocytes from different insect groups (Churchill *et al.* 1993).

VII GAP JUNCTION FORMATION IN COCKROACH HEMOCYTES

VII.1 Introduction

Hemocytes circulate freely in insect blood. They are chiefly responsible for at least two facets of the cellular immune response; phagocytosis of bacteria and other small invaders in the hemocoel, and encapsulation of larger foreign invaders such as parasites (review: Götz 1986). Encapsulation involves the surrounding and encasing of too-large-to-be-phagocytosed invaders of the hemocoel with many layers of adherent and highly flattened hemocytes (Grimstone *et al.* 1967; Götz 1986). During encapsulation hemocytes form various intercellular junctions with each other, including gap junctions, thus forming solid tissues in which only the innermost cells die (Baerwald 1975; Norton & Vinson 1977; Han & Gupta 1989). The presumed role of these gap junctions is to provide a direct intercellular pathway for the transport of nutrients to the inner cell mass (Pitts 1977). In the American cockroach, *Periplaneta americana,* gap junction-like plaques were present on freeze-fracture replicas of 48 hour-old hemocyte capsules (Baerwald 1975) and strong dye- and electrical-coupling was found in 72 hour-old hemocyte capsules (Caveney & Berdan 1982). In both cases the capsules were formed around synthetic material implanted in the hemocoel.

The *in vitro* formation of cockroach hemocyte gap junctions was demonstrated by fellow graduate student Sheppy Coodin in our lab (Churchill *et al.* 1993). This included the

discovery of small gap junction-like aggregations of E-faced particles (plaques) on freeze-fractured clumps of hemocytes that formed within 5 min of bleeding the cells. In addition, dye-transfer was detected between dye-loaded and unloaded cells within 3 min of the unloaded hemocytes being bled and immediately mixed with the dye-loaded cells. This rapid formation suggested that these cells are primed to make gap junctions soon after contact. In this chapter whole-cell voltage clamp was used to determine precisely when after initial contact the first functional GJ channels formed.

Early work on gap junction formation (GJ formation) used intracellular microelectodes to measure electrotonic and dye-coupling and showed that a wide variety of cell types are capable of forming gap junctions within 0.7 to 30 min of cell-to-cell contact (reviews: Revel *et al.* 1978; Bennett *et al.* 1981; Loewenstein 1981). Analysis of this early work suggested that gap junctions formed spontaneously on contact, on any location of the cell membrane (*i.e.* does not require a specialized region of membrane) and required no immediate protein synthesis (Loewenstein 1981). A mechanism of formation based on these observations has been proposed (Loewenstein 1981). It states that GJ hemichannels move laterally and freely in the plasma membrane and if close enough contact is made between the membranes of adjacent cells then two hemichannels, one from each cell, link up (dock) to form a complete GJ channel. Subsequently, the focal point in the

membrane created by this link traps this channel in position and seeds further aggregation of hemichannels which link up to form clusters of GJ channels eventually generating plaques of channels. At some point following linkup the channels open.

Double whole-cell voltage-clamp methods were used to detect clear step-like transitions in the junctional current measurable within 1 second of manipulating a hemocyte couplet into contact. These steps, all similar in size, appear to reflect the accretion of single channels as the nascent gap junction grows in size. The implications of the fast onset of coupling to the presented model of GJ formation is discussed. This work along with the freeze-fracture and dye-transfer studies by Sheppy Coodin has been published (Churchill *et al.* 1993).

VII.2 Materials and Methods

VII.2.1 Insect Culture

Adults of the American cockroach, *Periplaneta americana*, were reared on a ground dog chow refined sugar mixture and water ad libitum and were maintained at 27°C in a 12 h light/dark cycle (Coodin & Caveney 1992).

VII.2.2 *Periplaneta* Solutions

Pipette solution

PPS in mM: 100 KCl, 10 NaCl, 1 $CaCl_2$, 2 $MgCl_2$, 10 EGTA/45 KOH (added from a 50 mM EGTA/225 mM KOH stock solution), 10 Hepes; pH 7.2 with 1 M HCl.

Bath solutions:

SAL-EDTA in mM: 125 NaCl, 13 KCl, 17 EDTA-$2Na^+$, 10 Hepes, 1 $NaHCO_3$; pH 6.8 with 1 M NaOH.

Perisal in mM: 150 NaCl, 13 KCl, 10 Hepes, 1 $NaHCO_3$, 2 $CaCl_2$; pH 6.8 with 1 M NaOH

VII.2.3 Preparation of Hemocytes for Voltage Clamp

Glass coverslips were attached to 35 mm plastic Petri dishes with holes drilled in the bottom, and were coated with 50 μl of Perisal without added Ca^{++} containing 50 μg lipophorin /ml for 30 min, and then aspirated dry. Lipophorin was purified as described in Coodin and Caveney (1992).

Immediately before recording adult cockroaches were punctured at the base of a mesothoracic leg and 5 to 10 μl of hemolymph was quickly collected into a glass micropipette containing 10 μl of SAL-EDTA, and pipetted into 500 μl of SAL-EDTA. High [EDTA] was necessary to prevent the cells from clumping. Since insect plasma proteins were found to interfere with gigaohm-seal formation during whole-cell recording, hemocytes were pelleted (372 x g for 30 sec), and the supernatant discarded. Cells were immediately resuspended in 100 μl of SAL-EDTA + 100 μl of Perisal without Ca^{++} to prevent clumping, and plated onto lipophorin-coated coverslips containing 1.8 ml Perisal (final [EDTA] = 850 μM). These cells were not superfused in the recording chamber as loosely adherent cells necessary for these experiments would be washed away or damaged. Cells were kept at 25°C for the duration of the experiment, and were used within 5 to 140 min.

VII.2.4 Whole-Cell Recording

The whole-cell recording methods used for hemocytes are described in Chapter II. In a typical experiment gigaohm-seals were formed with slight mouth suction on neighbouring, but not touching, pairs of hemocytes that were positioned 1 to 5 cell diameters apart. This procedure had to be done very gently as the hemocytes, especially when starting to flatten, were easily damaged. Gigaohm-seals (mean 10 ± 1 GΩ (n = 131)) were obtained on both cells 60% of the time. After successful gigaohm-seal formation on both hemocytes the whole-cell recording mode was formed on both cells by rupturing the patch of membrane in the pipette with brief strong pulses of mouth suction. This was achieved in both cells 50% of the time. Immediately following break-in an example of the capacitive current was stored to disk for off-line analysis. Due to the short time that cells could be recorded from (mean: 5 ± 0.8 min; n = 67) the capacitance and series resistance compensation circuitry was not used on whole-cell currents, and changes in series resistance (R_S) were not monitored later in the experiment. Following break-in the baseline current of each cell was monitored for stability. If stable, one of the cells was then carefully freed from its loose substrate attachment and slowly moved into contact with the other cell. The baseline current was monitored for any shift which would indicate gigaohm-seal breakdown or cell damage. Many cells were discarded because of this. As soon as the moving cell

made contact with the fixed cell a mark was made on the chart recording to denote time zero.

VII.3 Results

VII.3.1 Series Resistances and Passive Electrical Properties

Series Resistance (R_S) just after break-in in 38 *Periplaneta* hemocytes was 28 ± 1 MΩ.

The values of whole-cell capacitance and membrane potential just after break-in in the same 38 cell pairs were 6.9 ± 0.3 pF and -33 ± 1 mV, respectively. From the leak current during the pulse used to elicit the capacitive current (I_L) at -30 to -50 mV holding voltage the nonjunctional membrane resistance in hemocytes ($R_M = \Delta V_P / I_L$) was estimated as 13 ± 4 GΩ (n = 38).

VII.3.2 Lipophorin-Coated Coverslips Reduce Cell Flattening

Within minutes of bleeding and settling out of solution, *Periplaneta americana* hemocytes adhere and flatten onto glass coverslips, either in the presence or absence of Ca^{++} (Coodin & Caveney 1992). Initial attempts to whole-cell voltage clamp these highly flattened cells proved unsuccessful due to the extreme difficulty of obtaining gigaohm-seals and break-ins on the cells. Recording in SAL-EDTA did slow flattening slightly but also introduced a large nonspecific leak current. In order to reduce hemocyte flattening I teamed up with Sheppy Coodin who had discovered that the insect plasma protein, lipophorin, when in suspension with the cells, prevented flattening and

Fig. VII-1. Hemocyte flattening is delayed by plating them onto lipophorin-coated glass coverslips

Thirty minutes after being plated onto untreated glass (**A**) hemocytes have become so extensively flattened that they could not be whole-cell voltage-clamped. However when plated onto lipophorin-coated coverslips, hemocytes remained only slightly adherent to the glass for 30 min or more (**B**) and were easily whole-cell voltage-clamped. When discoid hemocytes (arrowheads) were manipulated into contact GJ formation was not detected, but spherical or flattening cells (arrows) when pushed together did couple. Scale bar, 10 μm.

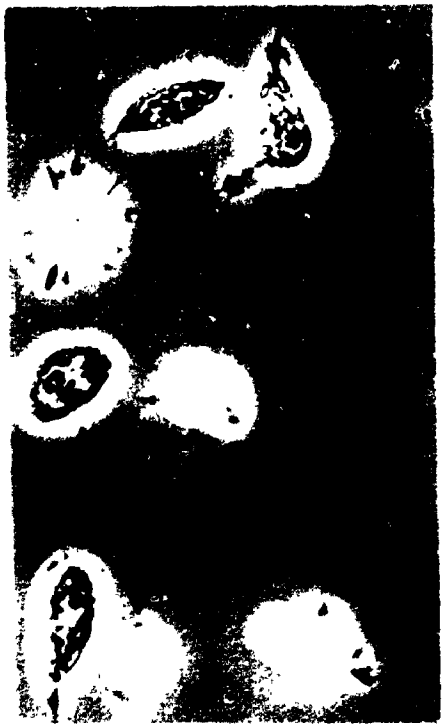

greatly reduced adhesion to glass coverslips (Coodin & Caveney 1992). S. Coodin prepared the lipophorin and the cells for these experiments. Although adding 5 μg lipophorin/ml to the bath solution did make the hemocyte morphology more suitable for recording, it hindered gigaohm-seal formation possibly by adhering to the patch-pipette. We therefore pre-coated coverslips for 30 min with 50 μg lipophorin/ml. This delayed hemocyte flattening onto the coverslips so that gigaohm-seals could be obtained (Fig. VII-1). Hemocytes remained rounded and loosely adherent for approximately 30 min or more on lipophorin-coated coverslips. Under these conditions it became possible to obtain gigaohm-seals and break-ins for up to 45 min and occasionally as late as 1 to 2 h after plating the cells.

VII.3.3 Whole-Cell Recording of Preformed Hemocyte Gap-Junctional Conductance

Cell pairs that had formed contacts within 20 to 30 min of plating were electrically-coupled. In 13 cell pairs G_j ranged from 2 to 75 nS immediately after break-in (mean: 33 ± 24 nS). Fig. VII-2 shows an example of macroscopic coupling in a well-coupled hemocyte pair. This trace illustrates how, almost immediately upon break-in, the junctional current rapidly dropped. Spontaneous uncoupling measured in 7 of these 13 cells (the other 6 cells were lost soon after break-in) had a time to half-maximal conductance of 25 to 100 sec (mean: 46 ± 10 sec). In several of these cell pairs a few single-channel

Fig. VII-2. Macroscopic coupling just after break-in in cell pairs already in contact

Voltage (V_1 & V_2) and current (I_1 & I_2) traces for both cells are shown. Both cells are held at -40 mV and pulsed alternately to -60 mV to generate junctional currents (upward current deflections). The macroscopic conductance immediately following break-in was 75 nS in this example and decreased rapidly and spontaneously during the recording to a half-maximal conductance in about 25 sec. (f_s = 50 Hz).

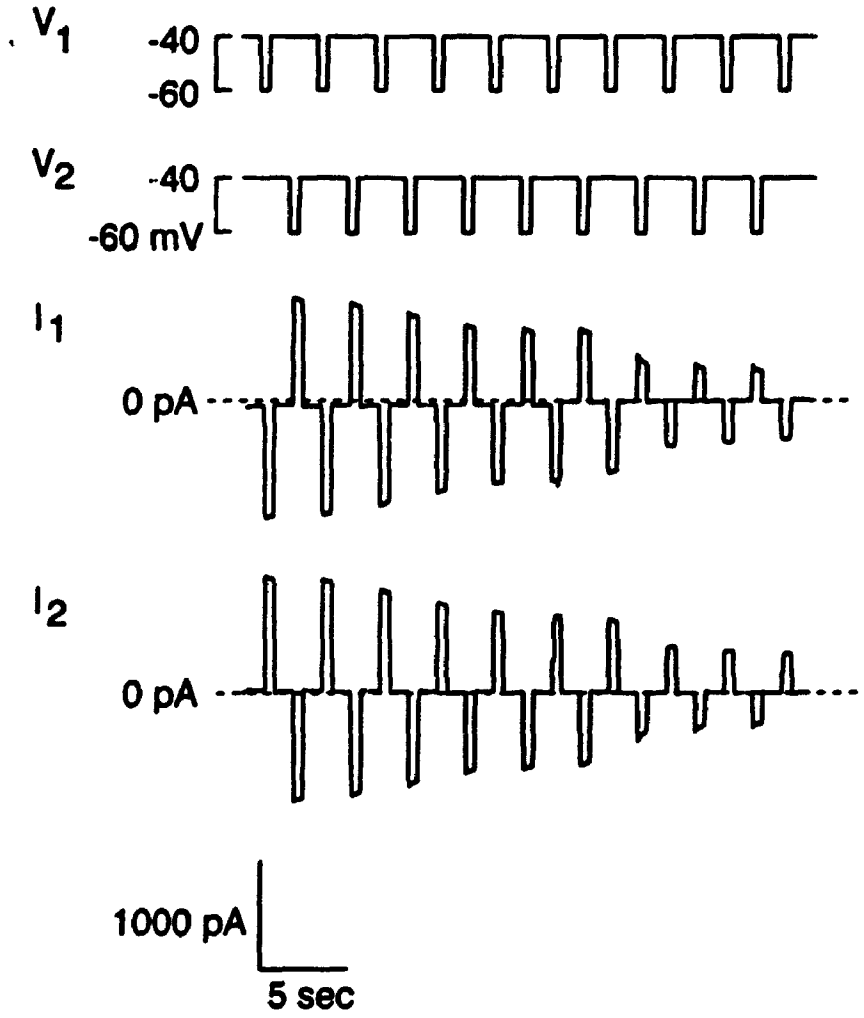
V1
-40
-60
V2
-40
-60 mV
I1
0 pA
I2
0 pA
1000 pA
5 sec

events were detected as spontaneous and quantal changes in the current traces of both cells while holding the voltages of both cells at constant but different levels. Measurable channel open-close events were used to estimate single-channel conductance (see below).

Although the cause for spontaneous uncoupling was not examined it is presumably due to the washout of cytoplasm that occurs in the whole-cell recording mode (see Chapter IV). Attempts were not made to reduce this by adding ATP to the pipette solution. In addition to the spontaneous uncoupling problem, it was difficult to record from these cells for long periods of time as they were highly mobile and often migrated away from the pipette, or tried to engulf it, thereby rupturing the gigaohm-seal. Some of the spontaneous uncoupling may have been due to this mechanical stress resulting from cell movement.

VII.3.4 Whole-Cell Recording of GJ Formation

To study GJ formation, single cells were whole-cell voltage-clamped, lifted away from their loose substrate attachments with patch-pipettes and manipulated into contact. In initial attempts discoid cells were used (Fig. VII-1B, arrowheads). These cells were difficult to break into and in 3 successful attempts failed to couple. In subsequent attempts using spherical, phase-bright cells (Fig. VII-1B, arrows) break-ins were easily obtained and the gigaohm-seal usually remained intact during cell manipulation thereby allowing the

precise moment of contact (within ± 1 sec) to be determined.

In the example shown in Fig. VII-3A, coupling was detected within seconds of bringing two spherical hemocytes together. Before contact the current traces were steady with relatively low noise. Eight seconds following the moment of contact (arrow) coupling was evident as a series of step-like transitions in both current signals that were similar in magnitude and opposite in sign. Since the steps in junctional current were nearly identical in both cells they presumably represent the opening of individual GJ channels which occurs as successive pairs of hemichannels linked up to form complete intercellular channels.

Three representative traces of rapid GJ formation are shown in Fig. VII-3B. Trace #1 records the most rapid formation seen, with the first step occurring about 1 sec after cell contact and junctional conductance reaching a plateau at 7.5 nS after 20 sec. Assuming a single-channel conductance of about 350 pS (see below) this represents approximately one channel being added to the growing gap junction per second. Coupling was detected in 8 of 32 such cell pairs. Of the negative results, 9 recordings lasted less than 60 sec after cell-cell contact. The mean time for the first event after contact was 16.6 ± 5.3 sec (range: 1 to 55 sec; n = 8). In 6 of these coupled pairs junctional conductance peaked at 1.3 to 7.8 nS in 20 to 150 sec (mean: 3.5 ± 0.9 nS). Following the plateau, junctional conductance

Fig. VII-3. Recordings of single-channel activity during gap junction formation in cells manipulated into contact

(A) Current traces (I_1 & I_2) from both cells are shown. Both cells were held at constant holding potentials of -55 and -40 mV creating a V_j of -15 mV. Step-like current transitions are evident starting 8 sec after the cells make contact (arrowhead). One channel opens and then closes and then many channels open as the steps sum on top of each other. The steps are equal in magnitude and opposite in polarity in both cells as evidence that these current patterns represent GJ-channel openings. After about 10 transitions the traces become too noisy to discern distinct steps. The first channel opening had a conductance of about 350 pS (dotted lines on upper trace). Some of the subsequent transitions clearly had smaller conductances; of 7 easily measured events γ_j ranged from 180 to 347 pS (mean: 283 ± 23 pS). I_2 appears noisier than I_1 probably due to nonjunctional-channel activity. (f_s = 50 Hz).

(B) Representative current traces of GJ formation in 3 different cell pairs. The trace from each pair with the best signal-to-noise ratio is shown with current converted to conductance for direct comparison. Holding voltages for each pair were: #1 and #3, -40 and -60 mV; and #2, -40 and -55 mV. #2 is the upper trace shown in (A). Dots joined by dotted lines are measurements taken from junctional current pulses in response to alternating transjunctional voltage jumps. Pulses were used to monitor junctional current after 20 to 30 sec so that the baseline current of the cells could be monitored. (f_s = 25 or 30 Hz).

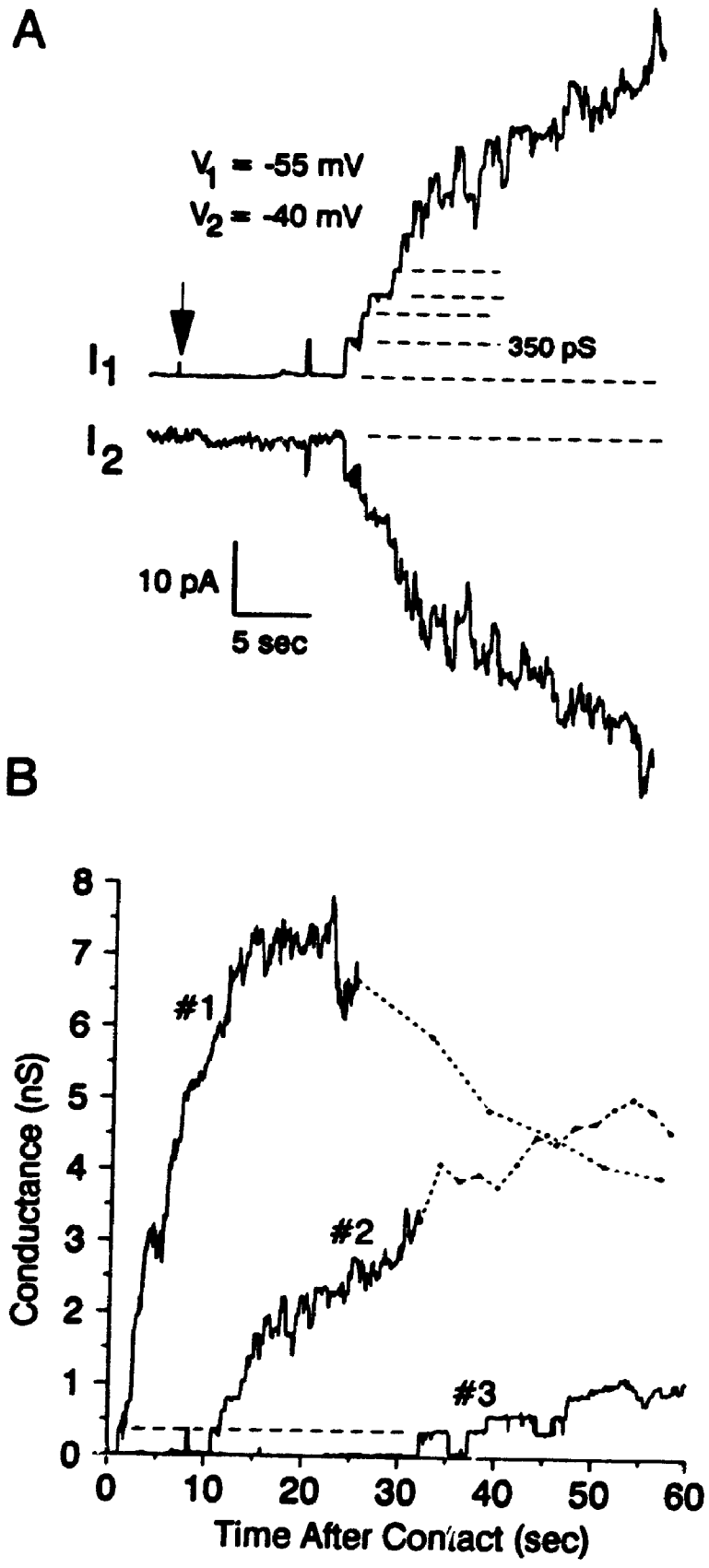
A
V_1 = -55 mV
V_2 = -40 mV
350 pS
I_1
I_2
10 pA
5 sec
B
Conductance (nS)
#1
#2
#3
Time After Contact (sec)

then declined to zero in 80 to 400 sec in the three pairs in which the recording lasted long enough to resolve single spontaneous steps in junctional current (< 1 nS). The time course of this subsequent decline was very close to the rate of spontaneous uncoupling found in hemocyte pairs coupled prior to break-in and presumably represents the same artifactual uncoupling process.

On two occasions cells were successfully pulled apart following the formation of coupling between hemocyte couplets, a steady baseline current reestablished, and the cells then manipulated back together to restore coupling.

VII.3.5 Single-Channel Conductance

Assuming that the successive step-like changes in junctional current that climbed during formation and dropped during uncoupling reflect the opening and closing of complete GJ channels, then the average main-state single-channel conductance can be estimated from the size of the current steps (see methods). The mean main-state single-channel conductance (γ_j) from 10 cell pairs was 339 ± 49 pS (n = 141 events). This small number of events was due to the short time available for recording single-channel activity (< 1 min per cell pair), the long open time of each event (40 to 6400 msec) and in forming junctions the rapidity at which channels were added (measurements could only be made on the first 10 or less steps before the signal noise added with each channel became too great). The frequency histogram for these data is

Fig. VII-4. Frequency histogram of single-channel events for 10 cell pairs

Weighted mean conductance was 342 ± 11 pS (n = 10). Mean conductance for each pair (in pS) was: 315 ± 7 (n = 27); 380 ± 4 (n = 2); 333 (n = 1); 320 ± 8 (n = 13); 343 ± 10 (n = 26); 383 ± 13 (n = 3); 395 ± 6 (n = 15); 333 ± 5 (n = 15); 283 ± 22 (n = 7); 344 ± 9 (n = 35). The distribution, which appeared to approximate a normal distribution, was best fit with a Gaussian curve which had a mean of 345 pS and SD of 47.

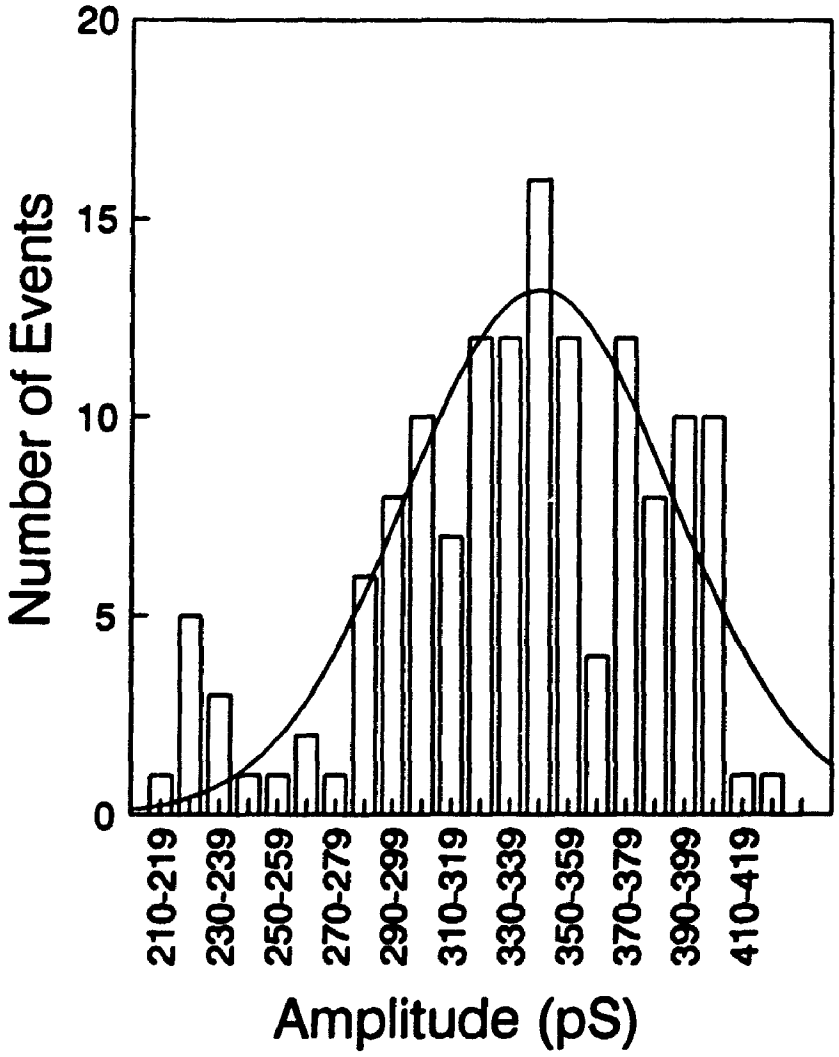
20
15
10
5
0
Number of Events
210-219
230-239
250-259
270-279
290-299
310-319
330-339
350-359
370-379
390-399
410-419
Amplitude (pS)

displayed in Fig. VII-4 and has been best fit with a single Gaussian distribution with a mean conductance of 345 pS and SD of 47.

VII.4 Discussion

VII.4.1 Onset and Rate of GJ Formation is Rapid

Quantal steps in junctional current early during GJ formation (within 0.7 to 1.5 min of cell-to-cell contact) were first demonstrated using an enhanced microelectrode technique on post-contact junctional signals between *Xenopus* blastomeres (Loewenstein *et al.* 1978). It was not until 1987 that a whole-cell voltage-clamped cell and a microelectrode impaled second embryonic *Xenopus* muscle cell were reaggregated to obtain the first direct recordings of current passage through single-GJ channels as they formed (Chow & Young 1987). These results were similar but channel formation slower than those obtained for hemocytes; 0.5 to 20 min to first onset of coupling and an accretion rate of one channel added every 0.5 to 3 min. Using double whole-cell recording in current-clamp mode to measure early GJ formation Rook *et al.* (1988) detected action potential propagation between paired neonatal rat heart cells 5 to 15 min post-contact. It was determined that 10 to 15 GJ channels were necessary for action potential propagation. Most recently Bukauskas and Weingart (1993) used double whole-cell voltage clamp to measure the onset of GJ formation in an established *Aedes albopictus* larvae cell line. They found the onset of coupling in these insect cells to occur an average

3.6 min after cell-to-cell contact.

The fastest reported onset of electrical coupling following cell-to-cell contact is the 1 sec value for contacting hemocyte couplets. It is not orders of magnitude faster than what has been reported for other cells and thus is probably not special. In fact both the onset and rate of GJ formation probably occurs on a millisecond time scale as the experiments in hemocytes were hampered by spontaneous uncoupling. Washout of cytoplasm occurs when the solution in the patch-pipette dilutes out soluble cytoplasmic components (Marty & Neher 1983), and has been shown to uncouple some vertebrate (*e.g.* Somogyi & Kolb 1988) and insect cell pairs (see Chapter IV). Similarly, washout probably caused the rapid decrease in junctional conductance measured in already-coupled hemocyte pairs and hence limits the measurement of both the onset and rate of GJ formation. Fast rates of accretion of 40 channels per sec have been reported between pairs of connexin-transfected *Xenopus* oocytes which are not prone to washout (Dahl *et al.* 1992). It is not known whether washout-induced uncoupling represents an inhibition of formation per se, or just of channel gating to the open state. Gap junctional plaques could feasibly continue to grow in size yet the channels remain closed due to washout of a cytoplasmic component necessary for opening the channel.

VII.4.2 Implications of Rapid Onset to Model of GJ Formation

Very rapid, possibly millisecond, post-contact onset of coupling in hemocytes has several implications for the model of GJ formation presented in the introduction. First, GJ channel precursors must exist as a rapidly deployable plasma membrane pool of randomly dispersed hemichannels as suggested by Loewenstein (1981). Alternative hypotheses, such as GJ channels forming from a pool of monomeric subunits that must first form multimeric hemichannels before docking or, a rapidly deployable pool of hemichannels in cytoplasmic vesicles that must first fuse with the plasma membrane in response to cell-cell contact both seem very unlikely given the rapid onset of coupling. Direct support for a plasma membrane pool of gap junction precursors comes from a recent study in *Xenopus* oocytes transfected with connexin mRNA and then probed with monoclonal antibodies for those connexins (Dahl *et al.* 1992).

The rapidity at which coupling occurred implies that docking of hemichannels from adjacent cells and channel gating to the open state must occur almost simultaneously; upon docking the channels do not appear to sit in the membrane for long before opening. Nevertheless, it is clear from hemocytes and cultured mosquito cells (Bukauskas & Weingart 1993) that docking precedes channel opening since the nonjunctional currents are steady prior to contact and do not change during

contact prior to the first junctional event.

The results presented here are consistent with the idea presented by Loewenstein *et al.* (1978) and Chow and Young (1987) that channels open 'one-channel-at-a-time' during GJ formation, not simultaneously. However, in hemocytes the time between opening of each successive channel can occur on a millisecond time scale, the rate of accretion being so fast that distinct steps of successive channel openings are not discerned. In Loewenstein's first review of GJ formation (Loewenstein 1981) a mathematical (Monte Carlo) simulation of this model of GJ formation is presented. This simulation assumed that GJ formation is a physical process limited only by the availability of gap junction precursors. This analysis showed that given reasonable estimates of the starting density of nonjunctional hemichannels and rates of their lateral mobility within the membrane that mature GJ channels would be concentrated to fairly high densities within hundreds of milliseconds. This prediction is not inconsistent with the new data from forming hemocyte gap junctions.

VII.4.3 Single-Channel Conductance

An estimate of 345 pS for the single-channel conductance of the hemocyte gap junction is among the largest for any cell type studied to date (see Chapter V for details). This large conductance is similar to other single-channel conductances found between cell pairs in other insect tissues including the 365 pS channel in cultured mosquito larval cells (Bukauskas &

Weingart 1993) and the 197 to 403 pS conductance in *Tenebrio* epidermal cells (Chapter V). From the data presented here it is difficult to assess the precise value of single-channel conductance and whether there are multiple channels. The 345 pS value was based on an average of 141 channel events from 10 hemocyte couplets in which the maximum number of events that could be recorded from any one couplet was 35. The averages for individual cell pairs ranged from 282 pS to 394 pS. Clearly, the single-channel conductance is large but given such a small data set it is difficult to say whether there is only one channel class, multiple channel classes with different main-state conductances or one channel with a range of conductances. Some of the variability in single-channel conductance may be attributable to series resistance errors. The initial average series resistance in these cells was 27 MΩ. This is already quite high and large increases in this value probably occur during manipulation of the cells and from cell motility (see Chapter V).

In spite of these difficulties, the measurement of the single-channel conductance of the first or second channel that opens during formation provides the most direct measure of single-channel conductance available. In most studies of single GJ-channel conductance the cells must be artificially uncoupled (Chapter V). Under these conditions it is impossible to know how many channels are active and whether the conductances measured represent actual single-channel

conductances or, for instance, the cooperative behaviour of several channels. By contrast, during GJ formation one can be reasonably certain that the first current step seen represents the current passing through one open channel. In insect epidermis a large-conductance channel (see Chapter V) was found during spontaneous uncoupling. These results in hemocytes during GJ formation suggests that such a large conductance channel does actually exist. Nevertheless, a practical illustration of this problem appeared recently in the two papers dealing with junctional conductance in the *Aedes albopictus* mosquito cell line. Single-channel recordings from poorly-coupled cell pairs with preformed gap junctions gave a single-channel conductance of 164 pS (Bukauskas *et al.* 1991), yet single-channel conductance was twice as large when channels were observed during GJ formation (Bukauskas & Weingart 1993).

VII.4.4 Possible Roles of Rapid GJ Formation in Hemocyte Encapsulation

Extensive gap-junctional coupling between hemocytes within capsules has been demonstrated to occur in a variety of invertebrates (Baerwald 1975; Norton & Vinson 1977; Han & Gupta 1989). The most likely function for gap junctions in hemocyte capsules, as in most tissues is a nutritive one. Capsules can be as much as 70 cell layers thick. Gap junctions would provide a pathway for nutrients from the outer cells of capsules, that have access to the hemolymph, to the inner

cells (Grimstone *et al.* 1967; Götz 1986). Since the encapsulation process can proceed rapidly (Götz 1986) rapid GJ formation would ensure that the innermost cells do not starve. In addition to a nutritive role, gap junctions may be involved in intercellular signalling. During capsule growth some kind of signal must be transmitted to terminate hemocyte addition to the capsule (as first proposed by Norton & Vinson 1977). This may occur via gap junctional mediated signalling. A new hemocyte just joining a growing capsule probably forms gap junctions almost immediately on contact with it (Baerwald 1975) and is able to sample all the gap junction permeable molecules within the collective cytoplasm of the capsule cells. One of those molecules could be a molecular signal regulating capsule thickness.

This chapter has described the rapid onset and rate of GJ formation between pairs of whole-cell voltage-clamped hemocytes. Although the measurements were limited by spontaneous cell uncoupling the onset of GJ formation in hemocyte couplets is the fastest yet reported. Further investigations using voltage-clamped hemocyte couplets along with molecular techniques (when probes to insect GJ proteins become available) might provide an excellent model system for supplying insight into the molecular basis of the early stages in GJ formation.

VIII SUMMARY AND GENERAL DISCUSSION

VIII.1 Summary of Results

Summary of results addressing the specific questions posed at the end of Chapter I:

1. Epidermal cells were isolated from two distinct stages of the larval *Tenebrio* moult cycle. Small numbers of pharate pupal epidermal (PPE) cells were completely dissociated with pronase and larger numbers of cuticle-attached newly-moulted epidermal (NME) cells were isolated by scraping the epidermal monolayer with a patch-pipette.
2. Epidermal cells suitable for whole-cell recording were isolated. Gigaohm-seals (> 5 GΩ) were easily obtained on cells from both stages which had large nonjunctional-membrane resistances (3 GΩ for NME & 14 GΩ for PPE cells). The current-voltage relationship of single PPE cells was linear making them ideal for recording GJ-channel activity and junctional-voltage dependence. In contrast, NME cells expressed a hyperpolarization-activated inward current that was time-dependent and sensitive to halothane.
3. Isolated epidermal cell pairs were functionally coupled by gap junctions. The distribution of initial junctional conductances (G_j) in PPE and NME cells ranged from 0 to 95 nS (mean: 11 nS) and from 31 to 818 nS (mean: 161 nS), respectively.
4. G_j dropped during recording in cell pairs from both

stages (7.5 and 4 min, resp.). In PPE cells, in contrast to NME cell, the initial low G_j allowed single GJ-channel activity to be observed just before complete uncoupling.

5. ATP added to the pipette solution significantly slowed uncoupling. ATP is probably used in an enzymatic process affecting GJ-channel gating since nonhydrolysable ATP analogues could not replace ATP. A simple capacitance measuring technique for detecting complete uncoupling in small groups of NME cells was developed and used to screen kinase inhibitors for their ability uncouple the cells. Those tried did not have a detectable effect.
6. The main-state single GJ-channel conductance in PPE cells was large (197 to 403 pS). This channel is capable of existing in a range of subconductance states (4 to 86% of the main-state). These substates are most likely partially-closed conductance states of single channels.
7. The presence of substates suggest a mechanism that may account for the selective regulation of gap junction permeability during insect epidermal development. Substates may have reduced permeability to larger molecules, thus restricting the cell-cell transfer of putative developmental signals.
8. Epidermal G_j and single-channel activity was primarily dependent on the nonjunctional-membrane potential (V_M), although transjunctional voltage also had an affect. The V_M at half-maximal G_j of the V_M-dependent response was -

26 mV suggesting that the whole-tissue V_M could regulate the overall level of G_j of the epidermis.

9. Hemocyte couplets manipulated into contact form gap junctions within seconds (mean: 16 sec). The fastest onset of coupling began 1 sec after contact. Rapid onset strongly suggests that gap junction precursors are already present in large amounts in the plasma membrane and channel opening occurs very soon after channel docking. Following the start of GJ formation G_j increased in distinct steps corresponding to the sequential addition of ~345 pS channels to the growing junction. The finding of large conductance channels in forming junctions provides direct support for the finding of large-conductance channels in uncoupling epidermal cells.

VIII.2 Summary Discussion

In this thesis I have completed one of the first biophysical characterizations of junctional conductances in acutely isolated insect cell pairs. Dual whole-cell recording methods have allowed high-resolution characterization of single-channel activity in uncoupling epidermal cells and of forming junctions in hemocyte couplets. My findings included one of the first clear demonstrations of partially-closed subconductance states in a GJ channel. In addition, this work provides further insight into the regulation of junctional conductance in the epidermis including the first detailed descriptions of voltage-dependence in this tissue, and by

suggesting a role for ATP in maintaining coupling. Each of these findings may play important roles in regulating cell-to-cell communication in the insect epidermis or in other insect tissues where this gap junction may be expressed. For instance, membrane-potential dependence of gap junctions could provide a means for regulating the overall tone of coupling in a tissue; ATP-dependence suggests a possible role for phosphorylation or another signalling mechanisms in regulating coupling; and single-channel subconductance states suggest a possible mechanism whereby junctional permeability could be selectively regulated during insect development. In addition to the work in the epidermis, recordings from forming junctions in hemocyte couplets has allowed a direct measurement of single gap-junction channels during a time when only one channel is active, providing direct support for the finding of a large-conductance channel in the uncoupling insect epidermis. Membrane-potential dependence and substate gating may be general properties of insect or other gap junctions. The biophysical profile developed in this study for epidermal gap-junction channels will enable meaningful comparisons of this insect gap junction with GJ channels of other cell types, especially those of other insects and eventually those encoded by cloned insect genes.

Appendix 1. Recording Setup

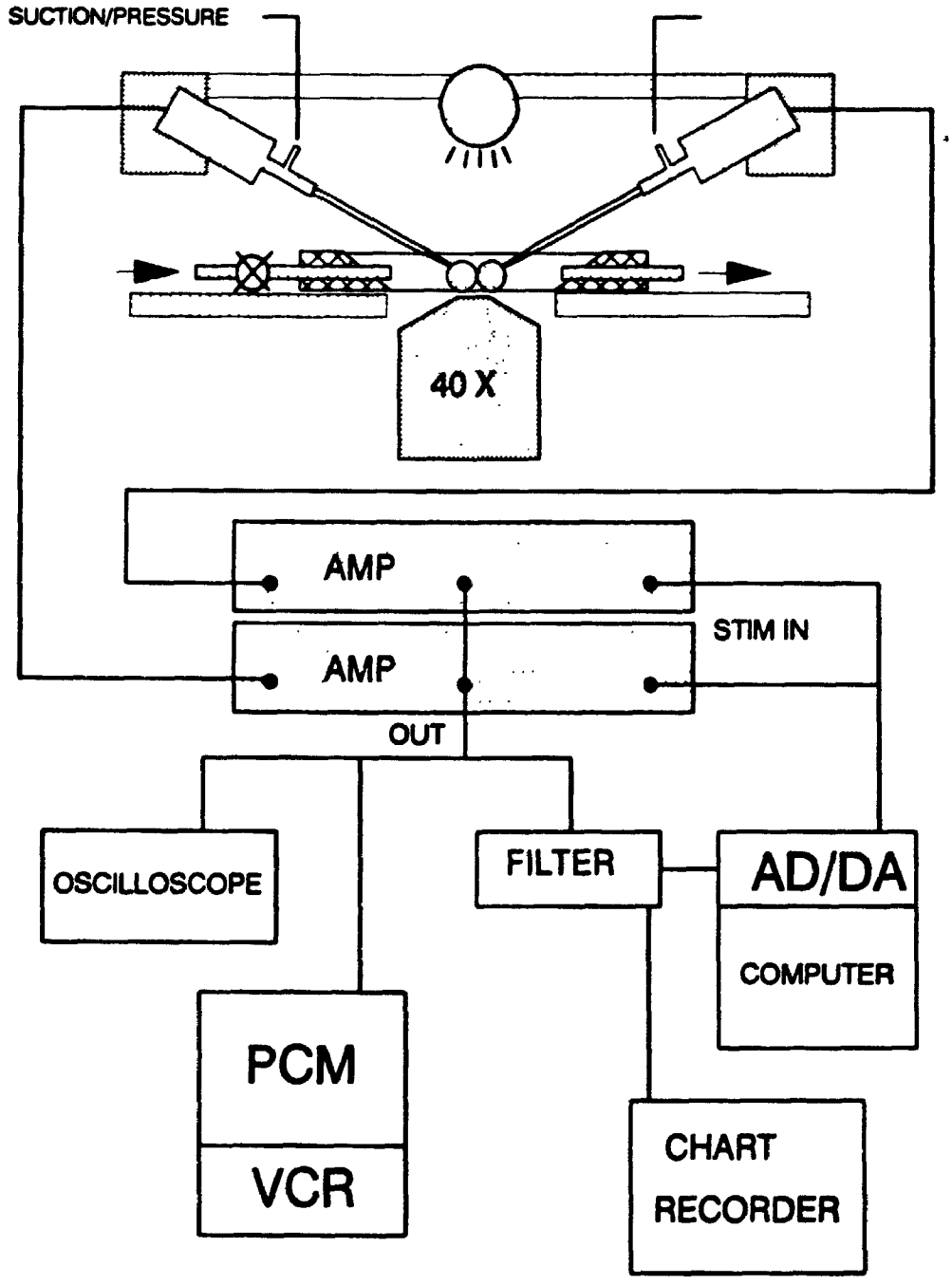
SUCTION/PRESSURE
40 X
AMP
AMP
STIM IN
OUT
OSCILLOSCOPE
FILTER
AD/DA
COMPUTER
PCM
VCR
CHART
RECORDER

Appendix 2. Recording Chamber

Recording chamber is made of Plexiglas. Tubes (16G) for attaching tygon tubing (1/16" ID, 1/8" OD) are stainless steel. Glass coverslip (22 X 40 mm, thickness #1) is fixed to the bottom of the chamber with white bees wax. The spring tissue clamp is made of stainless steel. The scale bar represents approximately 1 cm although the diagram is not drawn perfectly to scale.

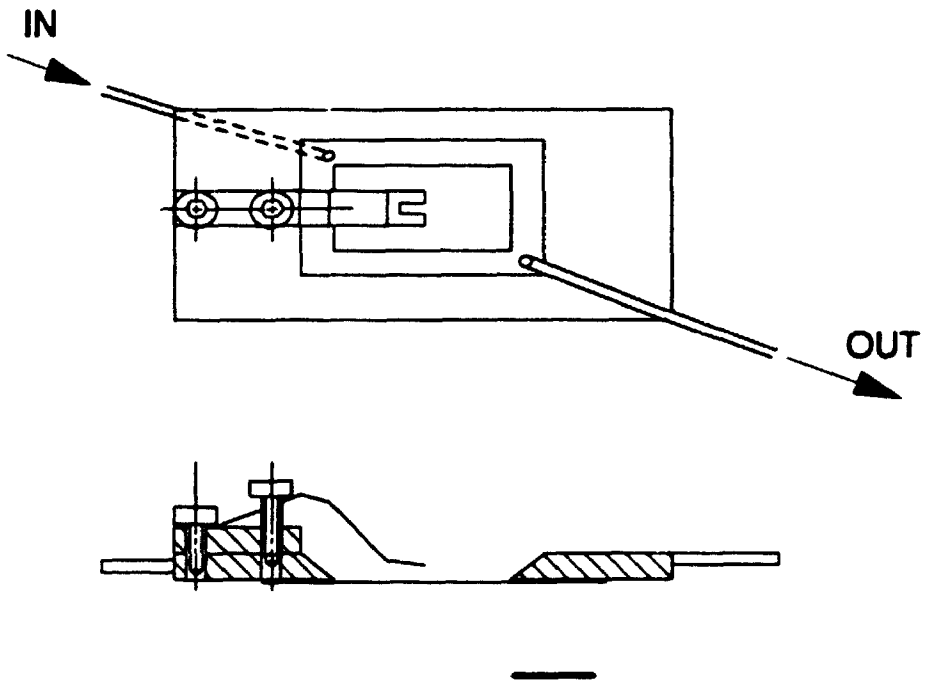
IN
OUT

APPENDIX 3 TWOCELL Program

Created Using Axobasic 1.0 (Axon Instruments, Foster City, California) and Quickbasic 4.0 (Microsoft, Bellevue, Washington).

INTRODUCTION

Basically this program works by first initializing and then cycling repeatedly through one main Do Loop. For each cycle of the Do Loop the program: 1. captures one key stroke from the key board (for selecting menu options); 2. writes data to the screen; 3. supplies an optional voltage pulse simultaneously to both cells for measuring cell capacitance (done only at a set interval selected by the investigator); 4. calls subroutines if a key from the main menu was selected (*e.g.* for changing the stimulus type, holding potentials or gain settings) and then 5. one stimulus pulse is supplied. Since the program cycles continuously (unless interrupted by a key stroke from the main menu) then a train of pulses is supplied. Data is displayed to the screen and if requested the data can be written to a file on disk. The main decision structure within the loop includes options found on the GO menu. When called by hitting one key on the keyboard (or using a mouse if available) the function is performed. Many of these functions involve a call to a subroutine, after which control returns to the loop with continuation of pulsing. Within the loop and with several of the menus in subroutines is the option to exit from the loop and hence the program. Exiting with hitting the <x> key brings the user to the EXIT MENU which has several options for: 1. exiting completely; 2. continuing; 3. going to STIM MENU to choose a new stimulus type and; 4. resetting several of the initialized values by going back up to various levels of the initializing section (1. below).

This program has modular construction. There is a short main module from which several subroutines are called. In order to save space only the main module and several key subroutines used in generating stimulus pulses and acquiring data are shown here. For more information see the Pclamp, Axobasic and Quickbasic manuals.

OUTLINE OF MAIN MODULE OF THE PROGRAM

The main module of the program has three parts (Calls to subroutines are *italicized*):

1. Initializing
    - A. declarations - declare subroutines
    - B. setting up axobasic quick library
    - C. setup screen colours
    - D. Call *Testepc7* - option to test patch-clamp amplifier
    - E. Call *FileNo.* - select starting filename file numbers
    - F. Call *DTcheck* - to check date and time on computer system
    - G. initialize variables - done automatically
    - H. set save intervals for transjunctional voltage pulses
    - I. set interval for measuring capacitance
    - J. set stimulation protocol to start with
    - K. Call *GOmenu* - to set up main menu on screen
    - L. initialize variable for whether and how data saved to file

2. Main Do Loop
    - A. key capture, *i.e.* according to main menu
    - B. display to screen
        - i. elapsed time
        - ii. gains
        - iii. holding voltage
    - C. CAP measuring at specified intervals; can be on or off
    - D. MAIN DECISION STRUCTURE An IF/ELSEIF/ELSE/ENDIF structure which uses key$ from key capture (according to

main menu) to briefly interrupt program flow and perform one of these 12 options.

IFs

1. Call *Gainset* - for changing gain of one or both cells (used for Gjstim, Nostim, Vjstim but not Capstim or Capmeas)
2. erase data from screen
3. zero the elapsed timer
4. Call *Stimenu* - for choosing stimulation type
5. Call *Savemenu* - for choosing how to save data; includes on/off switch and time intervals
6. Call *Vhold* - for changing holding potentials of both cells
7. Call *Capmeas* - for series resistance and capacitance measuring
8. Call *Capmenu* - for switching intermittent capacitance measuring on or off, and determining pulse intervals, pulse length, and gains for Capmeas and Capstim
9. Call *Cellswitch* - for determining if cell 1, cell 2 or both cells are to be pulsed during the Gjstim procedure
10. momentarily halt or pause program
11. Call *Vjstim* - for selecting single transjunctional pulses of any magnitude and duration
12. go to Exit Procedure, 3. below

ELSE

1. uses cell pulse switch info (C. 9.) to determine whether cell 1, cell 2 or both cells are to be pulsed
2. CALL STIMULATION PROCEDURE - depending on the voltage pulse type selected in *Stimenu* will call *Gjstim, Capstim, Nostim* or *Sealstim* which will produce a single voltage pulse before cycling again through the loop.

ENDIF

3. EXIT PROCEDURE
   1. Call *Savemenu* to decide if latest data collected is to be saved and if opened files are to be closed.
   2. Call *Exitmenu* to decide from several exiting options.

KEY FEATURES OF PROGRAM

Easy Changing of Holding Voltage of Both Cells of a Pair and Informing Program of Gain Changes at Amplifier

A key feature of the program is the ability to easily and rapidly change the holding voltage of both cells together by hitting a couple keys as well as informing the program of the change in gain with two key strokes (used in calculations of current amplitude). Both of these features are available from the *GO MENU* (*i.e.* main menu shown on screen). The gain changing procedure available from the *GO MENU* affects only pulsing types *Gjstim, Vjstim, Nostim.* There is an equivalent gain changing procedure available from the *CAP MENU* which affects only *CAPmeas* and *Capstim.* The two separate gain procedures make it possible to switch from *Gjstim* junctional current measurement and Capacitance measurement quickly and easily while having different gains for each and not having to continually change back and forth between gains.

Pclamp (Axon Instruments) Compatible Data Files

Another key feature is the production of Pclamp compatible files especially of capacitive spikes for series resistance measuring (*CAPmeas*) and responses to transjunctional voltage (*Vjstim*) which can be

analyzed by clampex of the Pclamp suite of programs (Axon, Instruments).

Spreadsheet Compatible Data Files

A second data file type is produced of junctional current data which is in ASCII in the PAF 5.0 format and is read by Supercalc/Lotus type spreadsheets. This file includes the average of the baseline currents (base I) before a junctional voltage pulse and the average of the currents during a junctional pulse. As well, the amplitude is calculated, and all these values are converted to absolute value with a column containing the cell that is pulsed. Finally this file contains amplifier gains, holding potential, elapsed time and a note of a file number where capacitive spikes are to be stored (including an estimate of the series resistance) if a series resistance measurement is made (similarly for *Vjstim* data).

File Naming Format

File names use the Pclamp format (see Pclamp manual). CAP meas files are YYMDDr##.dat and the Ascii files are YYMDDt##.prn and *Vjstim* data files are YYMDDv##.dat. File numbers are automatically incremented. There is an error message in case file ## is greater than 99. All files are stored in the subdirectory d:\tcdat which must exist in order for data to be written to disk.

Capacitance and Series Resistance Measuring (*i.e* Cap measuring)

CAP measuring can be specified to occur at a set interval during trains of junctional current measuring (*Gjstim*) and the interval can be changed by *Capmenu*. A single CAP measuring can be requested anytime by a single keystroke <r>.

Transjunctional Voltage Pulses

A single transjunctional voltage pulse of a specified size and duration and applied to a specified cell can be requested at any time from the *GO MENU* by using the *Vjstim* subroutine by hitting an uppercase <V>. These are stored in Pclamp compatible data files.

Easy Changing of the Holding Potential

Gjstim gives a train of junctional pulses of 20mV from the holding potential specified by *Vhold* (changed by hitting <*> on the number pad) either to cell 1 or cell 2 or to both cells alternately. This is controlled by *Cellswitch*.

Stopping Continuous Pulsing

There is three ways to stop pulsing. 1. hitting <p> of *GO MENU* to go to *Stimenu*. 2. Exit to *Exitmenu* by hitting <x>. 3. hitting <s> to go to the *Savemenu*. In all three cases the last opened t##-type Ascii file can be closed.

Save Menu

The *Savemenu* appears with all three keys where it is possible to close the file and continue pulsing without going to the *Stimenu* first and MOST importantly the time interval at which writing of junctional currents to the Ascii file occurs can be changed.

Setting Intervals for Data Capacitance Measuring and Storage of Data From Transjunctional Voltage Pulses (*Gjstim*)

The interval at which automatic CAP measuring is performed or writing of junctional currents to Ascii t## files is performed is determined by the elapsed timer. The control structure determining when writing occurs is found in the *Gjstim* subroutine where it is explained. The similar structure which determines when automatic CAP measuring will occur is in the main module at 2.C. in the outline above. In essence, if the interval for writing to a file is 0.25 min then a test value (ttt! or tttt!) is incremented by the interval once the interval has passed. Data write occurs when the elapsed time equals the test value. Once the write is finished the test value is incremented by the interval such that ttt! or tttt! = elapsed time + interval value. See the appropriate code in the program for more information.

Other Pulsing Protocol

Three pulsing protocol besides *Gjstim* is available from the *Stimenu*: 1. *Sealstim* gives a train of depolarizing pulses for monitoring

seal forming and measuring pipette resistances. Data cannot be written to a file. 2. *Capstim* which is like *sealstim* but 20mV hyperpolarizing pulses. *Vhold* can be changed but no files produced. 3. *Nostim* which has no voltage pulses or file writing but is great for changing *Vhold*. Transjunctional voltages can be set by using the vhold knobs on the patch clamp amplifiers.

Amplifier Testing Feature

Finally, at startup an option is given to go to a subroutine (*Testepc7*) which is designed for testing the amplifier. Pulses, sinewaves, trianguiar waves and constant outputs are available for testing the amplitude and frequency response of the current measuring circuitry of the patch-clamp amplifiers.

To save space the only subroutines shown here in addition to the main module are those that are key to performing stimulus generation and data acquisition. These include *CAPmeas, Capstim, Gjstim and Vjstim*. Two other stimulus generating subroutines not included are *Sealstim* and *Nostim* which are similar to those shown. Other subroutines not included are those for creating filenames (*Filemenu, FileNo.* and *Dateinfo*), opening and creating data files (*Openfile1, 2,* and *3*), creating Pclamp compatible file headers (*Pclampheader* and *Pclampheader3*), creating and running menus (*GOmenu, Stimenu, Savemenu, Exitmenu*), changing gain settings and holding potentials (*Gainset* and *Vhold*), changing the pulsed cell (*Cellswitch*) and testing the amplifier (*Testepc7*). In all only one quarter of the whole program is reproduced here.

BEGINNING OF PROGRAM CODE **********

```
'DEFINITIONS AND DECLARATIONS **********
'FILE NAMING, FILE OPENING, FILE HEADERING SUBROUTINES
DECLARE SUB Filemenu (savdat$)
DECLARE SUB FileNo. (ff1%, ff2%, ff3%)
DECLARE SUB Openfile1 (namefile1$, ff1%, stim$)
DECLARE SUB Openfile2 (namefile2$, ff2%, stim$, savdat$, sav$)
DECLARE SUB Openfile3 (namefile3$, ff3%, stim$, savdata$, savit$)
DECLARE SUB Pclampheader (ctics%, gn1!, gn2!, starttime!, endtime!,
namefile1$, yymmdd!, etime!)
DECLARE SUB Pclampheader3 (holdv!, vjpulse!, vjdpc!, plm!, gn1!, gn2!,
starttime!, endtime!, namefile3$, yymmdd!, etime!)
'OTHER UTILITY SUBROUTINES
DECLARE SUB Stimenu (stim$)
DECLARE SUB GOmenu ()
DECLARE SUB Savemenu (sint!, savmen$, namefile2$, sav$)
DECLARE SUB Exitmenu (exit$)
DECLARE SUB Dateinfo (D$, m$, mm$, dd$, yy$, yymmdd$, yymmdd!)
DECLARE SUB DTcheck ()
DECLARE SUB Capmenu (CAP$, cg1!, cg2!, ctics%, sss%, CAPint!, tttt!)
DECLARE SUB Cellswitch (cps$)
'HOLDING POTENTIAL AND GAIN CONTROLLING SUBROUTINES
DECLARE SUB Vhold (holdv%, voff%)
DECLARE SUB Gainset (g1!, g2!)
'STIMULATION PROTOCOL SUBROUTINES
DECLARE SUB CAPmeas (voff%, holdv%, cg1!, cg2!, ctics%, namefile1$,
yymmdd!, etime!, ff1%, savdat$, stim$)
DECLARE SUB Sealstim (g1!, g2!)
DECLARE SUB Capstim (voff%, ctics%, g1!, g2!)
DECLARE SUB Gjstim (kj%, sint!, ttt!, holdv%, voff%, cps%, g1!, g2!,
etime!, savdat$)
DECLARE SUB Nostim (ttt!, holdv%, voff%, g1!, g2!, etime!, savdat$)
DECLARE SUB Vjstim (plm%, plm!, holdv%, voff%, g1!, g2!, etime!,
yymmdd!, ff3%, savdat$, stim$)
DECLARE SUB Testepc7 ()
```

```
'INITIALIZING AXOBASIC.BI QUICK LIBRARY
************************************
REM $INCLUDE: 'axobasic.bi'
DEFINT I-Z
5 'LABEL >>>>>>>>>>>>>
```

```
'MAIN MODULE:
'2 CELL PULSING PROTOCOL IN A LOOP WITH DIRECTION VIA KEY CAPTURE TO
'     SEVERAL SUBROUTINE AS IN PURPOSE AND DESCRIPTION

'INITIALIZE SCREEN COLOURS ***********************************************
scolor = 15    'data on graph  0 black      5 pale violet 10 bright green
tcolor = 7     'message text   1 pale blue  6 pale brown  11 bright cyan
vcolor = 9     'vector         2 pale green 7 pale white  12 bright red
wcolor = 7     'text on graph  3 pale cyan  8 gray        13 bright
violet
mcolor = 14    'menu text      4 pale red   9 bright blue 14 bright
yellow
kcolor = 7     'cursor                                    15 bright white

'AMPLIFIER TESTING *******************************************************
'at startup an option is given to do an amplifier test; if 'yes' then
'proceed to test-epc7 subroutine
CALL Testepc7

'CHANCE TO EXIT **********************************************************
clrscrn
clearmsg
dispstring "**** EXIT? ****"
display -1950, -1600, 10
dispstring "DO YOU WANT TO STOP AND EXIT HERE   <y>  or  <n> ?"
display -1950, -1800, 10
yesno$ = INPUT$(1)
IF yesno$ = "y" THEN GOTO 23

'INITIALIZE DATE INFORMATION *********************************************
CALL Dateinfo(D$, m$, mm$, dd$, yy$, yymmdd$, yymmdd!)

'INITIALIZE FILENAME FILENUMBERS TO BE USED ******************************
6 'LABEL >>>>>>>>>>>>>
CALL FileNo.(ff1%, ff2%, ff3%)

'CHECK DATE AND TIME OF COMPUTER BEFORE STARTING *************************
CALL DTcheck

7 'LABEL >>>>>>>>>>>>>
'INITIALIZING VARIABLES **************************************************
'1. set vhold to -50mV to start off program
'2. set voff% to 0 to start; used to change the holding level from -50
' in steps of 10mV
'3. alternates between 1 & 0 with each time through main do loop to
'decide which pulse stim in Gjstim protocol dac command when "3" below
' set 0 for cell 1 and 1 for cell 2
'4. switch used to determine if alternate pulsing of both cells used "3"
'     or, of only cell 1 "1" or only cell 2 "2"
'5. set gains to 10 to start off program 'c' gains apply to cap and
'     CAPmeas, 'c'-less gains to everything else each is set
' independently and operates independently
'6. set elapsed time clock to zero
'7. switch to turn CAPmeas on or off
'8. used in CAPmeas at regular interval routine to display warning
'     tone/message once before measurement occurs
'9. switch used to keep track of whether a t## ASCII file is opened; if
'     file is opened "0" then the save menu shown, if closed "1" it is
'     not. This value is used when Exitmenu or Stimmenu is selected and
'     does not affect the selection of the Savemenu.
'10. set default # of clock tics between sampled points for Capstim and
'     CAPmeas
```

```
holdv% = -50        '1.
voff% = 0           '2.
cps% = 1            '3.
cps$ = "3"          '4.
g1! = 10            '5.
g2! = 10
cg1! = 10
cg2! = 10
clkzero             '6.
CAP$ = "0"          '7.
sss% = 0            '8.
sav$ = "1"          '9.
plm% = 0
plm! = 1
ctics% = 25         '10.

'INITIALIZE SAVE INTERVALS ********************************************
'1. set sint! which is the save interval
'2. set testtime! (ttt!) to elapsed time + some interval - used in stim
'      protocol to write to file at some interval -  this is reset to the
'      interval whenever clkzero called; ttt! = elapsed time + ttt!
wipe
clearmsg
dispstring "**** INTERVALS ****"
display -1950, -1600, 10
PRINT ""
INPUT "SAVE INTERVAL - minutes in decimal - default is 0.25 ?  >", sint!
IF sint! = 0 THEN sint! = .25
clearmsg
ttt! = sint!

'INITIALIZE CAPmeas INTERVALS ******************************************
'CAPint! and tttt! are the same as sint! and ttt! but instead sets a
'      specific interval for CAPmeas; tttt! = elapsed time CAPint!
wipe
clearmsg
dispstring "**** INTERVALS ****"
display -1950, -1600, 10
PRINT ""
INPUT "CAPmeas INTERVAL - minutes in decimal - default is 2   >",
CAPint!
IF CAPint! = 0 THEN CAPint! = 2
clearmsg
tttt! = CAPint!

'CHOOSE stim PROTOCOL TO START WITH ************************************
'stimenu used to select stim$ which used to determine stimulation type
' and also in exiting; IF stim$ = "x" then go to exiting procedure
clearmsg
CALL Stimenu(stim$)
IF stim$ = "x" THEN GOTO 4

'INITIALIZING GO MENU - WRITE TO MENU AREA ON GRAPHICS SCREEN *********
CALL GOmenu

'CALL FILE MENU TO DETERMINE IF FILE TO BE OPENED & THEN OPEN IT ******
'only performed for Gjstim protocol i.e. IF stim$ = "3"
IF stim$ = "3" THEN
        IF sav$ = "1" THEN
                CALL Filemenu(savdat$)
                CALL Openfile2(namefile2$, ff2%, stim$, savdat$, sav$)
        END IF
```

```
END IF
1 'LABEL >>>>>>>>>>>>>
```

```
'MAIN DO LOOP STARTS HERE ----------------------------------------------
'END LOOP IF <x> KEY HIT ----> GO INTO END OF PROGRAM routine
DO

'CAPTURE KEYSTROKE WITH EACH LOOP ----------------------------------------
'this key$ may be changed with every time through the loop since the
'     Quickbasic function INKEY$ looks for the input at all times; the
'     value of INKEY$ is returned to key$ at this line; key$ is used in
'     the decision structure of this loop to direct program flow; key$
'     values are indicated on the GO menu. Also esckey% is gathered as
'     well so that the escape key can be used to stop and go to the Exit
'     menu
key$ = INKEY$
esckey% = chasc(key$)

'CALC AND DISPLAY ELAPSED TIME IN MINUTES ---------------------------
elpsdtime! = time
etime! = elpsdtime! / 60000
dispflt etime!
display 1250, -1950, 10

'DISPLAY HOLDING VOLTAGE -------------------------------------------------
dispint holdv%
display -1650, 1750, 10

'CAP MEAS/INTERVAL ROUTINE -----------------------------------------------
'CAP MEAS AT A SPECIFIED TIME INTERVAL WITH A WARNING TONE/MESSAGE TO
' SET GAINS, FILTER, SWITCH.
'CAP$ is the main switch which decides if CAP meas is on "1" or off "0"
' if CAP$ is on then CAPmeas is performed at a specified interval
'     determined by tttt! which is initialized to elapsed time + some
'     interval e.g. 2 sec at start up initialization and in CAPswitch
'     subroutine
'                  SUMMARY OF 'IF' DECISION STRUCTURE
'       IF #3 - CAP$ switch to determine If interval CAP meas performed
'       IF #2 - at some specified time before do CAP meas give warning
'       IF #3 - sss% a switch used to make warning happen only once; set
'           to 1 in CAP MENU and then set to 0 once warning given and
'           set back to 1 once CAPmeas is performed
'       IF #4 - when elapsed time (etime!) surpasses tttt! (which is
'           initialized to etime! by CAP MENU + some interval then CAP
'           MEAS is performed after which tttt! is incremented by the
'           set interval so that CAP MEAS not performed until that
'           interval is again surpassed by etime!
IF CAP$ = "1" THEN
        IF etime! > tttt! - .1 THEN
                IF sss% = 1 THEN
                        FOR nsl = 500 TO 1000 STEP 100
                                SOUND nsl, .3
                        NEXT nsl
                        clearmsg
                        PRINT ""
                        PRINT "6 secs TO SET UP FOR CAPmeas"
                        PRINT ""
                        PRINT "1.  GAINS "
                        PRINT "2.  FILTERS TO 10 kHz"
                        PRINT "3.  SWITCH"
                        sss% = 0
                END IF
        END IF
        IF etime! > tttt! THEN
                clearmsg
```

```
                PRINT ""
                PRINT "CAP MEASURING NOW - HIT ANY KEY TO INTERRUPT"
                CALL CAPmeas(voff%, holdv%, cg1!, cg2!, ctics%,
namefile1$, yymmdd!, etime!, ff1%, savdat$, stim$)
                IF stim$ = "x" THEN GOTO 4
                tttt! = tttt! + CAPint!
                sss% = 1
                FOR ns1 = 500 TO 1000 STEP 100
                        SOUND ns1, .3
                NEXT ns1
                clearmsg
                PRINT ""
                PRINT "CAPmeas DONE  "; namefile1$; " closed"
                PRINT ""
                PRINT "RESET GAINS, FILTER, AND SWITCH !!!!!!!!!"
        END IF
END IF

'START MAIN DECISION STRUCTURE  ****************************************

'GAIN CHANGE PROCEDURE ---------------------------------------------
IF key$ = "g" THEN
        clearmsg
        CALL Gainset(g1!, g2!)

'SCREEN ERASE ------------------------------------------------------
ELSEIF key$ = "e" THEN
        wipe

'ZERO ELAPSED TIMER ------------------------------------------------
'NOTE: 'Z' IS UPPER CASE TO DECREASE MISTAKES
'RESET ttt! & tttt! to zero + interval over which CAP meas and write to
'     FILES performed
ELSEIF key$ = "Z" THEN
        clkzero
        ttt! = sint!
        tttt! = CAPint!

'CHOOSE stim PROTOCOL ----------------------------------------------
'1. close old file of t## type
'2. call stimenu where value of stim$ is chosen and graphics screen set
'     up
'3. if stim$ set to "x" in stimenu then proceed to exit procedure
'4. if stim$ = "3" (i.e. Gjstim performed) then go to file menu to
'     determine what if data is to be sent to a file or not; if yes then
'     openfile2 will proceed to open the file for use
'5. if stim$ set to "x" in openfile2 due to file number too large then
'     go to exit procedure
ELSEIF key$ = "p" THEN
8 'LABEL >>>>>>>>>>>>>
menuclear

'SAVE MENU
        IF sav$ = "0" THEN
                CALL Savemenu(sint!, savmen$, namefile2$, sav$)
                IF savmen$ = "p" THEN GOTO 25
                IF savmen$ = "x" THEN GOTO 23
                IF savmen$ = "i" THEN GOTO 25
        END IF
25 'label >>>>>>>>>>>>>>>>>

'STIM MENU
```

```
        CALL Stimenu(stim$)
        kj% = 0
        IF stim$ = "x" THEN GOTO 4
        IF stim$ = "3" THEN
                IF sav$ = "1" THEN
                        CALL Filemenu(savdat$)
                        CALL Openfile2(namefile2$, ff2%, stim$, savdat$,
sav$)
                        IF stim$ = "x" THEN GOTO 4
                END IF
        END IF
        CALL GOmenu
12 'LABEL >>>>>>>>>>>>>

'SAVE MENU ------------------------------------------------------------
'call save menu to close files or to change save interval IF savemen is
'     "p" then goto stimenu otherwise just continue looping
ELSEIF key$ = "s" THEN
2 'LABEL >>>>>>>>>>>>>
        menuclear
        CALL Savemenu(sint!, savmen$, namefile2$, sav$)
        IF savmen$ = "p" THEN GOTO 25
        IF savmen$ = "x" THEN GOTO 23
        IF savmen$ = "i" THEN GOTO 25
        CALL GOmenu

'CHANGE-Vhold PROCEDURE ----------------------------------------------
ELSEIF key$ = "*" THEN
        CALL Vhold(holdv%, voff%)

'CAP MEASUREMENT PROCEDURE ------------------------------------------
ELSEIF key$ = "r" THEN
        FOR ns1 = 500 TO 1000 STEP 100
                SOUND ns1, .3
        NEXT ns1
        clearmsg
        PRINT ""
        PRINT "SET UP FOR CAPmeas "
        PRINT ""
        PRINT "1.  GAINS "
        PRINT "2.  FILTERS TO 10 kHz"
        PRINT "3.  SWITCH"
        PRINT ""
        PRINT "STRIKE ANY KEY WHEN READY TO START !!!!!!"
        hold
        clearmsg
        PRINT ""
        PRINT "CAP MEASURING  NOW - HIT ANY KEY TO INTERRUPT"
        CALL CAPmeas(voff%, holdv%, cg1!, cg2!, ctics%, namefile1$,
yymmdd!, etime!, ff1%, savdat$, stim$)
        IF stim$ = "x" THEN GOTO 4
        FOR ns1 = 500 TO 1000 STEP 100
                SOUND ns1, .3
        NEXT ns1
        clearmsg
        PRINT ""
        PRINT "CAPmeas DONE  "; namefile1$; " closed"
        PRINT ""
        PRINT "RESET GAINS, FILTER, AND SWITCH !!!!!!!!!"

'CAP MEASUREMENT SWITCH ----------------------------------------------
'set CAPint! - the interval between CAP measurements when CAPmeas set
```

```
'       for interval use
ELSEIF key$ = "u" THEN
        CALL Capmenu(CAP$, cg1!, cg2!, ctics%, sss%, CAPint!, tttt!)

'CELL PULSING SWITCH ----------------------------------------------------
ELSEIF key$ = "q" THEN
        CALL Cellswitch(cps$)

'MOMENTARILY HALT EXECUTION ---------------------------------------------
ELSEIF key$ = "m" THEN
        clearmsg
        hold
        clearmsg

'TRANSJUNCTIONAL VOLTAGE PULSE GENERATING PROCEDURE ---------------------
-
ELSEIF key$ = "V" THEN
        CALL Vjstim(plm%, plm!, holdv%, voff%, g1!, g2!, etime!,
yymmdd!, ff3%, savdat$, stim$)

'EXIT LOOP -------------------------- ----------------------------------
ELSEIF esckey% = 27 THEN
        GOTO 4

'GET stim PROTOCOL ------------------------------------------------------
ELSE
'DETERMINE IF BOTH, CELL 1 OR CELL 2 PULSED
'1. alternate between 1 & 0 with each turn of Do Loop ONLY IF cps$ = "3"
'2. IF cps$ = "1" then set cps% to 0 so that cell 1 only is pulsed
'3. IF cps$ = "2" then set cps% to 1 so that cell 2 only is pulsed
        IF cps$ = "3" THEN
                IF cps% = 1 THEN
                        cps% = 0
                ELSE
                        cps% = 1
                END IF
        ELSEIF cps$ = "1" THEN
                cps% = 0
        ELSEIF cps$ = "2" THEN
                cps% = 1
        END IF

'CALL THE APPROPRIATE STIM PROTOCOL
        SELECT CASE stim$
                CASE "1"
                CALL Sealstim(g1!, g2!)
        CASE "2"
                CALL Capstim(voff%, ctics%, cg1!, cg2!)
        CASE "3"
                CALL Gjstim(kj%, sint!, ttt!, holdv%, voff%, cps%, g1!,
g2!, etime!, savdat$)
        CASE "4"
                CALL Nostim(ttt!, holdv%, voff%, g1!, g2!, etime!,
savdat$)
        CASE ELSE
                GOTO 8
        END SELECT

'END DECISION STRUCTURE ------------------------------------------------
END IF

'END OF MAIN LOOP -------------------------------------------------------
```

```
LOOP

'EXITING ROUTINE ************************************************************

'SET Vhold TO -50 FOR BOTH CELLS BUT FIRST GIVING A CHANCE TO EXIT,
'     SAVE, CONTINUE, OR START OVER
4 'LABEL >>>>>>>>>>>>>

'SAVE MENU *******************************************************************
menuclear
clearmsg
        IF sav$ = "0" THEN

                CALL Savemenu(sint!, savmen$, namefile2$, sav$)
                IF savmen$ = "p" THEN GOTO 25
                IF savmen$ = "i" THEN GOTO 25
        END IF
23 'LABEL >>>>>>>>>>>>>
clrscrn
clearmsg

'EXIT MENU *******************************************************************
CALL Exitmenu(exit$)

'EXIT MENU DECISION STRUCTURE ************************************************
IF exit$ = "i" THEN
        clearmsg
        GOTO 7
ELSEIF exit$ = "f" THEN
        clearmsg
        GOTO 6
ELSEIF exit$ = "x" THEN
        clearmsg
        clrscrn
        dispstring "BYE"
        display -1950, -1500, 10
        dispstring "TO GET OUT OF AXOBASIC"
        display -1950, -1700, 10
        dispstring "PRESS IN SEQUENCE <ANY KEY> then <ALT> then <F> then
<X>"
        display -1950, -1800, 10
ELSEIF exit$ = "p" THEN
        clearmsg
        GOTO 25
ELSE
        SOUND 1000, 2
        GOTO 23
END IF

'SET Vhold TO -50mV FOR BOTH CELLS ------------------------------------
dac 1, -105
dac 0, -105

END    '*********************************************************************

'END OF MAIN MODULE - TWOCELL.BAS ********************************************
```

```
'SUBROUTINES BEGIN HERE ************************************************
REM $DYNAMIC

'CAPmeas Subroutine

CAPACITANCE AND SERIES RESISTANCE MEASUREMENT SUBROUTINE WITH A CLAMPEX
COMPATIBLE DATA FILE CREATED

SUB CAPmeas (voff%, holdv%, cg1!, cg2!, ctics%, namefile1$, yymmdd!,
etime!, ff1%, savdat$, stim$)'

'DESCRIPTION: GIVE 1 SYNCHRONIZED PULSE TO BOTH CELLS Vh = -50 WITH 10mV
'      HYPERPOLARIZING PULSES DISPLAY DATA AND STORE IN USER BUFFER AND
'      THEN TO FILE - RETURN TO PULSING AS BEFORE CALLING THIS PROCEDURE
'      WITHOUT INTERRUPTION

'INITIALIZE OUTPUT REGION IN FILE ----------------------------------
p% = 0

'OPEN FILE FOR DATA INPUT ------------------------------------------
CALL Openfile1(namefile1$, ff1%, stim$)
IF stim$ = "x" THEN EXIT SUB

'START TIME --------------------------------------------------------
'GET STARTTIME FOR CLAMPEX FILE HEADER FOR CALCULATING ELAPSED TIME.
'      KEEP INACTIVATED EXCEPT FOR TESTING LENGTH OF TIME FOR CAPmeas BY
'      PUTTING starttime! value into Pclampheader at line [8] elpsdtime!
'      = time AND starttime! = elpsdtime! / 1000

'STIMULATION, DATA SAMPLING ********************************************

'CAP MEAS EXITING --------------------------------------------------
'HIT ANY KEY TO EXIT CAPmeasuring AND RETURN TO MAIN MODULE
IF INKEY$ <> "" THEN
        closeb 1
        EXIT SUB
ELSE
END IF

'STIMULUS TEMPLATE -------------------------------------------------
'STIMULATION AND SAMPLING USING EVOKE - STIMULUS TEMPLATE STORED IN
'      LOCATIONS 2048-4096
FOR nrf = 2048 TO 2348
        buf(nrf) = -105 + voff%
NEXT nrf
FOR nrf = 2349 TO 3349
        buf(nrf) = -126 + voff%
NEXT nrf
FOR nrf = 3350 TO 4096
        buf(nrf) = -105 + voff%
NEXT nrf

'STIM & SAMPLE -----------------------------------------------------
'1024 POINTS AT 25 usec
evoke1 ctics%, 2048, 2, 0, 2048, 1

'CYCLE TIMING ------------------------------------------------------
'add to make 2sec between pulses
waitclock 1727

'RAW DATA STORAGE --------------------------------------------------
'STORE DATA INTO DATA FILE AT BINARY LOCATION 1024+ or AXOTAPE BUFFER
```

```
'     BLOCK LOCATION 2
'1.  OUTPUT INTERLEAVED DATA TO FILE
outb 0, 8, 1, 2

'UNPACKING AND DATA DISPLAY ********************************************

'UNPACKING INTERLEAVED DATA ----------------------------------------
packl 0, 4096, 1024, 2, 1
packl 1, 5120, 1024, 2, 1

'DISPLAY OF UNPACKED DATA ------------------------------------------
wipe
dispstring "gain mV/pA:"
display -1250, 1800, 10
dispflt cg1!
display -600, 1800, 10
dispstring "gain mV/pA:"
display 350, 1800, 10
dispflt cg2!
display 1000, 1800, 10
scstart = -1800
scend = 1800
disl 4096, 1024
scstart = -1800
scend = 1800
disl 5120, 1024

'CALCULATIONS -----------------------------------------------------
'CALCULATIONS OF MAXIMUM CURRENT AND LEAK CURRENT FOR DISPLAY TO SCREEN.
'     Average 50 points for base current right before a voltage pulse
'     and 100 points for current during a voltage pulse (leak) and
'     convert from AD units to pA and apply gain correction. Absolute
'     value is taken of amp value (amp); the difference of base and
'     leak, i.e. the apparent leak. As well the min or minimum current
'     for the capacitive spike is found and the current is calculated
'     based on a gain of cg#!. From this series resistance is calculated
'     assuming delta Vpipette = 10 mV and gains = cg1! and cg2! If
'     measurement of pA is less than .1 then values are set to zero.
base2! = (suml(4096, 50) / 50) / (.2048 * cg2!)
leak2! = (suml(4790, 50) / 50) / (.2048 * cg2!)
amp2! = leak2! - base2!
IF amp2! < 0 THEN amp2! = amp2! * -1
IF amp2! < .1 THEN amp2! = 0
xxx% = minl(4096, 400)
min2! = (buf(xxx%) - base2!) / (.2048 * cg2!)
IF min2! < 0 THEN min2! = min2! * -1
Rs2! = (10 / min2!) * 1000
base1! = (suml(5120, 50) / 50) / (.2048 * cg1!)
leak1! = (suml(5670, 50) / 50) / (.2048 * cg1!)
amp1! = leak1! - base1!
IF amp1! < 0 THEN amp1! = amp1! * -1
IF amp1! < .1 THEN amp1! = 0
xxx% = minl(5120, 100)
min1! = (buf(xxx%) - base1!) / (.2048 * cg1!)
IF min1! < 0 THEN min1! = min1! * -1
Rs1! = (10 / min1!) * 1000

'WRITE AMPLITUDES TO SCREEN ---------------------------------------
dispstring "Ileak   pA:"
display -1250, 1700, 10
dispstring "Ipeak   pA:"
display -1250, 1600, 10
```

```
dispstring "Rs*   Mohm:"
display -1250, 1500, 10
dispflt amp1!
display -600, 1700, 10
dispflt min1!
display -600, 1600, 10
dispflt Rs1!
display -600, 1500, 10
dispstring "Ileak   pA:"
display 350, 1700, 10
dispstring "Ipeak   pA:"
display 350, 1600, 10
dispstring "Rs*   Mohm:"
display 350, 1500, 10
dispflt amp2!
display 1000, 1700, 10
dispflt min2!
display 1000, 1600, 10
dispflt Rs2!
display 1000, 1500, 10

'END LOOP ------------------------------------------------------------

'END TIME ------------------------------------------------------------
'END STORED IN CLAMPEX FILE HEADER TO CALCULATE ELAPSED TIME
elpsdtime! = time
etime! = elpsdtime! / 60000
endtime! = elpsdtime! / 1000

'CLOSE FILE ----------------------------------------------------------
closeb 1

'CREATE A CLAMPEX COMPATIBLE HEADER FOR DATA FILE **********************
gn1! = cg1! / 1000
gn2! = cg2! / 1000
CALL Pclampheader(ctics%, gn1!, gn2!, starttime!, endtime!, namefile1$,
yymmdd!, etime!)

'WRITE CALCULATED DATA TO ASCII FILE ************************************
'IF THIS CAPmeas IS PART OF A GjSTIM PROTOCOL AND IF AN ASCII/PAF FILE
'     HAS BEEN OPENED BY OPENFILE2 THEN AT THE END OF THIS CAPmeas
'     ROUTINE WRITE ONE LINE TO THE FILE WITH ELAPSED TIME, THE FILE
'     NUMBER IN THE FILENAME OF THIS JUST SAVED RAW DATA CAPmeas FILE
'     AND THE CALCULATED SERIES RESISTANCE
IF stim$ = "3" THEN
IF savdat$ = "n" THEN
        WRITE #2, ff1% - 1, "", "", "", "", "", "", "", cg1!, cg2!,
etime!, -50, 0, Rs1!, Rs2!
ELSEIF savedat$ = "o" THEN
        WRITE #2, ff1% - 1, "", "", "", "", "", "", "", cg1!, cg2!,
etime!, -50, 0, Rs1!, Rs2!
ELSE
        EXIT SUB
END IF
END IF

END SUB
```

Capstim Subroutine

```
PROTOCOL FOR MONITORING CELL CAPACITANCE IN CELL PAIRS WITHOUT DATA
SAVING
SUB Capstim (voff%, ctics%, cg1!, cg2!)

'STIMULATION PROCEDURE: HOLD AT -50 AND PULSE SIMULTANEOUSLY TO BOTH
'     CELLS TO -60; IF voff% IS NON-ZERO ENTIRE PROTOCOL WILL SHIFT SO
'     THAT -20mV PULSES ARE APPLIED FROM A DIFFERENT Vhold

'STIMULATION/SAMPLING ************************************************

'STIMULUS TEMPLATE ---------------------------------------------------
' STIMULATION AND SAMPLING USING EVOKE - WITH TEMPLATE STORED IN
LOCATIONS
' 2048-4096 - HOLD AT -50mV AND THEN PULSE TO -60 FOR 12msec
FOR nrf = 2048 TO 2348
        buf(nrf) = -105 + voff%
NEXT nrf
FOR nrf = 2349 TO 3349
        buf(nrf) = -126 + voff%
NEXT nrf
FOR nrf = 3350 TO 4096
        buf(nrf) = -105 + voff%
NEXT nrf

'STIM & SAMPLE -------------------------------------------------------
'1024 POINTS AT 25 usec
evokel ctics%, 2048, 2, 0, 2048, 1

'CYCLE TIMING --------------------------------------------------------
'add to make 2sec between pulses
waitclock 1727

'UNPACKING AND DATA DISPLAY ******************************************

'UNPACKING INTERLEAVED DATA ------------------------------------------
packl 0, 4096, 1024, 2, 1
packl 1, 5120, 1024, 2, 1

'DISPLAY OF UNPACKED RAW DATA ----------------------------------------
wipe
scstart = -1800
scend = 1800
disl 4096, 1024
scstart = -1800
scend = 1800
disl 5120, 1024

'CALCULATIONS --------------------------------------------------------
'CALCULATIONS OF MAXIMUM CURRENT AND LEAK CURRENT FOR DISPLAY TO SCREEN
'Average 50 points for base current right before a voltage pulse and 100
'     points for current during a voltage pulse (leak) and convert from
'     AD units to pA and apply gain correction. Absolute value is taken
'     of amp value (amp); the difference of base and leak, i.e. the
'     apparent leak. As well the min or minimum current for the
'     capacitive spike is found and the current is calculated based on a
'     gain. From this series resistance is calculated assuming delta
'     Vpipette = 10 mV. If measurement of pA is less than .1 then values
'     are set to zero.
base2! = (suml(4096, 50) / 50) / (.2048 * cg2!)
leak2! = (suml(4790, 50) / 50) / (.2048 * cg2!)
```

```
amp2! = leak2! - base2!
IF amp2! < 0 THEN amp2! = amp2! * -1
IF amp2! < .1 THEN amp2! = 0
xxx% = min1(4096, 400)
min2! = (buf(xxx%) - base2!) / (.2048 * cg2!)
IF min2! < 0 THEN min2! = min2! * -1
Rs2! = (10 / min2!) * 1000

base1! = (sum1(5120, 50) / 50) / (.2048 * cg1!)
leak1! = (sum1(5670, 50) / 50) / (.2048 * cg1!)
amp1! = leak1! - base1!
IF amp1! < 0 THEN amp1! = amp1! * -1
IF amp1! < .1 THEN amp1! = 0
xxx% = min1(5120, 100)
min1! = (buf(xxx%) - base1!) / (.2048 * cg1!)
IF min1! < 0 THEN min1! = min1! * -1
Rs1! = (10 / min1!) * 1000

'WRITE AMPLITUDES TO SCREEN ----------------------------------------
dispstring "Ileak   pA:"
display -1250, 1700, 10
dispstring "Ipeak   pA:"
display -1250, 1600, 10
dispstring "Rs*   Mohm:"
display -1250, 1500, 10
dispflt amp1!
display -600, 1700, 10
dispflt min1!
display -600, 1600, 10
dispflt Rs1!
display -600, 1500, 10
dispstring "Ileak   pA:"
display 350, 1700, 10
dispstring "Ipeak   pA:"
display 350, 1600, 10
dispstring "Rs*   Mohm:"
display 350, 1500, 10
dispflt amp2!
display 1000, 1700, 10
dispflt min2!
display 1000, 1600, 10
dispflt Rs2!
display 1000, 1500, 10

'DISPLAY GAINS for cell 1 & cell 2 ----------------------------------
dispstring "gain mV/pA:"
display -1250, 1800, 10
dispflt cg1!
display -600, 1800, 10
dispstring "gain mV/pA:"
display 350, 1800, 10
dispflt cg2!
display 1000, 1800, 10

'DISPLAY PULSE DURATION FOR CAPSTIM AND CAPmeas ---------------------
dispstring "CAPmeas and CAPstim"
display 500, -1000, 10
dispstring "  PULSE DUR (msec):  "
display 500, -1200, 10
dispint ctics%
display 1550, -1200, 10
END SUB
```

Gjstim Subroutine

SUBROUTINE FOR SUPPLYING TRAINS OF TRANSJUNCTIONAL VOLTAGE PULSES

```
SUB Gjstim (kj%, sint!, ttt!, holdv%, voff%, cps%, g1!, g2!, etime!,
savdat$)

'STIMULATING PROCEDURE: HOLD AT -50 AND PULSE ALTERNATELY TO EITHER CELL
'     TO -70; IF voff% IS NON-ZERO ENTIRE PROTOCOL WILL SHIFT SO THAT
'     -20mV PULSES ARE APPLIED FROM A DIFFERENT Vhold
'
'PROTOCOL FOR MONITORING JCNAL CURRENTS WITH BOTH CELLS HELD AT THE
'     SAME STARTING VOLTAGE
'          CALIBRATED FOR ONE PULSE EVERY 3 SECONDS

'ALTERNATING STIMULATION WITH SAMPLE ************************************

'STIMULATION & SAMPLING -------------------------------------------------
'cps% determines which cell pulsed
'1.  cells to -50 for 3s
'2.  CYCLE TIMING - add to make 3s between pulses
'3.  sample 106pts every 3.33msec (353msec)
'4.  one cell to -70 s 100ms according to cps%
'5.  sample 300pts every 3.33msec (1sec)
'6.  cells back to -50
'7.  sample 106pts every 3.33msec (353msec)
dac 1, -105 + voff%                          '1.
dac 0, -105 + voff%
waitclock 775                                '2.
samplel 500, 106, 2, 0, 0, 2                 '3.
dac cps%, -147 + voff%                       '4.
samplel 333, 300, 2, 106, 0, 2               '5.
dac 1, -105 + voff%                          '6.
dac 0, -105 + voff%
samplel 500, 106, 2, 406, 0, 2               '7.

'ELAPSED TIME ----------------------------------------------------------
'CALC AND DISPLAY ELAPSED TIME IN minutes
elpsdtime! = time
etime! = elpsdtime! / 60000

'UNPACKING, DISPLAYING, CALCULATING AND SAVING **************************

'UNPACK DATA ------------------------------------------------------------
'1.  cell 2 data
'2.  cell 1 data
packl 0, 512, 256, 2, 1              '1.
packl 1, 768, 256, 2, 1              '2.

'DISPLAY OF DATA -------------------------------------------------------
'1.  cell 2 data
'2.  cell 1 data
wipe
scstart = 100          '2.
scend = 1800
disb 2, 1
scstart = -1800        '1.
scend = -100
disb 3, 1

'CALCULATIONS ----------------------------------------------------------
'Average 50 points for base current right before a voltage pulse and 100
```

```
'     points for current during a voltage pulse (peak) and convert from
'     AD units to pA and apply gain correction. Absolute value is taken
'     of amp value (amp); the difference of base and peak, i.e. the
'     apparent Ij. If amp is less than .1 it is set to zero.
base2! = (suml(512, 50) / 50) / (.2048 * g2!)
peak2! = (suml(600, 100) / 100) / (.2048 * g2!)
amp2! = peak2! - base2!
IF amp2! < 0 THEN amp2! = amp2! * -1
IF amp2! < .1 THEN amp2! = 0

base1! = (suml(768, 50) / 50) / (.2048 * g1!)
peak1! = (suml(865, 100) / 100) / (.2048 * g1!)
amp1! = peak1! - base1!
IF amp1! < 0 THEN amp1! = amp1! * -1
IF amp1! < .1 THEN amp1! = 0

'WRITE AMPLITUDES TO SCREEN ----------------------------------------
dispstring "Iamp    pA:"
display -1250, 1700, 10
dispflt amp1!
display -600, 1700, 10
dispstring "Iamp    pA:"
display 350, 1700, 10
dispflt amp2!
display 1000, 1700, 10

'DISPLAY GAINS for cell 1 & cell 2 ----------------------------------
dispstring "gain mV/pA:"
display -1250, 1800, 10
dispflt g1!
display -600, 1800, 10
dispstring "gain mV/pA:"
display 350, 1800, 10
dispflt g2!
display 1000, 1800, 10

'WRITE DATA TO OPEN FILE #2 -----------------------------------------
'1.  STOP HERE IF SAVDAT$ IS "D" i.e. DON'T SAVE DATA
'2.  ONLY SAVE DATA AT defined interval (sint!)
'3.  SWITCH SO THAT DATA FROM TWO CONSECUTIVE PULSES IS SAVED
'    if sint! >= time for three pulses then data from two consecutive
'     pulses will be saved and then not again until the interval has
'     passed; if sint! <= time for two pulses then every pulse will be
'     saved; if, time for two pulses > sint! > time for three pulses,
'     then be careful since saving will not occur at perfectly timed
'     intervals
IF savdat$ = "d" THEN EXIT SUB          '1.
IF etime! > ttt! THEN                   '2.
        WRITE #2, "", base1!, peak1!, amp1!, base2!, peak2!, amp2!,
cps%, g1!, g2!, etime!, holdv%
        SOUND 500, .5
   IF kj% = 1 THEN                      '3.
       ttt! = ttt! + sint!
       kj% = 0
   ELSEIF kj% = 0 THEN
       kj% = 1
   END IF
END IF
END SUB
```

Vjstim Subroutine

```
SUBROUTINE FOR SUPPLYING SINGLE TRANSJUNCTIONAL VOLTAGE PULSES OF ANY
SIZE AND DURATION AND FOR STORAGE TO PCLAMP COMPATIBLE DATA FILES

SUB Vjstim (plm%, plm!, holdv%, voff%, g1!, g2!, etime!, yymmdd!, ff3%,
savdat$, stim$)

'STIMULATING PROCEDURE: HOLD BOTH CELLS AT -50 AND PULSE ONE CHOSEN CELL
'      TO THE COMMANDED TRANSJUNCTIONAL POTENTIAL; IF voff% IS NON-ZERO
'      ENTIRE PROTOCOL WILL SHIFT SO THAT PULSES ARE APPLIED FROM
'      DIFFERENT Vhold.

37 'LABEL >>>>>>>>>>>>>

'FILE MENU ------------------------------------------------------------
'savdata$ is used in determining if raw data is to be saved in a Pclamp
'      compatible file. Also, Openfile3 subroutine uses it to determine
'      if a new or old data file is to be opened.
wipe
clearmsg
dispstring " **** Vjstim ****"
display -1600, -400, 10
dispstring "**** FILE MENU ****"
display -1600, -500, 10
dispstring "<d> DON'T SAVE TO FILE"
display -1600, -700, 10
dispstring "<n> MAKE NEW"
display -1600, -900, 10
dispstring "<o> APPEND TO OLD"
display -1600, -1100, 10
dispstring "      <key> ?"
display -1600, -1300, 10

'INPUT savdata$ -------------------------------------------------------
'savdata$ USED IN DECIDING IF WRITING TO FILE WILL OCCUR
savdata$ = INPUT$(1)
wipe
clearmsg

'CHECK FOR CORRECT INPUT -----------------------------------------------
IF savdata$ = "d" THEN
        GOTO 38
ELSEIF savdata$ = "n" THEN
        CALL Openfile3(namefile3$, ff3%, stim$, savdata$, savit$)
        IF stim$ = "x" THEN EXIT SUB
        plm% = 0
        plm! = 1
        GOTO 38
ELSEIF savdata$ = "o" THEN
        CALL Openfile3(namefile3$, ff3%, stim$, savdata$, savit$)
        IF stim$ = "x" THEN EXIT SUB
        GOTO 38
ELSE
        SOUND 1000, 2
        GOTO 37
END IF
38 'LABEL >>>>>>>>>>

'SIZE OF Vj PULSE TO USE -----------------------------------------------
wipe
dispstring "Vj pulse size?"
```

```
display -1600, -1300, 10
PRINT ""
INPUT "Vj pulse size and sign in mV:  "; vjpulse!
IF vjpulse! > 200 THEN
        SOUND 1000, 2
        GOTO 38
END IF
vjp! = vjpulse! * 2.1

'DURATION OF PULSE ------------------------------------------------
wipe
clearmsg
dispstring "Vj pulse duration?"
display -1600, -1300, 10
PRINT ""
INPUT "Vj pulse duration in seconds:  "; vjdur!
IF vjdur! = 0 THEN
        SOUND 1000, 2
        GOTO 38
END IF
vjd% = vjdur! * 125
vjdpc! = vjdur! * 1250
40 'LABEL >>>>>>>>>>

'CELL TO PULSE ----------------------------------------------------
wipe
clearmsg
dispstring "*** Cell to Pulse? ***"
display -1600, -500, 10
dispstring "   <1> CELL ONE"
display -1600, -700, 10
dispstring "   <2> CELL TWO"
display -1600, -900, 10
dispstring "      <key> ?"
display -1600, -1100, 10

'INPUT -----------------------------------------------------------
'INPUT cps$ to determine if cell 1, cell 2, or both cells will be pulsed
ctp$ = INPUT$(1)

'CHECK FOR CORRECT INPUT ------------------------------------------
wipe
IF ctp$ = "1" THEN
        ctp% = 0
ELSEIF ctp$ = "2" THEN
        ctp% = 1
ELSE
        SOUND 1000, 2
        GOTO 40
END IF
wipe
clearmsg

'STIMULATION WITH SAMPLE ******************************************

'STIMULATION & SAMPLING -------------------------------------------
'ctp% determines which cell pulsed
'1.  cells to -50 for 3s
'3.  sample 112pts every 18.75msec (2100msec)
'4.  one cell to -70 s 100ms according to cps%
'5.  sample 800pts every 18.75msec (15sec)
'6.  cells back to -50
```

```
'7.  sample 112pts every 18.75msec (2100msec)
dac 1, -105 + voff%                          '1.
dac 0, -105 + voff%
samplel vjd%, 112, 2, 0, 0, 2                '3.
dac ctp%, vjp! - 105 + voff%                 '4.
samplel vjd%, 800, 2, 112, 0, 2              '5.
dac 1, -105 + voff%                          '6.
dac 0, -105 + voff%
samplel vjd%, 112, 2, 912, 0, 2              '7.

'ELAPSED TIME ------------------------------------------------------
'CALC AND DISPLAY ELAPSED TIME IN minutes
elpsdtime! = time
etime! = elpsdtime! / 60000

'RAW DATA STORAGE ---------------------------------------------------
'STORE DATA INTO DATA FILE AT BINARY LOCATION 1024 or AXOTAPE BUFFER
'      BLOCK
'LOCATION 2 (there are 2 file bytes/location)
'1.  OUTPUT INTERLEAVED DATA TO FILE
'2.  for new files data is stored at location 2 but for storage of data
'     to old files the data location is incremented
IF savdata$ = "d" THEN
        GOTO 41
ELSEIF savdata$ = "n" THEN
        outb 0, 4, 3, 2
        plm% = plm% + 4
        plm! = 1
ELSEIF savdata$ = "o" THEN
        outb 0, 4, 3, 2 + plm%
        plm% = plm% + 4
        plm! = plm! + 1
END IF
41 'LABEL >>>>>>>>>>>

'UNPACKING, DISPLAYING, CALCULATING AND SAVING **************************

'UNPACK DATA --------------------------------------------------------
'1.  cell 2 data
'2.  cell 1 data
packl 0, 1024, 512, 2, 1          '1.
packl 1, 1536, 512, 2, 1          '2.

'DISPLAY OF DATA ----------------------------------------------------
'1.  cell 2 data
'2.  cell 1 data
wipe
scstart = 100          '2.
scend = 1800
disb 1, 2

scstart = -1800        '1.
scend = -100
disb 6, 2

'CALCULATIONS -------------------------------------------------------
'Average 50 points for base current right before a voltage pulse and 50
'     points for current during a voltage pulse (peak) and convert from
'     AD units to pA and apply gain correction. Absolute value is taken
'     of amp value (amp); the difference of base and peak, i.e. the
'     apparent Ij. If amp is less than .1 it is set to zero.
base2! = (suml(1024, 50) / 50) / (.2048 * g2!)
```

```
peak2! = (suml(400, 50) / 50) / (.2048 * g2!)
amp2! = peak2! - base2!
IF amp2! < 0 THEN amp2! = amp2! * -1
IF amp2! < .1 THEN amp2! = 0

base1! = (suml(1536, 50) / 50) / (.2048 * g1!)
peak1! = (suml(1942, 50) / 50) / (.2048 * g1!)
amp1! = peak1! - base1!
IF amp1! < 0 THEN amp1! = amp1! * -1
IF amp1! < .1 THEN amp1! = 0

'WRITE AMPLITUDES TO SCREEN ----------------------------------------
dispstring "Iamp    pA:"
display -1250, 1700, 10
dispflt amp1!
display -600, 1700, 10
dispstring "Iamp    pA:"
display 350, 1700, 10
dispflt amp2!
display 1000, 1700, 10

'DISPLAY GAINS for cell 1 & cell 2 ----------------------------------
dispstring "gain mV/pA:"
display -1250, 1800, 10
dispflt g1!
display -600, 1800, 10
dispstring "gain mV/pA:"
display 350, 1800, 10
dispflt g2!
display 1000, 1800, 10

'END TIME -----------------------------------------------------------
'END STORED IN CLAMPEX FILE HEADER TO CALCULATE ELAPSED TIME
elpsdtime! = time
etime! = elpsdtime! / 60000
endtime! = elpsdtime! / 1000

'CLOSE FILE ---------------------------------------------------------
closeb 3

'CREATE A CLAMPEX COMPATIBLE HEADER FOR DATA FILE **********************
IF savdata$ = "d" THEN GOTO 39
gn1! = g1! / 1000
gn2! = g2! / 1000
holdv! = (-105 + voff%) / 2.1
CALL Pclampheader3(h  dv!, vjpulse!, vjdpc!, plm!, gn1!, gn2!,
starttime!, endtime!, namefile3$, yymmdd!, etime!)
39 'LABEL >>>>>>>>>>>>>

'WRITE CALCULATED DATA TO ASCII FILE ************************************
'IF THIS CAPmeas IS PART OF A GjSTIM PROTOCOL AND IF AN ASCII/PAF FILE
'     HAS BEEN OPENED BY OPENFILE2 THEN AT THE END OF THIS CAPmeas
'     ROUTINE WRITE ONE LINE TO THE FILE WITH ELAPSED TIME, THE FILE
'     NUMBER IN THE FILENAME OF THIS JUST SAVED RAW DATA CAPmeas FILE
'     AND THE CALCULATED SERIES RESISTANCE
IF stim$ = "3" THEN
IF savdat$ = "n" THEN
       WRITE #2, ff3% - 1, base1!, peak1!, amp1!, base2!, peak2!,
amp2!, ctp%, g1!, g2!, etime!, holdv%, vjpulse!, "", ""
ELSEIF savedat$ = "o" THEN
       WRITE #2, ff3% - 1, base1!, peak1!, amp1!, base2!, peak2!,
amp2!, ctp%, g1!, g2!, etime!, holdv%, vjpulse!, "", ""
```

```
ELSE
        EXIT SUB
END IF
END IF

waitclock 2000

END SUB
```

REFERENCES

Anumonwo JMB, Wang H-Z, Trabka-Janik E, Dunham B, Veenstra RD, Delmar M & Jalife J. 1992. Gap junctional channels in adult mammalian sinus nodal cells. Immunolocalization and electrophysiology. *Circulation Research* **71**:229-239

Arvanitaki A & Chalazonitis N. 1959. Interactions electriques intre le soma géant et les somata immediatement contigus (ganglion pleurobronchial d'*Aplysia*). *Bulletin de l'Institut Oceanoghraphique* **1143**:1-30

Auerbach AA & Bennett MVL. 1969. A rectifying synapse in the central nervous system of a vertebrate. *Journal of General Physiology* **53**:211-237

Baerwald RJ. 1975. Inverted gap and other cell junctions in cockroach hemocyte capsules: A thin section and freeze-fracture study. *Tissue and Cell* **7**:575-585

Barrio LC, Suchyna T, Bargiello T, Roginsky R, Zukin RS, Nicholson B & Bennett MVL. 1991. Kinetic properties of voltage dependence of rat connexin 26 and 32 junctions expressed in *Xenopus* oocytes. *Biophysical Journal* **59**:440a

Bennett MVL, Barrio LC, Bargiello TA & Spray DC, Hertzberg E, Sáez JC. 1991. Gap junctions: new tools, new answers, new questions. *Neuron* **6**:305-320

Bennett MVL, Spray DC & Harris AL. 1981. Electrical coupling in development. *American Zoologist* **21**:413-427

Bennett MVL, Verselis V, White RL & Spray DC. 1988. Gap junctional conductance: gating. **In**: *Gap Junctions*. EL Hertzberg & RG Johnson, Ed. Alan R. Liss, New York. pp.287-304

Berdan RC & Caveney S. 1985. Gap junction ultrastructure in three states of conductance. *Cell and Tissue Research* **239**:111-122

Bevilacqua A, Loch-Caruso R & Erickson RP. 1989. Abnormal development and dye-coupling produced by anti-sense RNA to gap junction protein in mouse preimplantation embryos. *Proceedings of the National Academy of Science of U.S.A.* **86**:5444-5448

Beyer EC, Paul DL & Goodenough DA. 1990. Connexin family of gap junction proteins. *Journal of Membrane Biology* **116**:187-194

Binnington K & Retnakaran A, Ed. 1991. *Physiology of the Insect Epidermis*. CSIRO, Australia.

Blennerhassett MG. 1984. Selectivity in Junctional Communication. University of Western Ontario. Ph D Thesis.

Blennerhassett MG & Caveney S. 1984. Separation of developmental compartments by a cell type with reduced junctional permeability. *Nature* **309**:361-364

Boitano S, Dirksen ER & Sanderson MJ. 1992. Intercellular propagation of calcium waves mediated by inositol trisphosphate. *Science* **258**:292-295

Brink PR & Fan S-F. 1989. Patch clamp recordings from membranes which contain gap junction channels. *Biophysical Journal* **56**:579-593

Bruzzone R & Meda P. 1988. The gap junction: a channel for multiple functions? *European Journal of Clinical Investigation* **18**:444-453

Bukauskas F, Kempf C & Weingart R. 1991. Electrical coupling between cells of the insect *Aedes albopictus*. *Journal of Physiology* **448**:321-337

Bukauskas FF, Kempf C & Weingart R. 1992. Cytoplasmic bridges and gap junctions in an insect cell line (*Aedes albopictus*). *Experimental Physiology* **77**:903-911

Bukauskas FF & Weingart R. 1993. Short communication. Multiple conductance states of newly formed single gap junction channels between insect cells. *Pflügers Archives* **423**:152-154

Burt JM. 1991. Modulation of cardiac gap junction channel activity by the membrane lipid environment. **In**: *Biophysics of Gap Junction Channels*. C Peracchia, Ed. CRC Press, Boca Raton, Fl. pp.75-96

Burt JM & Spray DC. 1988a. Inotropic agents modulate gap junctional conductance between cardiac myocytes. *American Journal of Physiology* **254 (Heart Circ. Physiol. 23)**:H1206-H1210

Burt JM & Spray DC. 1988b. Single-channel events and gating behaviour of the cardiac gap junction channel. *Proceedings of the National Academy Science of the U.S.A.* **85**:3431-3434

Burt JM & Spray DC. 1989. Volatile anaesthetics block intercellular communication between neonatal rat myocardial cells. *Circulation Research* **65**:829-837

Caveney S. 1978. Intercellular communication in insect development is hormonally controlled. *Science* **199**:192-195

Caveney S. 1985a. Intercellular communication. **In:** *Comprehensive Insect Physiology Biochemistry and Pharmacology*. GA Kerkut & LI Gilbert, Ed. Pergamon Press, Toronto. vol.2, pp.319-370

Caveney S. 1985b. The role of gap junctions in development. *Annual Reviews of Physiology* **47**:319-335

Caveney S. 1988. Developmental physiology of insect gap junctions. **In:** *Gap Junctions*. EL Hertzberg & RG Johnson, Ed. Alan R. Liss, New York. pp.495-504

Caveney S & Berdan R. 1982. Selectivity in junctional coupling between cells of insect tissues. **In:** *Insect Ultrastructure*. RC King & H Akai, Ed. Plenum Press, New York. vol.1, pp.434-465

Caveney S, Berdan RC, Blennerhassett MG & Safranyos RGA. 1986. Cell-to-cell coupling via membrane junctions: methods that show its regulation by a developmental hormone in an insect epidermis. **In:** *Techniques in In Vitro Invertebrate Hormones and Genes*. E Kurstak, Ed. Elsevier Scientific Publishers, Ireland. pp.1-23

Caveney S, Berdan RC & McLean S. 1980. Cell-to-cell ionic communication stimulated by 20-hydroxyecdysone occurs in the absence of protein synthesis and gap junction growth. *Journal of Insect Physiology* **26**:557-567

Caveney S & Blennerhassett MG. 1980. Elevation of ionic conductance between insect epidermal cells by ß-ecdysone *in vitro*. *Journal of Insect Physiology* **26**:13-25

Caveney S & Safranyos RGA. 1989. Developmental physiology of insect epidermal gap junctions. **In:** *Cell Interactions and Gap Junctions*. N Sperelakis & WC Cole, Ed. CRC Press, Baton Rouge, Fl. vol.1, pp.107-123

Chanson M, Bruzzone R, Spray DC, Regazzi R & Meda P. 1988. Cell uncoupling and protein kinase C: correlation in a cell line but not in a differentiated tissue. *American Journal of Physiology* **255 (Cell Physiol. 24)**:C699-C704

Chen Y-H & DeHaan RL. 1992. Multiple-channel conductance states and voltage regulation of embryonic chick cardiac gap junctions. *Journal of Membrane Biology* **127**:95-111

Chow I & Young SH. 1987. Opening of single gap junction channels during formation of electrical coupling between embryonic muscle cells. *Developmental Biology* **122**:332-337

Churchill D & Caveney S. 1993a. Double whole-cell patch-clamp characterization of gap junctional channels in isolated insect epidermal cell pairs. *Journal of Membrane Biology* **135**:165-180

Churchill D & Caveney S. 1993b. Double whole-cell patch-clamp of gap junctions in insect epidermal cell pairs: single channel conductance, voltage dependence and spontaneous uncoupling. **In**: *Gap Junctions*. JE Hall, GA Zampighi & RM Davis, Ed. Elsevier, New York. pp.239-245

Churchill D & Caveney S. 1993c. Isolation of epidermal cell pairs from an insect, *Tenebrio molitor*, for dual whole-cell recording of large-conductance gap-junctional channels. *Journal of Experimental Biology* **178**:261-267

Churchill D, Coodin S, Shivers RR & Caveney S. 1993. Rapid *de novo* formation of gap junctions between insect hemocytes *in vitro*: a freeze-fracture, dye-transfer and patch-clamp study. *Journal of Cell Science* **104**:763-772

Collins A, Somlyo AV & Hilgemann DW. 1992. The giant cardiac membrane patch method: stimulation of outward Na^{+}-Ca^{2+} exchange current by MgATP. *Journal of Physiology* **454**:27-57

Coodin S & Caveney S. 1992. Lipophorin inhibits the adhesion of cockroach (*Periplaneta americana*) haemocytes *in vitro*. *Journal of Insect Physiology* **38**:853-662

Cooper K, Rae JL & Gates P. 1989. Membrane and junctional properties of dissociated frog lens epithelial cells. *Journal of Membrane Biology* **111**:215-227

Cornell-Bell AH & Finkbeiner SM. 1991. Ca^{2+} waves in astrocytes. *Cell Calcium* **12**:185-204

Cornell-Bell AH, Finkbeiner SM, Cooper MS & Smith SJ. 1990. Glutamate induces calcium waves in cultured astrocytes: long-range glial signalling. *Science* **247**:470-473

Cserhåti T & Szögyi M. 1993. Interaction of phospholipids with proteins and peptides. New advances III. *International Journal of Biochemistry* **25**:123-146

DeHaan RL & Chen Y-H. 1990. Development of gap junctions. *Annals of the New York Academy of Science* **588**:164-173

Dahl G, Miller T, Paul D & Voellmy R. 1987. Expression of functional cell-cell channels from cloned rat liver gap junction complementary DNA. *Science* **236**:1290-1293

Dahl G, Werner R, Levine E & Rabadan-Diehl C. 1992. Mutational analysis of gap junction formation. *Biophysical Journal* **62**:172-182

De Mello WC. 1991. Further studies on the influence of cAMP-dependent protein kinase on junctional conductance in isolated heart cell pairs. *Journal of Molecular and Cellular Cardiology* **23**:371-379

Dermietzel R, Hertzberg EL, Kessler JA & Spray DC. 1991. Gap junctions between cultured astrocytes: immunocytochemical, molecular, and electrophysiological analysis. *Journal of Neuroscience* **11**:1421-1432

Dermietzel R, Hwang TK & Spray DC. 1990. The gap junction family: structure, function and chemistry. *Anatomical Embryology* **182**:517-528

Devaux PF. 1988. Phospholipid flipases. *FEBS Letters* **234**:8-12

Devaux PF. 1991. Static and dynamic lipid asymmetry in cell membranes. *Biochemistry* **30**:1163-1173

Diehl-Jones W & Huebner E. 1993. Ionic basis of bioelectric currents during oogenesis in an insect. *Developmental Biology* **158**:301-316

Dorresteijn AWC, Wagemaker HA, deLaat SW & van den Biggelaar JAM. 1983. Dye-coupling between blastomeres in early embryos of *Patella vulgata* (Mollusca Gasteropoda): Its relevance for cell determination. *Wilhelm Roux's Archives of Developmental Biology* **192**:262-269

Fischmeister R, Ayer Jr. RK & DeHaan RL. 1986. Some limitations of the cell-attached patch clamp technique: a two-electrode analysis. *Pflügers Archives* **406**:73-82

Flagg-Newton J, Simpson I & Loewenstein WR. 1979. Permeability of the cell-to-cell membrane channels in mammalian cell junction. *Science* **205**:404-407

Fox JA. 1987. Ion channel subconductance states. *Journal of Membrane Biology* **97**:1-8

Fraser SE & Bryant PJ. 1985. Patterns of dye coupling in the imaginal disk of *Drosophila melanogaster*. *Nature* **317**:533-536

Fraser SE, Green CR, Bode HR & Gilula NB. 1987. Selective disruption of gap junctional communication interferes with a patterning process in *Hydra*. *Science* **237**:49-55

Furshpan EJ & Potter DD. 1959. Transmission at the giant motor synapses of the crayfish. *Journal of Physiology* **145**:289-325

Gevers P & Timmermans LPM. 1991. Dye-coupling and the formation and fate of the hypoblast in the teleost fish embryo, *Barbus Conchonius*. *Development* **112**:431-438

Giaume C. 1991. Application of the patch-clamp technique to the study of junctional conductance. **In**: *Biophysics of Gap Junction Channels*. C Peracchia, Ed. CRC Press, Boca Raton, Fl. pp.175-190

Giaume C, Fromaget C, Aoumari AE, Cordier J, Glowinski J & Gros D. 1991. Gap junctions in cultured astrocytes: single-channel currents and characterization of channel-forming protein. *Neuron* **6**:133-143

Giaume C, Kado RT & Korn H. 1987. Voltage-clamp analysis of a crayfish rectifying synapse. *Journal of Physiology* **386**:91-112

Götz P. 1986. Encapsulation in arthropods. **In**: *Immunity in Invertebrates*. M Brehélin, Ed. Springer-Verlag, New York. pp.153-170

Grimstone AV, Rotheram S & Salt G. 1967. An electron-microscope study of capsule formation by insect blood cells. *Journal of Cell Science* **2**:281-292

Gunn MD, Sen A, Chang A, Willerson JT, Buja LM & Chien KR. 1985. Mechanisms of accumulation of arachidonic acid in cultured myocardial cells during ATP depletion. *American Journal of Physiology* **249 (Heart Circ. Physiol. 18)**:H1188-H1194

Guthrie SC & Gilula NB. 1989. Gap junctional communication and development. *Trends in Neuroscience* **12**:12-16

Hamill OP, Marty A, Neher E, Sakmann B & Sigworth FJ. 1981. Improved patch-clamp techniques for high-resolution current recording from cells and cell-free membrane patches. *Pflügers Archives* **391**:85-100

Han SS & Gupta AP. 1989. Arthropod immune system. II. encapsulation of implanted nerve cord and "plain gut" surgical suture by granulocytes of *Blattella germanica* (L.) (Dictyoptera: Blattellidae). *Zoological Science* **6**:303-320

Hardie DG & MacKintosh RW. 1992. AMP-activated protein kinase- an archetypal protein kinase cascade. *BioEssays* **14**:699-704

Harris AL, Spray DC & Bennett MVL. 1981. Kinetic properties of a voltage-dependent junctional conductance. *Journal of General Physiology* **77**:95-117

Harris AL, Spray DC & Bennett MVL. 1983. Control of intercellular communication by a voltage dependent junctional conductance. *Journal of Neuroscience* **3**:79-100

Hepburn HR, Ed. 1976. *The Insect Integument*. Elsevier, New York.

Hilgemann DW & Collins A. 1992. Mechanism of cardiac Na^{+}-Ca^{2+} exchange current stimulation by MgATP: possible involvement of aminophospholipid translocase. *Journal of Physiology* **454**:59-82

Hille B. 1992. *Ionic Channels of Excitable Cells*. Sinauer Associates Inc., Sunderland, Massachussetts, 2nd ed

Horn R & Marty A. 1988. Muscarinic activation of ionic currents measured by a new whole-cell recording method. *Journal of General Physiology* **92**:145-159

Jaffe LF. 1981. The role of ionic currents in establishing developmental pattern. *Philosophical Transactions of the Royal Society of London. Series B. (Biology)* **295**:553-566

Jan LY & Jan YN. 1989. Voltage-sensitive ion channels. *Cell* **56**:13-25

Johnson LN & Barford D. 1993. The effects of phosphorylation on the structure and function of proteins. *Annual Reviews of Biophysics and Biomolecular Structure* **22**:199-232

Johnston MF & Ramon F. 1982. Voltage independence of an electrotonic synapse. *Biophysical Journal* **39**:115-117

Johnston MF, Simon SA & Ramon F. 1980. Interaction of anesthetics with electrical synapses. *Nature* **286**:509-518

Jongsma HJ, Wilders R, van Ginneken ACG & Rook MB. 1991. Modulatory effect of the transcellular electric field on gap-junction conductance. **In:** *Biophysics of Gap Junction Channels*. C Peracchia, Ed. CRC Press, Boca Raton, Fl. pp.163-174

Kameyama M. 1983. Electrical coupling between ventricular paired cells isolated from guinea-pig heart. *Journal of Physiology* **336**:345-357

Kimmel C & Law R. 1985. Cell lineage of zebrafish blastomeres II. Formation of the yolk syncytial layer. *Developmental Biology* **108**:86-93

King RC & Akai HA, Ed. 1982. *Insect Ultrastructure*. Plenum Press, New York.

Klöckner U & Isenberg G. 1992. ATP suppresses activity of Ca^{2+}-activated K^{+} channels by Ca^{2+} chelation. *Pflügers Archives* **420**:101-105

Koefoed BM. 1987. The ability of an epithelium to survive removal of the basal lamina by enzymes: fine structure and content of sodium and potassium of the midgut epithelium of the larva of *Tenebrio molitor* after withdrawal of the basal lamina by elastase—a short note. *Tissue and Cell* **19**:65-70

Laird DW, Puranam KL & Revel J-P. 1991. Turnover and phosphorylation dynamics of connexin43 gap junction protein in cultured cardiac myocytes. *Biochemical Journal* **273**:67-72

Lal R, Laird DW & Revel J-P. 1993. Antibody perturbation analysis of gap-junction permeability in rat cardiac myocytes. *Pflügers Archives* **422**:449-457

Lane NJ. 1982. Insect intercellular junctions: their structure and development. **In**: *Insect Ultrastructure*. RC King & HA Akai, Ed. Plenum Press, New York. pp.402-433

Lasater EM & Dowling JE. 1985. Electrical coupling between pairs of isolated fish horizontal cells is modulated by dopamine and cAMP. **In**: *Gap Junctions*. MVL Bennett & DC Spray, Ed. Cold Spring Harbor Laboratory, New York. pp. 393-404

Latorre R, Bacigalupo J, Delgado R & Labarca P. 1991. Four cases of direct ion channel gating by cyclic nucleotides. *Journal of Bioenergetics and Biomembranes* **23**:577-597

Lau AF, Kanemitsu Y, Kurata WE, Danesh S & Boynton AL. 1992. Epidermal growth factor disrupts gap-junctional communication and induces phosphorylation of connexin43 on serine. *Molecular Biology of the Cell* **3**:865-874

Laufer M, Salas R, Medina R & Drujan B. 1989. Cyclic adenosine monophosphate as a second messenger in horizontal cell uncoupling in the teleost retina. *Journal of Neuroscience Research* **24**:299-310

Lawrence PA. 1973. A clonal analysis of segment development in *Oncopeltus* (Hemiptera). *Journal of Embryology and Experimental Morphology* **30**:681-699

Lawrence PA & Green SM. 1975. The anatomy of a compartment border. The intersegmental boundary in *Oncopeltus*. *Journal of Cell Biology* **65**:373-382

Lee S, Gilula NB & Warner AE. 1987. Gap junctional communication and compaction during implantation stages of mouse development. *Cell* **51**:851-860

Lees-Miller JP & Caveney S. 1982. Drugs that block calmodulin activity inhibit cell-to-cell coupling in the epidermis of *Tenebrio molitor*. *Journal of Membrane Biology* **69**:233-245

Levinson G & Bradley TJ. 1984. Removal of insect basal laminae using elastase. *Tissue and Cell* **16**:367-375

Levitan IB. 1985. Phosphorylation of ion channels. *Journal of Membrane Biology* **87**:177-190

Lo CW & Gilula NB. 1979. Gap junctional communication in the preimplantation mouse embryo. *Cell* **18**:399-409

Locke M. 1959. The cuticular pattern in an insect, *Rhodnius prolixus* Stal. *Journal of Experimental Biology* **36** 459-477

Locke M. 1987. The very rapid induction of filopodia in insect cells. *Tissue and Cell* **19**:301-318

Loewenstein WR. 1966. Permeability of membrane junctions. *Annals of the New York Academy of Science* **137**:441-472

Loewenstein WR. 1981. Junctional intercellular communication: The cell-to-cell membrane channel. *Physiological Reviews* **61**:829-913

Loewenstein WR. 1986. The cell-to-cell membrane channel. Its regulation by cellular phosphorylation. **In**: *Ionic Channels in Cells and Model Systems*. R Latorre, Ed. Plenum Press, New York. pp.335-351

Loewenstein WR, Kanno Y & Socolar SJ. 1978. Quantum jumps of conductance during formation of membrane channels at cell-cell junction. *Nature* **274**:133-136

Loewenstein WR, Nakas M & Socolar SJ. 1967. Permeability transformations at a cell membrane junction. *Journal of General Physiology* **50**:1865-1891

Manivannan K, Ramanan SV, Mathias RT & Brink PR. 1992. Multichannel recordings from membranes which contain gap junctions. *Biophysical Journal* **61**:216-227

Marty A & Neher E. 1983. Tight-seal whole-cell recording. **In**: *Single-Channel Recording*. B Sakmann & E Neher, Ed. Plenum Press, New York. pp.107-122

Mazet J-L, Jarry T, Gros D & Mazet F. 1992. Voltage dependence of liver gap-junction channels reconstituted into liposomes and incorporated into planar bilayers. *European Journal of Biochemistry* **210**:249-256

Mazzei GJ, Katoh N & Kuo JF. 1982. Polymyxin B is a more selective inhibitor for phospholipid-sensitive Ca^{2+}-dependent protein kinase than for calmodulin-sensitive Ca^{2+}-dependent protein kinase. *Biochemical and Biophysical Research Communications* **109**:1129-1133

McMahon DG, Knapp AG & Dowling JE. 1989. Horizontal cell gap-junctions: single-channel conductance and modulation by dopamine. *Proceedings of the National Academy of Science of the U.S.A.* **86**:7639-7643

Metzger P & Weingart R. 1985. Electric current flow in cell pairs isolated from adult rat hearts. *Journal of Physiology* **366**:177-195

Meves H & Nagy K. 1989. Multiple conductance states of the sodium channel and of other ion channels. *Biochimica et Biophysica Acta* **988**:99-105

Miller AG, Zampighi GA & Hall JE. 1992. Single-membrane and cell-to-cell permeability properties of dissociated embryonic chick lens cells. *Journal of Membrane Biology* **128**:91-102

Moore LK, Beyer EC & Burt JM. 1991. Characterization of gap junction channels in A7r5 vascular smooth muscle cells. *American Journal of Physiology* **260 (Cell Physiol. 29)**:C975-C981

Moreno AP, Campos de Carvalho AC, Christ G, Melman A & Spray DC. 1993. Gap junctions between human corpus cavernosum smooth muscle cells: gating properties and unitary conductance. *American Journal of Physiology* **264 (Cell Physiol. 33)**:C80-C92

Moreno AP, Campos de Carvalho AC, Verselis V, Eghbali B & Spray DC. 1991a. Voltage-dependent gap junction channels are formed by connexin32, the major gap junction protein of rat liver. *Biophysical Journal* **59**:920-925

Moreno AP, Eghbali B & Spray DC. 1991b. Connexin32 gap junction channels in stably transfected cells. Equilibrium and kinetic properties. *Biophysical Journal* **60**:1267-1277

Moreno AP, Eghbali B & Spray DC. 1991c. Connexin32 gap junction channels in stably transfected cells: unitary conductance. *Biophysical Journal* **60**:1254-1266

Moreno AP, Fishman GI & Spray DC. 1992. Phosphorylation shifts unitary conductance and modifies voltage dependent kinetics of human connexin43 gap junction channels. *Biophysical Journal* **62**:51-53

Münster PN & Weingart R. 1993. Effects of phorbol ester on gap junctions of neonatal rat heart cells. *Pflügers Archives* **423**:181-188

Musil LS, Beyer EC & Goodenough DA. 1990. Expression of the gap junction protein connexin 43 in embryonic chick lens: molecular cloning, ultrastructural localization, and post-translational phosphorylation. *Journal of Membrane Biology* **116**:163-175

Musil LS & Goodenough DA. 1990. Gap junctional intercellular communication and the regulation of connexin expression and function. *Current Opinions in Cell Biology* **2**:875-880

Musil LS & Goodenough DA. 1991. Biochemical analysis of connexin43 intracellular transport, phosphorylation, and assembly into gap junctional plaques. *Journal of Cell Biology* **115**:1357-1374

Nagajski DJ, Guthrie SC, Ford CC & Warner AE. 1989. The correlation between patterns of dye transfer through gap junctions and future developmental fate in *Xenopus*: the consequences of u.v. irradiation and lithium treatment. *Development* **105**:747-752

Nakahiro M, Yeh JZ, Brunner E & Narahashi T. 1989. General anesthetics modulate GABA receptor channel complex in rat dorsal root ganglion neurons. *FASEB Journal* **3**:1850-1854

Newton AC. 1993. Interactions of proteins with lipid headgroups: Lessons from protein kinase C. *Annual Reviews of Biophysics and Biomolecular Structure* **22**:1-25

Neyton J & Trautmann A. 1985. Single-channel currents of an intercellular junction. *Nature* **317**:331-335

Neyton J & Trautmann A. 1986a. Acetylcholine modulation of the conductance of intercellular junctions between rat lacrimal cells. *Journal of Physiology* **377**:283-295

Neyton J & Trautmann A. 1986b. Physiological modulation of gap junction permeability. *Journal of Experimental Biology* **124**:93-114

Nicholls JG & Purves D. 1972. Monosynaptic chemical and electrical connexions between sensory and motor cells in the central nervous system of the leech. *Journal of Physiology* **209**:647-667

Nichols CG & Lederer WJ. 1991. Adenosine triphosphate-sensitive potassium channels in the cardiovascular system. *American Journal of Physiology* **261 (Cell Physiol. 30)**:C1675-C1686

Niggli E, Rüdisüli A, Maurer P & Weingart R. 1989. Effects of general anesthetics of current flow across membranes in guinea pig myocytes. *American Journal of Physiology* **256 (Cell Physiol. 25)**:C273-C281

Noma A & Tsuboi N. 1987. Dependence of junctional conductance on proton, calcium and magnesium ions in cardiac paired cells of guinea-pig. *Journal of Physiology* **382**:193-211

Norton WN & Vinson SB. 1977. Encapsulation of a parasitoid egg within its habitual host: An ultrastructural investigation. *Journal of Invertebrate Pathology* **30**:55-67

Obaid AL, Socolar SJ & Rose B. 1983. Cell-to-Cell channels with two independently regulated gates in series: analysis of junctional conductance modulation by membrane potential, calcium, and pH. *Journal of Membrane Biology* **73**:69-89

Ordway RW, Singer JJ & Walsh Jr. JV. 1991. Direct regulation of ion channels by fatty acids. *Trends in Neuroscience* **14**:96-100

Paschke D, Eckert R & Hülser DF. 1992. High-resolution measurements of gap-junctional conductance during perfusion with anti-connexin antibodies in pairs of cultured mammalian cells. *Pflügers Archives* **420**:87-93

Peracchia C. 1991. Effects of the anesthetics heptanol, halothane and isoflurane on gap junction conductance in Crayfish septate axons: a calcium- and hydrogen-independent phenomenon potentiated by caffeine and theophylline, and inhibited by 4-aminopyridine. *Journal of Membrane Biology* **121**:67-78

Pérez-Armendariz M, Roy C, Spray DC & Bennett MVL. 1991. Biophysical properties of gap junctions between freshly dispersed pairs of mouse pancreatic β-cells. *Biophysical Journal* **59**:76-92

Pitts JD. 1977. Direct communication between animal cells. **In:** *International Cell Biology 1976-1977*. BR Brinkley & KR Porter, Ed. Rockerfeller University Press, New York. pp.43-49

Politoff AL, Socolar SJ & Loewenstein WR. 1969. Permeability of a cell membrane junction. Dependence on energy metabolism. *Journal of General Physiology* **53**:498-515

Pusch M & Neher E. 1988. Rates of diffusional exchange between small cells and a measuring patch pipette. *Pflügers Archives* **411**:204-211

Ramón F & Rivera A. 1986. Gap junction channel modulation—A physiological viewpoint. *Progress in Biophysics and Molecular Biology* **48**:127-153

Randriamampita C, Giaume C, Neyton J & Trautmann A. 1988. Acetylcholine-induced closure of gap junction channels in rat lacrimal glands is probably mediated by protein kinase C. *Pflügers Archives* **412**:462-468

Revel JP. 1986. Gap junctions in development. *American Zoologist* **26**:529-533

Revel JP, Griepp EB, Finbow M & Johnson R. 1978. Possible steps in gap junction formation. *Zoon* **6**:139-144

Reverdin EC & Weingart R. 1988. Electrical properties of the gap junctional membrane studied in rat liver cell pairs. *American Journal of Physiology* **254 (Cell Physiol. 23)**:C226-C234

Reynhout JK, Lampe PD & Johnson RG. 1992. An activator of protein kinase C inhibits gap junction communication between cultured bovine lens cells. *Experimental Cell Research* **198**:337-342

Ringham GL. 1975. Localization and electrical characteristics of a giant synapse in the spinal cord of the lamprey. *Journal of Physiology* **251**:395-407

Rook MB, de Jonge B, Jongsma HJ & Masson-Pévet MA. 1990. Gap junction formation and functional interaction between neonatal rat cardiocytes in culture: a correlative physiological and ultrastructural study. *Journal of Membrane Biology* **118**:179-192

Rook MB, Jongsma HJ & van Ginneken ACG. 1988. Properties of single gap junctional channels between isolated neonatal rat heart cells. *American Journal of Physiology* **255 (Heart Circ. Physiol. 24)**:H770-H782

Rook MB, van Ginneken ACG, de Jonge B, El Aoumari A, Gros D & Jongsma HJ. 1992. Differences in gap junction channels between cardiac myocytes, fibroblasts, and heterologous pairs. *American Journal of Physiology* **263 (Cell Physiol. 32)**:C959-C977

Rose B & Loewenstein WR. 1976. Permeability of a cell junction and the local cytoplasmic free ionized calcium concentration: A study with aequorin. *Journal of Membrane Biology* **28**:87-119

Ruangvoravat CP & Lo CW. 1992. Restrictions in gap junctional communication in the *Drosophila* larval epidermis. *Developmental Dynamics* **193**:70-82

Rubin JB, Verselis VK, Bennett MVL & Bargiello TA. 1992. Molecular analysis of voltage dependence of heterotypic gap junctions formed by connexins 26 and 32. *Biophysical Journal* **62**:183-195

Rüdisüli A & Weingart R. 1989. Electrical properties of gap junction channels in guinea-pig ventricular cell pairs revealed by exposure to heptanol. *Pflügers Archives* **415**:12-21

Sáez JC, Connor JA, Spray DC & Bennett MVL. 1989. Hepatocyte gap junctions are permeable to the second messenger inositol 1,4,5-trisphosphate, and to calcium ions. *Proceedings of the National Academy of Science of the U.S.A.* **86**:2708-2712

Sáez JC, Spray DC, Nairn AC, Hertzberg E, Greengard P & Bennett MVL. 1986. cAMP increases junctional conductance and stimulates phosphorylation of the 27-kDa principle gap junction polypeptide. *Proceedings of the National Academy of Science of the U.S.A.* **83**:2473-2477

Safranyos RGA. 1985. Diffusion via cell-to-cell channels. University of Western Ontario. Ph.D. Thesis.

Safranyos RGA & Caveney S. 1984. Rates of diffusion of fluorescent molecules via cell-to-cell membrane channels in a developing tissue. *Journal of Cell Biology* **100**:736-747

Sakai N, Blennerhassett MG & Garfield RE. 1992. Intracellular cyclic AMP concentration modulates gap junction permeability in parturient rat myometrium. *Canadian Journal of Physiology and Pharmacology* **70**:358-364

Sandberg K, Bor M, Ji H, Markwick A, Millan MA & Catt KJ. 1990. Angiotensin II-induced calcium mobilization in oocytes by signal transfer through gap junctions. *Science* **249**:298-301

Schwarzmann G, Wiegandt H, Rose B, Zimmerman A, Ben-Haim D & Loewenstein WR. 1981. Diameter of the cell-to-cell junctional membrane channels as probed with neutral molecules. *Science* **213**:551-553

Serras F & van den Biggelaar JAM. 1987. Is a mosaic embryo also a mosaic of communication compartments? *Developmental Biology* **120**:132-138

Serras F, Baud C, Moreau M, Guerrier P & van den Biggelaar JAM. 1988. Intercellular communication in the early embryo of the ascidian *Ciona intestinalis*. *Development* **102**:55-63

Sheridan JD & Atkinson MM. 1985. Physiological roles of permeable junctions: some possibilities. *Annual Reviews of Physiology* **47**:337-353

Sherman A & Rinzel J. 1991. Model for synchronization of pancreatic ß-cells by gap junction coupling. *Biophysical Journal* **59**:547-559

Slater SJ, Cox KJA, Lombardi JV, Ho C, Kelly MB, Rubin E & Stubbs CD. 1993. Inhibition of protein kinase C by alcohols and anaesthetics. *Nature* **364**:82-84

Smith TG & Baumann F. 1969. The functional organization within the ommatidium of the lateral eye of *Limulus*. *Progress in Brain Research* **31**:313-349

Somogyi R & Kolb H-A. 1988. Cell-to-cell channel conductance during loss of gap junctional coupling in pairs of pancreatic acinar and Chinese hamster ovary cells. *Pflügers Archives* **412**:54-65

Spitzer NC. 1982. Voltage- and stage-dependent uncoupling of Rohon-Beard neurones during embryonic development of *Xenopus* tadpoles. *Journal of Physiology* **330**:145-162

Spray DC. 1990. Electrophysiological properties of gap junction channels. **In:** *Parallels in Cell to Cell Junctions in Plants and Animals*. AW Robards, WJ Lucas, JD Pitts, HJ Jongsma & DC Spray, Ed. Springer-Verlag, Berlin

Spray DC & Bennett MVL. 1985. Physiology and pharmacology of gap junctions. *Annual Reviews of Physiology* **47**:261-303

Spray DC, Bennett MVL, Campos de Carvalho AC, Eghbali B, Moreno AP & Verselis V. 1991a. Transjunctional voltage dependence of gap junction channels. **In:** *Biophysics of Gap Junction Channels*. C Peracchia, Ed. CRC Press, Boca Raton, Fl. pp.175-190

Spray DC, Chanson M, Moreno AP, Dermietzel R & Meda P. 1991b. Distinctive gap junction channel types connect WB cells, a clonal cell line derived from rat liver. *Journal of Physiology* **260 (Cell Physiol. 29)**:C513-C527

Spray DC, Ginzberg RD, Morales EA, Gatmaitan Z & Arias IM. 1986. Electrophysiological properties of gap junctions between dissociated pairs of rat hepatocytes. *Journal of Cell Biology* **103**:135-144

Spray DC, Harris AL & Bennett MVL. 1979. Voltage dependence of junctional conductance in early amphibian embryos. *Science* **204**:432-434

Spray DC, Harris AL & Bennett MVL. 1981. Equilibrium properties of a voltage-dependent junctional conductance. *Journal of General Physiology* **77**:77-93

Spray DC, Moreno AP & Campos de Carvalho AC. 1993. Biophysical properties of the human cardiac gap junction channel. *Brazilian Journal of Medicine and Biological Research* **26**:541-552

Spray DC, Moreno AP, Eghbali B, Chanson M & Fishman GI. 1992. Gating of gap junction channels as revealed in cells stably transfected with wild type and mutant connexin cDNAs. *Biophysical Journal* **62**:48-50

Spray DC, Sáez JC, Brosius DA, Bennett MVL & Hertzberg EL. 1986. Isolated liver gap junctions: gating of transjunctional current is similar to that in intact pairs of rat hepatocytes. *Proceedings of the National Academy of Science of U.S.A.* **83**:5494-5497

Spray DC, White RL, Campos de Carvalho AC, Harris AL & Bennett MVL. 1984. Gating of gap junction channels. *Biophysical Journal* **45**:219-230

Spray DC, White RL, Mazet F & Bennett MVL. 1985. Regulation of gap junctional conductance. *American Journal of Physiology* **248 (Heart Physiol. 17)**:H753-H764

Stagg RB & Fletcher WH. 1990. The hormone-induced regulation of contact-dependent cell-cell communication by phosphorylation. *Endocrine Reviews* **11**:302-325

Standen NB. 1992. Potassium channels, metabolism and muscle. *Experimental Physiology* **77**:1-25

Stellwaag-Kittler F. 1954. Zur physiologie der käferhautung. Untersuchungen am mehlkäfer *Tenebrio molitor* L. *Biol Zbl* **73**:12-49

Stern JH & Macleish PR. 1985. Isolated pairs of rod photoreceptors are electrically coupled by a large, voltage-dependent junctional conductance. *Investigative Ophthamology and Visual Science* **26 suppl.**:193

Sugiura H, Toyama J, Tsuboi N, Kamiya K & Kodama I. 1990. ATP directly affects junctional conductance between paired ventricular myocytes isolated from guinea pig heart. *Circulation Research* **66**:1095-1102

Sun FF, Fleming WE & Taylor BM. 1993. Degradation of membrane phospholipids in the cultured human astroglial cell line UC-11MG during ATP depletion. *Biochemical Pharmacology* **45**:1149-1155

Swenson KI, Jordan JR, Beyer EC & Paul DL. 1989. Formation of gap junctions by expression of connexins in *Xenopus* oocyte pairs. *Cell* **57**:145-155

Takens-Kwak BR & Jongsma HJ. 1992. Cardiac gap junctions: three distinct single channel conductances and their modulation by phosphorylating treatments. *Pflügers Archives* **422**:198-200

Takens-Kwak BR, Jongsma HJ, Rook MB & van Ginneken ACG. 1992. Mechanisms of heptanol-induced uncoupling of cardiac gap junctions: a perforated patch-clamp study. *American Journal of Physiology* **262 (Cell Physiol. 31)**:C1531-1538

Terrar DA & Victory JGG. 1988. Influence of halothane on electrical coupling in cell pairs isolated from guinea-pig ventricle. *British Journal of Pharmacology* **94**:509-514

Traub O, Look J, Paul D & Willecke K. 1987. Cyclic adenosine monophosphate stimulates biosynthesis and phosphorylation of the 26 kDa gap junction protein in cultured mouse hepatocytes. *European Journal of Cell Biology* **43**:48-54

Unwin PNT & Zampighi G. 1980. Structure of the junction between communicating cells. *Nature* **283**:545-549

Veenstra RD. 1990. Voltage-dependent gating of gap junction channels in embryonic chick ventricular cell pairs. *American Journal of Physiology* **258 (Cell Physiol. 27)**:C662-672

Veenstra RD & DeHaan RL. 1986. Measurement of single channel currents from cardiac gap junctions. *Science* **233**:972-974

Veenstra RD & DeHaan RL. 1988. Cardiac gap junction channel activity in embryonic chick ventricle cells. *American Journal of Physiology* **254 (Heart Circ. Physiol. 23)**:H170-180

Verselis V & Brink PR. 1984. Voltage-clamp of the earthworm septum. *Biophysical Journal* **45**:147-150

Verselis VK & Bargiello TA. 1991. Dual voltage control in a *Drosophila* gap junction channel. **In**: *Biophysics of Gap Junction Channels*. C Peracchia, Ed. CRC Press, Boca Raton, Fl. pp.117-130

Verselis VK, Bennett MVL & Bargiello TA. 1991. A voltage-dependent gap junction in *Drosophila melanogaster*. *Biophysical Journal* **59**:114-126

Vogel H. 1992. Structure and dynamics of polypeptides and proteins in lipid membranes. *Quarterly Review of Biophysics* **25**:433-457

Wang H-Z, Li J, Lemanski LF & Veenstra RD. 1992. Gating of mammalian cardiac gap junction channels by transjunctional voltage. *Biophysical Journal* **63**:139-151

Warner AE, Guthrie SC & Gilula NB. 1984. Antibodies to gap-junctional protein selectively disrupt junctional communication in the early amphibian embryo. *Nature* **311**:127-131

Warner AE & Lawrence PA. 1982. Permeability of gap junctions at the segmental border in insect epidermis. *Cell* **28**:243-252

Weingart R. 1986. Electrical properties of the nexal membrane studied in rat ventricular cell pairs. *Journal of Physiology* **370**:267-284

Weingart R & Bukauskas FF. 1993. Gap junction channels of insects exhibit a residual conductance. *Pflügers Archives* **424**:192-194

Weir MP & Lo CW. 1984. Gap-junctional communication compartments in the *Drosophila* wing imaginal disk. *Developmental Biology* **102**:130-146

Weir MP & Lo CW. 1985. An anterior/posterior communication compartment border in engrailed wing discs: possible implications for *Drosophila* pattern formation. *Developmental Biology* **110**:84-90

White RL, Spray DC, Campos de Carvalho AC & Bennett MVL. 1982. Voltage dependent gap junctional conductance between fish embryonic cells. *Society of Neuroscience Abstracts* **8**:944

White RL, Spray DC, Campos de Carvalho AC, Wittenberg BA & Bennett MVL. 1985. Some electrical and pharmacological properties of gap junctions between adult ventricular myocytes. *American Journal of Physiology* **249 (Cell Physiol. 18)**:C447-C455

Wigglesworth VB. 1937. Wound healing in an insect (*Rhodnius prolixus* Hemiptera). *Journal of Experimental Biology* **14**:364-381

Wigglesworth VB. 1948. The structure and deposition of the cuticle in the adult mealworm, *Tenebrio molitor* L. (Coleoptera). *Quarterly Journal of Microscopical Science* **89**:197-217

Wigglesworth VB. 1959. The role of the epidermal cells in the 'migration' of tracheoles in *Rhodnius prolixus* (Hemiptera). *Journal of Experimental Biology* **36**:632-640

Wigglesworth VB. 1977. Structural changes in the epidermal cells of *Rhodnius* during tracheole capture. *Journal of Cell Science* **26**:161-174

Wigglesworth VB. 1984. The integument. **In**: *Insect Physiology*. Chapman and Hall, New York. pp.1-17

Wilders R & Jongsma HJ. 1992. Limitations of the dual voltage clamp method in assaying conductance and kinetics of gap junction channels. *Biophysical Journal* **63**:942-953

Willecke K, Hennemann H, Dahl E, Jungbluth S & Heynkes R. 1991. The diversity of connexin genes encoding gap junctional proteins. *European Journal of Cell Biology* **56**:1-7

Wolpert L. 1978. Gap junctions: channels for communication in development. **In:** *Intercellular Junctions and Synapses*. J Feldman, NB Gilula & JD Pitts, Ed. Chapman and Hall, London. pp.79-96

Wu J, McHowat J, Saffitz JE, Yamada KA & Corr PB. 1993. Inhibition of gap junctional conductance by long-chain acylcarnitines and their preferential accumulation in junctional sarcolemma during hypoxia. *Circulation Research* **72**:879-889

Xiao RP & De Mello WC. 1991. Intracellular resistance in rat papillary muscle: interaction between cyclic AMP and calcium. *Journal of Cardiovascular Pharmacology* **17**:754-760

Yang J, Isenberg KE & Zorumski CF. 1992. Volatile anesthetics gate a chloride current in postnatal rat hippocampal neurons. *FASEB Journal* **6**:914-918

Young JD-E, Cohn ZA & Gilula NB. 1987. Functional assembly of gap junction conductance in lipid bilayers: demonstration that the major 27 kd protein forms the junctional channel. *Cell* **48**:733-743

Zampighi GA, Hall JE & Kreman M. 1985. Purified lens junctional protein forms channels in planar lipid films. *Proceedings of the National Academy of Science of the U.S.A.* **82**:8468-8472

Zimmerman AL & Rose B. 1985. Permeability properties of cell-to-cell channels: kinetics of fluorescent tracer diffusion through a cell junction. *Journal of Membrane Biology* **84**:269-283